MASARYK UNIVERSITY IN BRNO
FACULTY OF SCIENCE

Ondřej Šráček – Josef Zeman

INTRODUCTION TO ENVIRONMENTAL HYDROGEOCHEMISTRY

BRNO 2004

ISBN 80-210-3586-2

Content

Chapter 1: Introduction **1**

Chapter 2: Water pollutants **3**
2.1 Introduction 3
2.2 Heavy metals 3
2.3 Organic compounds 4
2.4 Pesticides 4
2.5 Acid deposition 4
2.6 Nutrients 5
2.7 Thermal pollution 5
2.8 Pathogens 5
2.9 Oxygen-demanding wastes 5
2.10 Salts 6

Chapter 3: Principles of hydrogeochemistry **7**
3.1 Basic approaches 7
3.2 Thermodynamics 8
3.3 Kinetics 11
3.4 Oxidation-reduction (redox) reactions 12
3.5 Inorganic adsorption 14

Chapter 4: Carbonate system **19**
4.1 Introduction 19
4.2 Acid-base reactions in carbonate system 19
4.3 Dissolution and precipitation reactions 28
4.4 Regulation of natural waters pH by carbonate system 32

Chapter 5: Sampling of water and solids **37**
5.1 Basic considerations 37
5.2 Field parameters 37
5.3 Collection and preservation of samples 38
5.4 Sampling of solids 39

Chapter 6: Principles of geochemical modeling **41**
6.1 Introduction 41
6.2 Speciation models 41
6.3 Mass balance models 43
6.4 Forward models 44
6.5 Coupled transport and geochemical models 46

CHAPTER 7: INTRODUCTION TO TRANSPORT PROCESSES 49
7.1 Importance of transport processes 49
7.2 Diffusion 49
7.3 Advection 49
7.4 Dispersion 50
7.5 Adsorption 51
7.6 Decay 51
7.7 Equations of transport and their solutions 52
7.8 Breakthrough curve and tracer tests 53

CHAPTER 8: CONTAMINATION BY METALS 55
8.1 Behavior of metals in water 55
8.2 Examples of contaminants 57
8.3 Investigation of sites contaminated by metals 58

CHAPTER 9: ACID MINE DRAINAGE 61
9.1 Formation of acid mine drainage 61
9.2 Supply of oxygen 62
9.3 Neutralization of acid mine drainage 63
9.4 Hydrogeology of mining wastes 64
9.5 Prevention and remediation of acid mine drainage. 65
9.6 Investigation of acid mine drainage sites 65

CHAPTER 10: BEHAVIOR OF RADIONUCLIDES 67
10.1 Introduction 67
10.2 The structure of nuclei 67
10.3 The decay of excited and unstable nuclei 69
10.4 Basics of radiogenic isotope geochemistry 71
10.5 Geochronology 72
10.6 Decay systems and their applications 73

CHAPTER 11: ORGANIC CONTAMINATION 83
11.1 Types of organic contaminants 83
11.2 Hydraulics of free phase migration 84
11.3 Partitioning of organics between phases 85
11.4 Biodegradation 87
11.5 Mass balance calculations 89
11.6 Investigation of contaminated sites 90
11.7 Evaluation of natural attenuation 91

CHAPTER 12: GEOCHEMICAL ASPECTS OF REMEDIATION OF CONTAMINATED AQUIFERS 93
12.1 Introduction 93
12.2 Geochemical aspects 93
12.3 Basic types of remediation 95

CHAPTER 13: RISK ANALYSIS 99
13.1 Basic concepts 99
13.2 Concept of toxicity 99
13.3 Carcinogenic contaminants 100
13.4 Non-carcinogenic contaminants 101
13.5 Risk analysis methodology 101

Chapter 1: Introduction

There is an increasing interest in environmental issues. Hydrogeochemistry is very important from viewpoint of environmental impact assessment. Both surface water and ground water are used as sources of water for many purposes. Water also is transfer medium for many inorganic and organic contaminants and for pathogenic organisms. The purpose of our text is to present a basic information necessary for treatment and interpretation of environmental hydrogeochemical data. The level of text roughly corresponds to introductory master's level and basic knowledge of chemistry, mathematics and intrudoctury hydrogeochemistry is expected.

The structure of our text is as follows: Principal ground water pollutants are briefly indicated and then basic hydrogeochemical principals are discussed. More profound treatment of introductory hydrogeochemistry can be found in books such as Drever (1997) and Langmuir (1997). Then carbonate system is discussed in more detail because buffering in contaminated water and, thus, behavior of pH-sensitive contaminants is closely linked to the behavior of carbonates. Sampling of water and solids are an important part of contaminant studies and basic principals are introduced. Especially collection of solid phase samples is often neglected, but solid phase composition can be as important as water chemistry at many contaminated sites. More quantitative interpretation of collected data is discussed in chapters about geochemical modeling and transport. Then several types of contamination are discussed, including metals, acid mine drainage, radionuclides, and organics. Geochemical problems of remediation and principal remediation methods are also introduced. More detailed treatment of the topic is covered, for example, by Appelo and Postma (1999) and by Suthersan (1996). Finally, principals of risk analysis are discussed because calculation of risk became an important part of contamination studies. We will welcome comments from readers, which could help us to improve a potential re-edition of the text.

Chapter 2: Water Pollutants

2.1 Introduction

There are many types of water pollutants. Water which is withdrawn, used for some purposes and returned, is generally polluted. For example, water contaminated by agriculture activities contains nitrates, pesticides, and pathogens; mining activities produce water with low pH, elevated concentrations of sulfate, iron and other metals; thermal plants produce water that is elevated in temperature, with low dissolved oxygen concentration and so on. Chemical industry is very important source of water pollution because produces thousands of toxic compounds. In this chapter we focus on principal water pollutants, but this review is by no means complete and more detailed information can be found at U.S. EPA Home Page and in specialized books such as Masters (1998) and Fetter (1999).

2.2 Heavy Metals

Definition of metals is based on their physical properties like high thermal and electrical conductivity, high reflectivity, ductility, and strength. From chemical viewpoint, metals are elements which can give up one or more electrons and, thus, form cations in aqueous solution. The term heavy metals generally refers to metal with specific weight greater than about 4.0 g/cm^3. Principal metals from environmental viewpoint are *mercury, lead, cadmium,* and *arsenic* (arsenic is considered as semi-metal because has both metalic and non-metalic properties). Other toxic metals are beryllium, aluminum, chromium, bismuth, cobalt, nickel, strontium, thallium, zinc, tin, selenium, and titanium. Some of them like chromium are essential nutrients at low doses, but they become toxic at high concentrations.

Metals differ from organic pollutants because they are persistent in environment. For example, benzene can be degraded by bacteria, but lead can be only transferred from water to solid phase by precipitation of minerals like cerussite, $PbCO_3$, or galenite, PbS. It can be also adsorbed on ferric oxide and hydroxides, but always stays in environment and may be later remobilized during changes of pH and Eh conditions.

Metals may be inhaled or ingested with consumed water. Their toxicity depends on *exposition pathway* (see Chapter 13). For example, mercury in liquid form is not very toxic and most of ingested mercury is excreted from human body. In contrast, mercury vapor is very toxic because enters blood stream and after passing to brain can damage central nervous system. In the case of lead the situation is inverse, e.g., the most toxic is dissolved lead present as free ion Pb^{2+} and lead vapor is not very dangerous. Typical target organ damaged by metals are kidneys because most metals are excreted via kidneys. Typical metals toxic to kidneys and called nephrotoxins are cadmium, lead, and mercury.

There are several sources of metals in environment. Principal source of metals is mining industry, where concentrations of dissolved metals like iron, zinc, arsenic, lead etc., may reach extreme values (Chapter 9). Other sources are landfills, application of fertilizers (they frequently contain metals like cadmium, electroplating (chromium), and so on. High concentrations of dissolved metals are also typical for organic contamination plumes because initially adsorbed metals are released from Fe(III) oxide and hydroxides, which are unstable in very reducing environment.

2.3 Organic Compounds

There are thousands organic compounds produced in chemical industry. However, only some of them are important from environmental viewpoint. There is a group of toxic compounds related to dissolution of commercial gas. The group is called *BTEX* on the basis of names of compounds: *B*enzene, *T*oluene, *E*thylbenzene, and *X*ylene. They have a lower specific weight than that of water and, thus, they float on water table. The BTEX comprise only a small fraction of commercial gas (less than 10 %), but they are relatively more soluble than compounds with higher molecular weight (> C7, e.g., with more than 7 atoms of carbon), and they are very carcinogenic (more in Chapter 11 and Chapter 13).

Important group of contaminants also are *chlorinated solvents* like tetrachloroethylene (PCE), trichloroethylene (TCE), 1,2-dichloroethylene (DCE), 1,2-dichloroethane (DCA), vinylchloride (VC), and carbon tetrachloride (CTC). These compounds have higher specific weight than that of water and, consequently, they sink towards the base of an aquifer. They are carcinogenic, with vinylchloride as the most toxic compound. In many cases, there is formation of TCE, 1,2-DCE, and VC from PCE as parent compound (more in Chapter 11). Some organic compounds like trichloromethane (TCM) may form as a consequence of artificial chlorination of water containing natural dissolved organic carbon compounds.

Finally, there is contamination by *polyaromatic hydrocarbons* (PAH) like naphtalene, anthracene, and benzopyrene at some sites. These compounds comprise several benzene nuclei and they are relatively insoluble, with tendency to partition into soil organic matter. Thus, their occurrence is generally limited to the proximity of contaminant sources. They are very persistent in environment and some of them like benzopyrene are strong carcinogens. More in-depth reviews of organic contaminants are in Domenico and Schwartz (1998) and Fetter (1999).

2.4 Pesticides

Pesticides are chemicals used to kill undesirables organisms. Based on their use, they can be divided into *insecticides, fungicides, herbicides,* and *rodenticides.*

There are 3 principal groups of organic pesticides: *organochlorines, organophosphates, and carbamates.* The typical organochlorine is DDT (dichlorodiphenyltrichlorethane) which was frequently used to control mosquitoes carrying malaria and yellow fever. Toxicity of DDT to humans is relatively low, but the most serious problem related to this compound was its accumulation in food chain. DDT and its metabolite dichlorodiphenyldichloroethene (DDE) interferes with the enzyme that regulates distribution of calcium in birds, with resulting very thin shells of eggs. Other common organochlorines are aldrine, dildrin, endrin, endosulfan, and heptachlor.

Organophosphates such as parathion, malathion, and diazinon, are not very persistent, but they are more toxic than organochlorines. Exposure results in a wide range of symptoms like tremor, convulsions etc.

Carbamates are derived from carbamic acid, H_2NCOOH. Common carbamates are aldicarb, carbaryl, and propoxur. Acute human exposure may cause vomiting, blurred vision, and in some cases also death.

Most of compounds indicated above are insecticides. Chlorinated hydrocarbons are also used as pesticides. Clorophenoxy compounds like 2,4,5-T, and 2,4-D are known because they were used in mixture called Agent Orange as defoliants in the Vietnam War.

2.5 Acid Deposition

Rain water is naturally slightly acidic, with pH about 5.7 (Chapter 4). This is result of presence of carbonic acid, H_2CO_3, in the air at equilibrium with p_{CO2} equal to $10^{-3.5}$ atm. However, typical pH values of precipitation in industrial zones of Europe and North America are as low as 4.0. This is referred as acid rain caused by *anthropogenic emissions* of sulfur and nitrogen oxides. Sources of emissions can be *stationary* (thermal plants burning coal with high sulfur content) or *mobile* (cars releasing emissions from combustion of fuel).

Principal input from emissions are ions H^+, NO_3^-, and SO_4^{2-}. Sulfate ions are not very detrimental, but they may contribute to high salinity of water. Nitrate ions may contribute to eutrophication of surface water bodies, and, first of all, they can cause *methemoglobinemia* in little kids as a consequence of oral consumption (see section about nutrients). Thus, their concentration in consumed water is closely controlled. Nitrogen oxides in the air also contributes to formation of *ground level ozone* (GLO), harmful for both human health and plants.

Important impact of acidification is also dissolution of aluminosilicate and aluminum hydroxide minerals. In that case, toxic aluminum is released. Concentration of aluminum is generally controlled by precipitation of amorphous aluminum hydroxide, $Al(OH)_3$. This mineral phase becomes soluble at pH about 4.2 and water with lower pH often has high aluminum concentration. Aluminum is very detrimental for aquatic life because precipitates as $Al(OH)_3$ in more basic environment of the gills of fish and may cause their clogging.

2.6 Nutrients

Nutrients are chemicals necessary for growth of living organisms. Typical examples are carbon, nitrogen, iron, sulfur, and phosphorus. In excessive concentrations, they can be considered as pollutants because they stimulate growth of aquatic plants such as algae. Presence of algae in surface water bodies is detrimental for their use as drinking water and for recreational purposes.

Excessive growth of algae leads to *algae blooms* and to *eutrophication* of water. When algae die and decompose, they remove dissolved oxygen (DO) from water. The nutrient, which is the least available for algae growth is called a *limiting nutrient.* Carbon is generally available and either nitrogen or phosphorus are limiting nutrients for algae growth. Principal sources of nitrogen are chemical fertilizers, runoff from animal feedlots, septic systems, waste water discharge, and nitrogen deposition from atmosphere. Thus, nitrogen is rarely limiting nutrient for algae growth. In contrast, phosphorus is generally less abundant. However, concentration of phosphorus in the form of phosphate, PO_4^{3-}, may be high in agriculture runoff from heavily fertilized areas, in sewage water, and in outflow from septic systems.

Detergents produced after World War II also contained large amount of phosphate and were not biodegradable. Recent detergents are already biodegradable and phosphate present as sodium tripolyphosphate (STP) was often replaced by sodium nitrilotriacetate (NTA).

2.7 Thermal Pollution

Thermal pollution is generally related to waste waters from power plants. Water is not generally contaminated, but has higher temperature than ambient water. Thus, concentration of dissolved oxygen (DO) is lower. Also, metabolic rates of aquatic organisms double for each 10°C of increasing temperature. Increased metabolic rates also result in higher consumption of oxygen. Thus, consequences of thermal pollution are similar to the input of nutrients, e.g., water with low DO concentration with limited aquatic life. Furthermore, toxic impact of some contaminants like aluminum increases in low DO water because their input by gills increases as a consequence of higher rate of water exchange.

2.8 Pathogens

Pathogens are disease-causing organisms that can multiply and grow within bodies of humans and animals. Our text is focused on hydrogeochemistry of contamination and only brief outline of pathogens is presented here.

Growth of pathogens in body of a host is called infection. Pathogens can be broadly divided into *bacteria,* responsible for diseases like cholera, bacillary dysentery, and typhoid; *viruses,* responsible, for example, for hepatitis and poliomyelitis; *protozoa,* causing amebic dysentery and giardiasis, and *helminths* (parasitic worms), which cause diseases like schistosomiasis and dracunculiasis. Epidemics may be caused by penetration of intestinal discharges of an infected individual called carrier. Carriers themselves may not even exhibit symptoms of disease. This means that it is necessary to protect water supplies from any human and animal waste contamination. A common classification distinguishes between waterborne diseases like cholera and typhoid, which are spread by ingestion of contaminated water, water-washed diseases like scabia and trachoma, associated with lack of water to maintain cleanliness, water-based diseases, such as schistosomiasis and dracunculiasis, transmitted by contact with water without ingestion, and water-related diseases, such as dengue fever and malaria, transmitted by hosts (like mosquitoes) which depend on water, but without direct human contact with water.

Initially, coliform bacteria were considered as indicators of contamination of water by pathogens from human waste. However, it was found that presence *enteroviruses* is a better criterion for evaluation of contamination by human waste. Suggested indicators are presence of *polioviruses* and *hepatitis A* (HAV) viruses. Transport of viruses can be modeled just like transport of inorganic and organic contaminants and probably the most important modeling parameter is *inactivation rate* (e.g., removal of viruses by processes like their die-off) of viruses (Azadpour-Keeley et al., 2003).

2.9 Oxygen-demanding Wastes

Besides of nutrients and thermal pollution the DO concentration may be reduced by decomposition of *oxygen-demanding wastes.* The saturated oxygen concentration in water is relatively low, from 8 to 15 mg/L, depending on temperature. The minimum recommended DO concentration for fish population is 5 mg/L, but cold water species require even higher concentrations of oxygen.

Oxygen-demanding wastes are generally biodegradable organic compounds which consume oxygen during their biodegradation. Biodegradable organic compounds are contained, for example, in municipal waste waters and in effluents from industries like food processing and paper production.

The most common measures of oxygen demand are *chemical oxygen demand* (COD) and *biochemical oxygen demand* (BOD). The BOD is generally measured for 5 days period and is indicated as BOD_5. The COD refers to the amount of oxygen necessary to oxidize the waste chemically and BOD refers to amount of oxygen necessary to degrade waste biologically. Because not all organic compounds can be degraded biologically, then it holds that COD > BOD.

2.10 Salts

Water accumulates a variety of dissolved solids. A commonly used measure of salinity the concentration of *total dissolved solids* (TDS). Recommended TDS for drinking water is about 500 mg/L. Limits for livestock are higher, for example beef cattle can tolerate concentration up to 10,000 mg/L. In temperate and cold climate, one of sources of salinity can be related to the *application of road salts* in winter. Concentrations of cations like Na is generally lowered by cation exchange, but chloride concentration in water may reach high values.

In semiarid and arid climates, there is an increasing salinity linked to *irrigation* of fields. Irrigation water evaporates in soil and there is build-up of concentrations of ions like Na and Cl because ions like Ca and Mg are incorporated to precipitated carbonates. Furthermore, precipitated minerals form salt crust at ground surface and they may be re-dissolved during precipitation period. Ground water discharges to surface water bodies and salinity in rivers increases in the direction of their flow. This process is enhanced by excessive withdrawal of river water for irrigation (for example, from Colorado River in the Southwest of USA).

References

Azadpour-Keeley A., Faulkner B.R., Chen J.-S., 2003: *Movement and Longevity of Viruses in the Subsurface*, U.S. EPA Issue Papers, 24 p.

Domenico P.A., Schwartz F.W., 1998: *Physical and Chemical Hydrogeology*, 2nd Edition, John Wiley and Sons, New York.

Fetter C.W., 1999: *Contaminant Hydrogeology*, 2nd Edition, Prentice Hall, Upper saddle River, NJ 07458.

Masters G.M., 1998: *Introduction to Environmental Engineering and Science*, 2nd Edition, Prentice Hall, Upper Saddle River, New Jersey 07 458.

Chapter 3: Principles of Hydrogeochemistry

3.1 Basic Approaches

Dilution factor (DF): Ratio between final and initial concentration of a conservative ion like chloride, assuming that there was no input of the ion along flow path. The DF value can be used to evaluate the influence of physical processes like dispersion in transport of contaminants. An analogy of dilution factor is *concentration factor (CF),* which is used, for example, to evaluate a fraction of infiltrated precipitation after evapotranspiration. In that case, this is the ratio of chloride concentration in precipitation to chloride concentration in deep unsaturated zone water or in ground water.

Problem: In piezometer close to mining wastes, the concentrations of Cl^- and Al^{3+} were 100 mg/L and 40 mg/L, respectively. In piezometer located about 50 m downgradient the same concentrations were 60 mg/L and 10 mg/L. Which part of Al^{3+} concentration change was caused by geochemical processes?

Solution: The dilution factor DF for Cl^- is DF = 100/60 = 0.6. When we multiply initial concentration of Al^{3+} by DF we get 40×0.6 = 24 mg/L. This is expected concentration after physical processes. However, measured concentration was 10 mg/L. This means that 24 – 10 = 14 mg/L of the change was probably caused by chemical processes like precipitation of minerals as gibbsite, $Al(OH)_3$. We can check saturation index for gibbsite, which should have a value close to zero (see later).

Thermodynamic approach: There is assumption of very fast reaction rate with instantaneous equilibrium and no time factor is included. This assumption may be valid in the case of slow ground water flow and long residence time in ground water system.

Kinetic approach: Time factor plus other factors which have an impact on rate of reactions are included. Kinetic approach is much less used than thermodynamic approach because data on reaction kinetics are limited. However, some slow reactions like silicate weathering and redox reactions require kinetic description. One of the best known reaction kinetics is the kinetics of pyrite oxidation.

Mass balance approach: It is based on determination of concentration changes in different phases of an investigated system. It cannot be applied in some situations because solid phase composition changes may be difficult or even impossible to determine.

Problem: Calculate the volume of water with pH = 3.5 necessary to dissolve calcite in 1 m^3 of sand with 0.5 wt% of calcite. Specific weight of sand is 1 600 kg/m^3 and 1 mol of calcite is 100 g.

Solution:

- calculate number of moles of calcite in 1 m^3 of sand = (1 600 000 g × 0.005)/100 g = 80 mol
- calculate the volume of water to dissolve 80 mol of calcite: $V = 80\ \text{mol}/10^{-3.5} = 2.5\times10^5\ \text{L} = 2.5\times10^2\ \text{m}^3$

Master parameters (variables) are pH, redox potential Eh and ionic strength. They determine speciation (e.g., distribution of total concentrations among free ions and complexes) and behavior of dissolved species.

Macrocontaminants generally occur in high concentrations and influence master parameters of water. Examples are SO_4^{2-} and Fe^{2+} (only in acid mine drainage because in other environments Fe^{2+} generally has low concentration). The concentration of sulfate and Fe^{2+} in acid mine drainage, for example, has an impact on ionic strength (see later) and, thus, on activity coefficients, and Fe^{2+} concentration also has an impact on redox potential Eh. Macrocontaminants influence behavior of *microcontaminants* like Pb^{2+}, Zn^{2+} through ionic strength impact on activity coefficients and formation of complexes. When Pb^{2+} enters ground water, it has no influence on master parameters and macrocontaminants. On the other hand, formation of complexes like $PbSO_4^0$ has strong impact on lead behavior, but not on sulfate behavior because generally concentration of lead is negligible compared to the concentration of sulfate. When only contamination by microcontaminants takes place, we do not have to predict changes of master parameters like in the case of contamination by macrocontaminants. This means that modeling of behavior of contaminants is much simpler.

3.2 Thermodynamics

Common concentration units in hydrogeochemistry are *molarity M*, defined as mass in moles in 1 litr of solution and *molality m*, defined as mass in moles in 1 kilogram of solution. In dilute solution molarity is approximately equal to molality. Concentrations in miliequivalents per liter is concentration in milimoles per liter multiplied by charge of an ion.

Problem: Concentration of Ca in water is 65.1 mg/L. Calculate concentrations in mmol/L and meq/L. Atomic weight of Ca is 40.08.

Solution: Concentration in mmol/L is 65.1/40.08 = 1.62, concentration in meq/L is 1.62×2=3.24.

Activity a_i is "thermodynamic concentration" or the fraction of total concentration which participates in geochemical reactions. It is calculated as a product of *activity coefficient* γ_i and concentration m_i:

$$a_i = \gamma_i m_i \tag{3.1}$$

Activity coefficient is a function of *ionic strength I*, which is calculated as

$$I = \frac{1}{2}\sum m_i z_i^2 \tag{3.2}$$

where m_i is concentration and z_i is charge of ion *i*.

Problem: Calculate ionic strength of 0.2 mol solution of $NaSO_4$.

Solution:

$$I = \frac{1}{2}\left(m_{Na^+} z_{Na^+}^2 + m_{SO_4^{2-}} z_{SO_4^{2-}}^2\right)$$

$$I = \frac{1}{2}\left(0.2 \times 1^2 + 0.2 \times 2^2\right) = 0.5$$

Ionic strength is a measure of mineralization of a solution. When ionic strength increases, activity coefficient decreases (Fig. 3.1). In very diluted solutions activity coefficient is ≅ 1.0 and activity is equal to concentration. The decreasing trend is related to the "cage" of opposite charge particles around ions. There is reversal of the trend in extremely concentrated solutions (brines) because beyond of ionic strength of about 1.0 mol/L because there is an increase of activity coefficients with increasing ionic strength. This is related to decreasing amount of free water because most of water is already binded around particles. In the case of uncharged species like $H_2CO_3^0$, $H_4SiO_4^0$ or $H_3AsO_3^0$ only second effect takes place and their activity coefficients are always ≥ 1.0.

Activity coefficients are calculated using Debye-Hückel equation for ionic $I < 0.1$, Davies equation $I < 0.5$, and Pitzer's equations for very high ionic strength (Langmuir, 1997; Drever, 1997). However, Pitzer's parameters are generally available for 25°C only.

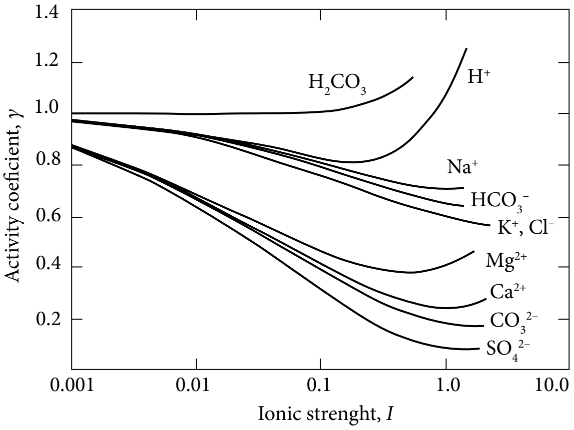

Fig. 3.1 Relation between ionic strength and activity coefficients (after Freeze and Cherry, 1979).

The Debye-Hückel equation in extended form is

$$\log \gamma_i = -Az_i^2 \frac{\sqrt{I}}{1 + Ba\sqrt{I}} \tag{3.3}$$

where γ_i is activity coefficient of ion *i*, z_i is its charge, *A*, *B* are temperature-dependent constant, and *a* is parameter corresponding to the size of an ion.

For higher ionic strength ($I > 0{,}1$), the Davies equation is used:

$$\log \gamma_i = \frac{-Az_i^{\,2}\sqrt{I}}{1+\sqrt{I}} + 0.2Az_i^{\,2}I \qquad 3.4$$

where A is temperature-dependent constant, and the final term is purely empirical. Constants and ion sizes used in both equations can be found, for example, in Stumm and Morgan (1996) and in Langmuir (1997). Hand calculation of activity coefficients becomes complicated and tedious when more species are involved. Thus, the equations above are used in speciation programs like PHREEQC (Parkhurst, 1995) to calculate distribution of total concentrations among free ions and complexes.

Law of mass action (also called Guldberg-Waag Law): In reaction

$$a\,\mathrm{A} + b\,\mathrm{B} \longleftrightarrow c\,\mathrm{C} + d\,\mathrm{D} \qquad 3.5$$

where small letters indicate stechiometric coefficients and capital letters are concentrations, the Gibbs free energy, which is driving force of the reaction, is expressed as

$$\Delta G_R = \Delta G_R^0 + RT\ln \frac{a_\mathrm{C}^c a_\mathrm{D}^d}{a_\mathrm{A}^a a_\mathrm{B}^b [A]^a [B]^b} \qquad 3.6$$

where $\Delta G_R^{\,0}$ is standard Gibbs free energy of the reaction, R is universal gas constant, and T is temperature. For equilibrium applies that $\Delta G_R = 0$ and then

$$\Delta G_\mathrm{R}^0 = -\;RT\;\ln K \qquad 3.7$$

where K is equilibrium constant for the reaction. The standard Gibbs free energy is calculated as

$$\Delta G_R^0 = \Delta G_{f\ \mathrm{products}}^0 - \Delta G_{f\ \mathrm{reactants}}^0 \qquad 3.8$$

where G_f is Gibbs formation energy (from thermodynamic tables).

At equilibrium, there is no more change of reactants and products concentrations and $\Delta G_R = 0$. If $\Delta G_R < 0$, then a reaction proceeds from the left to the right, if $\Delta G_R > 0$, then a reaction proceeds from the right to the left.

Van't Hoff equation is used to correct a value of equilibrium constant generally available for 25°C. When the constant is K_{T1} for temperature T_1, its value for temperature T_2 is

$$\log K_{T_2} = \log K_{T_1} + \frac{\Delta H_R^0}{2.303R}\left(\frac{1}{T_1} - \frac{1}{T_2}\right) \qquad 3.9$$

where ΔH^0_R is enthalpy of reaction (from tables), and R is universal gas constant.

Solubility product K_{sp} is equilibrium constant for dissolution/precipitation of a mineral. Let us have dissolution of gypsum in water:

$$\mathrm{CaSO_4 \cdot 2H_2O}(s) = \mathrm{Ca^{2+} + SO_4^{2-} + 2H_2O}$$

Mass action equation is

$$\frac{[\mathrm{Ca^{2+}}][\mathrm{SO_4^{2-}}][\mathrm{H_2O}]^2}{[\mathrm{CaSO_4 \times 2H_2O}]} = K_{equil}$$

where terms in brackets are activities. By definition, activities of pure solid phases and water (except for very mineralized solutions) are equal to 1.0, and we can write

$[\mathrm{Ca^{2+}}]\ [\mathrm{SO_4^{\,2-}}] = K_{equil} = K_{sp} = 10^{-4.60}$ for 25°C

where K_{sp} is equilibrium constant called solubility product. This constant applies for the reaction as it is written, e.g., for dissolution. For precipitation its value is $1/10^{-4.60} = 10^{4.60}$.

Saturation index SI indicates the degree of saturation with respect to a given mineral. It is defined as

$$SI = \log \frac{IAP}{K_{sp}} \qquad 3.10$$

where IAP is ion activity product, for example in the case of gypsum dissolution it is

$IAP = [\mathrm{Ca^{2+}}]\ [\mathrm{SO_4^{\,2-}}]$

where brackets denote activities.

When $IAP = K_{sp}$, the SI value is 0 and water is at equilibrium with respect to a given mineral. If $SI > 0$, water is supersaturated and the mineral should precipitate, and if $SI < 0$, water is undersaturated and the mineral should dissolve (of course, if the mineral is present in solid phase in contact with water). It has to be emphasized that the SI value indicates direction, but does provide information about rate of a reaction. Furthermore, there are reactions which never attain equilibrium and reactants are gradually transformed into products. An example is the oxidation of organic matter:

$CH_2O + O_2 \rightarrow CO_2 + H_2O$

In this reaction, organic matter is consumed and even when concentration of products such as CO_2 increases, organic matter cannot be re-created. This means that this type of reactions requires kinetic description.

Only some minerals dissolve and precipitates relatively fast and they are called *reactive minerals*. In this case we can apply thermodynamic approach. Common reactive minerals are (adapted from Deutsch, 1997):

Carbonates:
- calcite, $CaCO_3$
- dolomite, $CaMg(CO_3)_2$
- siderite, $FeCO_3$
- rodochrozite, $MnCO_3$

Sulfates:
- gypsum, $CaSO_4.2H_2O$
- jarosite, $KFe_3(SO_4)_2(OH)_6$
- melanterite, $FeSO_4.7H_2O$
- alunite $KAl_3(SO_4)_2(OH)_6$(questionable)

Oxides and hydroxides:
- ferrihydrate, $Fe(OH)_3$
- goethite, FeOOH
- gibbsite, $Al(OH)_3$
- manganite, MnOOH
- amorphous silica, $SiO_2(am)$
- brucite, $Mg(OH)_2$

Congruent dissolution: when a mineral dissolves, the ratio between ions in solution is the same as in the mineral. For example, the ratio $Ca^{2+}:SO_4^{2-}$ is 1:1 in both gypsum and in water.

Incongruent dissolution: the ratio is different in dissolving mineral and in water. This is typical for dissolution of silicates, when secondary minerals are formed. An example is dissolution of anorthite with formation of kaolinite:

$CaAl_2Si_2O_8 + H^+ + H_2O \rightarrow Al_2Si_2O_5(OH)_4 + Ca^{2+}$

The ratio $Ca^{2+}:Al^{3+}:Si^{4+}$ is 1:2:2 in ortoclase, but 1:0:0 in water because all Al^{3+} and Si^{4+} are retained in secondary mineral kaolinite.

Stability diagrams for silicates: They are constructed for selected silicate minerals and with assumption of all aluminum conserved in solid phase. There is no guarantee that a water sample is at equilibrium with a mineral, when water samples fall into the field of the mineral. This behavior just indicates that the water is relatively closer to equilibrium with the mineral compared to other mineral phases used for construction of the diagram. An example of stability diagram for system with K_2O is in Fig. 3.2.

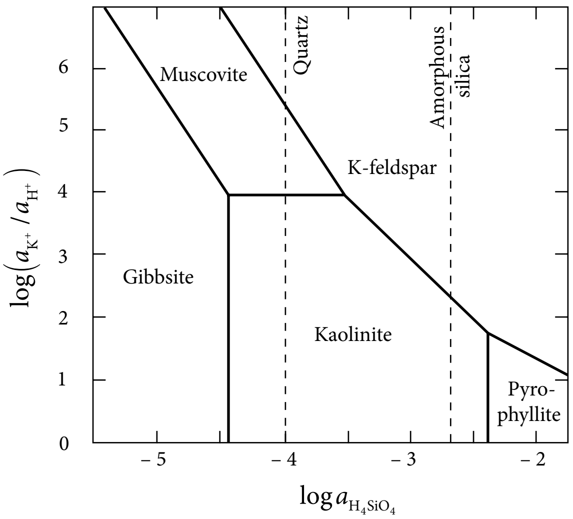

Fig. 3.2 Stability diagram for system with K_2O.

Influence of complexation: there is formation of *aquatic complexes* of ions, for example calcium can be in solution as free ion Ca^{2+} and in the form of complexes like $CaSO_4^0$, $CaHCO_3^+$ etc. These complexes increase solubility of calcium minerals, which would be lower if only Ca^{2+} would have been present in water.

Let us consider dissolution of anglesite,

$PbSO_4(s) \longleftrightarrow Pb^{2+} + SO_4^{2-} \qquad K_{sp} = 10^{-7.79}$

If there are Mg^{2+} and Cl^- already present in water, there is formation of complexes

$Mg^{2+} + SO_4^{2-} \longleftrightarrow MgSO_4^0$ and $Pb^{2+} + Cl^- \longleftrightarrow PbCl^+$ (and also $PbSO_4^0$)

and total dissolved lead concentration will be

$[Pb]_{total} = (Pb^{2+}) + (PbSO_4^0) + (PbCl^+)$

There also is an influence of ionic strength on dissolution of anglesite. In water with Mg^{2+} and Cl^-, the activity coefficients for Pb^{2+} and SO_4^{2-} are lower than in distilled water and more anglesite dissolves. In that case we can write that

$$\gamma_{Pb^{2+}} m_{Pb^{2+}} \gamma_{SO_4^{2-}} m_{SO_4^{2-}} = K_{\text{anglesite}}$$

The value of solubility product of $K_{anglesite}$ is a constant, and, thus, when values of activity coefficients γ are reduced as a consequence of high ionic strength, then values of concentrations *m* have to increase to compensate for the change.

Common ion effect: If water is at equilibrium with less soluble mineral and encounters more soluble mineral, which contains an ion from the first mineral already dissolved in water, then the first mineral precipitates (Drever, 1997). An example is precipitation of calcite during dissolution of gypsum:

$$Ca^{2+} + HCO_3^- + CaSO_4 \cdot 2H_2O(s) \longleftrightarrow$$
$$\longleftrightarrow Ca^{2+} + SO_4^{2-} + CaCO_3(s) + H^+ + 2H_2O$$

Water of Ca-HCO_3 type at equilibrium with calcite encounters gypsum and resulting water is of Ca-SO_4 type. Calcite is less soluble than gypsum and dissolution of gypsum with input of large quantity of Ca^{2+} forces precipitation of calcite and reduction of bicarbonate concentration. Similarly, if the water dissolving anglesite in previous case contains SO_4^{2-} instead of Cl^-, there will be very limited dissolution of anglesite because sulfate is in both anglesite and in water.

Order of encounter refers to the order in which strata with different minerals are encountered by flowing ground water. Even when the same strata with the same mineral assemblage are encountered, resulting ground water chemistry at outflow will be different if the order of strata is different (Palmer and Cherry, 1984). For example, if first sequence contains shale layer with Na-montmorillonite, limestone layer, and gypsum layer and second sequence contains limestone layer, gypsum layer, and shale layer with Na-montmorillonite and organic matter, the water at the first sequence outflow will have high Ca^{2+} and SO_4^{2-}–concentrations and low Na^+ concentration, and the water at the second sequence outflow will have high Na^+, and low SO_4^{2-} Ca^{2+} concentrations. This is a consequence of common ion effect, cation exchange and sulfate reduction in different orders.

3.3 Kinetics

Kinetic approach includes time factor. Let us have dissolution of halite, NaCl. When we plot concentration of Na^+ *vs.* time (Fig. 3.3), concentration of Na^+ increases initially, but at time $t = t_2$ reaches a maximum, and then remains constant. Since time t_2, the concentration of Na^+ does not depend on time and is determined by the solubility product of halite.

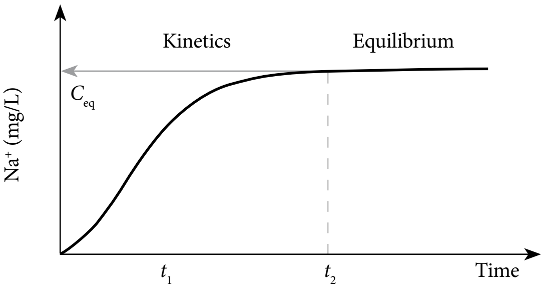

Fig. 3.3 Dissolution of halite (adapted from Appelo and Postma, 1999).

Behavior in the region where $t > t_2$ is described by thermodynamics, and behavior in region where $t < t_2$ is described by kinetics. The time t_2 necessary to attain equilibrium is different for different minerals. It is relatively short for reactive minerals like calcite and gypsum and long for non-reactive minerals like quartz. However, if a reaction is "fast" or "slow" also depends on the relation between velocity of ground water flow and reaction rate (the faster the flow is, the less probable is equilibrium) and on time scale of investigation (for example, predictions for radioactive disposal sites are up to more than 10,000 years).

Order of reaction kinetics: depends on exponent of independent variable, for example reaction

$$-\frac{dC}{dt} = k\ C \qquad 3.11$$

is of first order because the exponent of concentration C is one. In the reaction t is time and k is reaction constant linked to half-life $t_{1/2}$ as $k = ln\ 2 / t_{1/2}$. Solution of the equation obtained by integration for C_0 at t_0 is

$$C_t = C_0\ e^{-kt} \qquad 3.12$$

where C_0 and C_t are concentrations at time $t = 0$ (initial concentration) and at time t. Rate of reaction decreases with declining concentration and this reaction is used to describe radioactive decay of isotopes like ^{14}C and tritium and is also used for biodegradation of petroleum products like benzen and toluen and chlorinated solvents like PCE and TCE.

In the case of zero order kinetics, the reaction is

$$-\frac{dC}{dt} = k \qquad 3.13$$

and

$$C_t = C_0 - kt \qquad 3.14$$

Rate of zero order reaction is always the same and does not depend on concentration. In the case of 2nd order reaction concentration is squared,

$$-\frac{dC}{dt} = k\ C^2 \qquad 3.15$$

Example of second order reaction is oxidation of Fe^{2+} by oxygen,

$$-\frac{dm_{Fe^{2+}}}{dt} = k\ m_{Fe^{2+}} \left[OH^-\right]^2 p_{O_2} \qquad 3.16$$

This reaction is of 2nd order with respect to pH, but of first order with respect to Fe^{2+} concentration and partial pressure of O_2.

Homogeneous vs. *heterogeneous reaction:* Homogeneous reaction includes only one phase. Example is formation of $PbSO_4^0$ complex in solution. Heterogeneous reactions include more phases and an example is dissolution of CO_2 in water.

Relation between reaction constant and temperature is given by the *Arrhenius equation*,

$$k = A\exp\frac{-E_a}{RT} \qquad 3.17$$

where A is pre-exponential (Arrhenius) factor, E_a is activation energy, R is universal gas constant and T is temperature. If we know reaction constants for different temperatures, we can plot a graph $\log k = f(1/T)$ in order to determine activation energy from its slope equal to $-E_a/2.3\,R$ (Fig. 3.4).

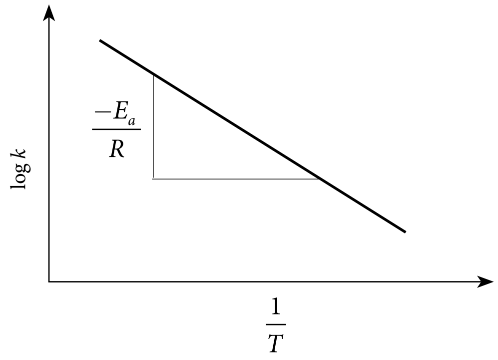

Fig. 3.4. Determination of activation energy.

3.4 Oxidation-reduction (redox) Reactions

In these reactions there is change of oxidation state of ions. Oxidation is a loss of electrons and reduction is a gain of electrons. Electrons cannot freely exist in solution, thus there is no oxidation without reduction and vice versa. Example is oxidation of Fe^{2+} combined with precipitation of ferric hydroxide:

$$Fe^{2+} + 0.25\,O_2 + 2.5\,H_2O \longleftrightarrow Fe(OH)_3(s) + 2\,H^+$$

In this reaction iron is oxidized from +2 state to +3 state and oxygen is reduced from 0 state to –2 state. On the other hand, dissolution of calcite,

$$CaCO_3(s) + CO_2 + H_2O \longleftrightarrow Ca^{2+} + 2HCO_3^-$$

is not redox reaction because oxidation numbers of calcium and carbon are always +2 and +4, respectively.

Each redox reaction can be written as a combination of two half-reactions, oxidation and reduction. For example, oxidation of Fe^0 by oxygen can be written as

$Fe^0(s) \rightarrow Fe^{2+} + 2e^-$	oxidation of Fe^0 to Fe^{2+}
$0.5O_2 + 2H^+ + 2e^- \rightarrow H_2O$	reduction of O^0 to O^{2-}
$Fe^0(s) + 0.5\,O_2 + 2H^+ \rightarrow Fe^{2+} + H_2O$	complete reaction

In this reaction, Fe^0 is oxidized and is donor of electrons and reducing agent, and oxygen is acceptor of electrons and oxidizing agent.

There are two basic types of redox notation:
First of them is *redox potential*, Eh [V], which is expressed with respect to hydrogen electrode. However, it is generally measured with respect to a different electrode (kalomel electrode etc.) and measured values have to be corrected for hydrogen electrode. The correction for kalomel electrode and temperature 25°C is about 0.245 V. The *Nernst equation* describes the relation between redox potential and activities of a redox couple. For example, for redox couple of iron the equation is

$$Eh = Eh^0 + \frac{RT}{nF}\ln\frac{\left[Fe^{3+}\right]}{\left[Fe^{2+}\right]} \qquad Eh^0 = 0.77\ \mathrm{V} \qquad 3.18$$

where Eh^0 is standard potential (from tables), n is number of transferred electrons, F is Faraday constant and terms in squared brackets are activities. The Eh^0 values for other redox reactions are in Appelo and Postma (1993).

Second type of notation is the *activity of electrons*, p*e*, notation. This is expressed in analogy with pH as $pe = -\log[e^-]$. However, in contrast to H^+, electrons cannot exist separately in a solution. Equation for iron redox couple is in this notation

$$pe = pe^0 + \ln\frac{\left[Fe^{3+}\right]}{\left[Fe^{2+}\right]} \qquad pe^0 = 13.0 \qquad 3.19$$

In this case, the manipulation of equation is simpler than in the case of the Eh notation because the equation can be treated as an ordinary equilibrium equation. Conversion between both notations is

$$Eh[V] = 0.059\,pe \qquad \text{for } 25°C \qquad 3.20$$

Different forms of the same element with different oxidation number can have completely different behavior (soluble Fe^{2+} compared to insoluble Fe^{3+}) and toxicity (very toxic Cr^{6+} compared to Cr^{3+} with low toxicity).

Thus, information about oxidation number is necessary in investigation of contaminated sites.

Determination of oxidation number can be done:

(a) Directly, by analytical determination on perfectly preserved (filtered and acidified in the field) sample. This determination has a priority.

(b) By splitting of total concentration, for example Fe_{total}, on the basis of field Eh value and the Nernst equation. This determination is problematic because the Eh value may correspond to the strongest redox couple (which is often, but not always, iron couple) and other redox couples may not be with the strongest couple at equilibrium. Especially poor is match between Eh and O_2/H_2O couple.

(c) By calculating Eh value from one redox couple like Fe^{2+}/Fe^{3+} and using the calculated Eh or pe value to determine concentration of second redox couple (for example, Mn^{2+}/Mn^{4+}) by splitting of total concentration. This approach suffers of the same problem as the application of field Eh, e.g., there frequently is a lack of equilibrium between different redox couples. In geochemical programs like PHREEQC it is possible to choose between all options mentioned above.

The Eh-pH diagrams: they are used for interpretation of contaminants behavior. An example of the Eh-pH diagram for iron is in Fig. 3.5. Key points are:

- The diagrams are constructed for specified concentrations of metals and anions (for example, $Pb_{total} = 10^{-6}$ mol/L, $S_{total} = 10^{-3}$ mol/L etc.). If there is a significant difference between specified concentrations and concentrations at a studied site, then boundary in the diagram have to be recalculated.
- They is assumption of equilibrium.
- Boundaries between fields indicate equal concentrations for aqueous species. This means that, for example, Fe^{2+} can be present at lower concentration in the Fe^{3+} field.
- In solid phase fields, the aqueous ions are present at very low concentrations. In the contrary, there is no presence of solid phase in dissolved species fields. When total concentration of a metal increases, the size of solid phase field also increases.

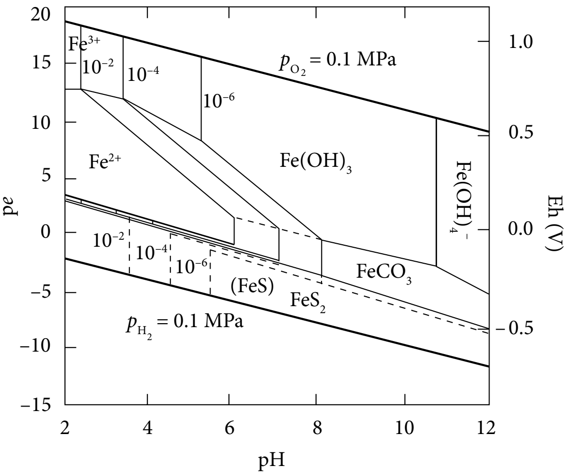

Fig. 3.5 The Eh-pH diagram for iron.

Redox sequence (also redox ladder): There is a natural sequence of redox reactions during oxidation of organic matter. Dissolved oxygen is consumed first and methane is generated last, Fig. 3.6. The sequence is: $O_2 \rightarrow NO_3^- \rightarrow Mn^{4+} \rightarrow Fe^{3+} \rightarrow SO_4^{2-} \rightarrow CH_4$. The sequence is based on free energy released at each redox reaction, which decreases from consumption of oxygen to methanogenesis. There is the same sequence observed along a flow path in a pristine flow system, e.g., dissolved oxygen is generally found close to recharge area and methane, if present, at deep confined zone. When biodegradation of petroleum products occurs, electron acceptors are also consumed in the same order. In the case of sanitary landfills and dissolved petroleum products plumes, the sequence is reversed, e.g., methane is found close to (or directly in) a source zone (landfill or free phase zone) and dissolved oxygen is found at the periphery of a plume.

Problem: Ground water sample with pH about 7.0 has 5.0 mg/L of total iron and 160 mg/L of sulfate. Is there a possibility of significant concentrations of nitrate and methane?

Solution: Iron is present as Fe^{2+} at this pH range (Fe^{3+} precipitates as $Fe(OH)_3$), which is incompatible with nitrate. Iron comes from dissolution of $Fe(OH)_3$ after nitrate reduction. High sulfate concentration shows that there has not been a significant sulfate reduction. Thus, the sample does not already have nitrate and still does not have methane. There should be analysis for other metals (Pb, Zn etc.) generally adsorbed on $Fe(OH)_3$, which are generally released during reductive dissolution of $Fe(OH)_3$.

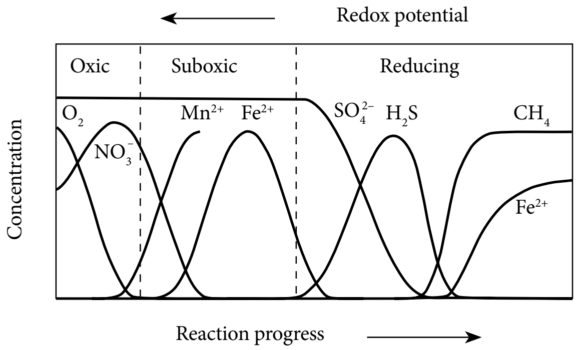

Fig. 3.6 Redox sequence of electron acceptors consumption.

3.5 Inorganic Adsorption

This section deals with adsorption of inorganic species. Adsorption of organics is treated in chapter about organic contamination. Adsorption refers to attachment of dissolved solids to surface of adsorbent (clay, hydroxide etc.), whereas absorption refers to penetration of dissolved solids into structure of an adsorbent. In many cases it is not possible to distinguish between both processes.

Clays have adsorption capacity relatively independent of pH. On the other hand, hydroxides and soil organic matter have adsorption capacity highly dependent on pH.

Clays have large specific surface, which generally has negative charge at close to neutral pH due to substitution of Si^{4+} and Al^{3+} in their crystal lattice by ions with lower valency.

Table 3.1 Properties of clay minerals (adapted from Deutsch, 1997).

Property/clay mineral	Montmorillonite	Illite	Kaolinite
Particle size [μm]	0.01–1.0	0.1–2.0	0.1–5.0
Ion substitution	high	intermediate	low
Surface [m^2/g]	600–800	100–120	5–20
CEC [meq/100g]	80–100	15–40	3–15

Cation exchange capacity (CEC): characterizes adsorption capacity for cations. It is determined by saturation of exchange sites by a cation (generally NH_4^+) and then by determination of its concentration after expulsion from exchange sites by other cation (Na^+ in concentrated solution of NaCl). Values of CEC are reported in meq/100 g of soil for specified pH (generally 7.0). Properties of clay minerals are in Table 3.1.

Montmorillonite has the largest specific surface and the highest CEC values, and kaolinite exhibits the lowest values. In the case of clays also occurs protonation of surface at low pH values and thus, adsorption capacity changes. However, bulk adsorption capacity of clay is pH-independent, for example, for montmorillonite it is about 90 % of total adsorption capacity.

Sand has low CEC values, generally less than 1 meq/100 g or less. However, even this value is by no means negligible.

Problem: Sand at Borden site in Ontario, Canada, has CEC equal to 0.5 meq/100 g. Calculate the amount of Na^+ which can be adsorbed, when grain density is 2.68 kg/dm^3 and porosity is 0.33.

Solution: 1 m^3 has 670 dm^3 of solids and 330 dm^3 of water, thus 1L of water is in contact with 670/330 = 2.03 dm^3 or 2.03 x 2.68 = 5.44 kg of solids, and this amount of solids can adsorb

$$54.4 \times 0.5 = 27.2 \text{ meq of } Na^+$$

which correspond to

$$27.2 \times 22.99 = 625.33 \text{ mg/L}$$

of Na^+ - this is more than usual Na^+ concentration in most ground waters.

Organic matter in solid phase (SOM-solid organic matter) plays an important role in adsorption of organic contaminants (see later), but also is important adsorbent for inorganic contaminants. This is related to deprotonation of carboxylic group –COOH and phenolic group –OH due to changes of pH, with resulting negative surface charge. Soil humus may have CEC up to 200 meq/100 g and can adsorb a significant fraction of metals like chromium (Nikolaidis et al., 1994). Appelo and Postma (1999) present an equation for calculation of CEC on the basis of both clay content and organic matter content:

$$\text{CEC[meq/100 g]} = 0.7\times(\%\ \text{clay}) + 3.5\times(\%\ \text{C}) \quad 3.21$$

The *ion exchange* comprises replacement of one species adsorbed on solid phase surface by another one present initially in solution. Cation exchange is generally much more important than anion exchange. Ions with higher charge are preferentially adsorbed, but ion exchange also depends on concentrations in solution. For example, Ca^{2+} has higher affinity for adsorption than Na^+ when dissolved concentrations are comparable, but Na^+ is more adsorbed than Ca^{2+} in sea water with much higher Na^+ concentrations. Adsorption affinity decreases in the sequence

$$Al^{3+} > Ca^{2+} > Mg^{2+} > K^+ > Na^+$$

When both charge and concentration of two ions are similar, then an ion with lower hydrated radius is preferred for adsorption. Hydrated radius is lower for ions with higher ion radius because in their case the ratio charge/ion radius is lower. Thus, Ca^{2+} has higher ion radius and lower hydrated radius than Mg^{2+} and is preferentially adsorbed.

There often are *colloids* (particles of size <1μm) in water. *Stern layer* with tightly held ions (generally cations) is close to surface of colloids and *Gouy layer* with mobile ions (cations still predominate) is further from surface, between Stern layer and bulk solution with the same concentrations of cations and anions. Stability of colloids depends on the thickness of the Gouy layer which in turn depends on ionic strength of solution.

When ionic strength increases, there is compression of the layer and flocculation of colloids (for example, during mixing of river water and sea water in estuaries).

In the case of Fe and Mn hydroxides the adsorption is strongly pH-dependent. When pH increases, there is de-protonation of surface,

$$\equiv SOH_2^+ \longleftrightarrow \equiv SOH^0 + H^+ \tag{3.22}$$

$$\equiv SOH^0 \longleftrightarrow \equiv SO^- + H^+ \tag{3.23}$$

and adsorbed ions also change surface charge of adsorbent, for example, in the case of Zn^{2+} adsorption we can write

$$\equiv SO^- + Zn^{2+} \longleftrightarrow \equiv SOZn^+ \tag{3.24}$$

In equations above, the sign ≡ indicates adsorption sites on solid phase and *S* indicates element in solid phase (in the case of ferric hydroxide it is Fe). When average charge at adsorbent surface is equal to zero, the numbers of positive and negative charge sites are equal and we can write that

$$\equiv SOH_2^+ \longleftrightarrow \equiv SO^- \tag{3.25}$$

Value of pH at the point is called pH_{ZPC} (pH of zero point of charge). Typical pH_{ZPC} values for different minerals are: clays 2.0 – 4.0, feldspars 2.0 – 2.5, $Fe(OH)_3$ 8.3, and calcite 8.4.

When pH of solution changes, there also is a change of electrostatic component of adsorption related to adsorption/desorption of H^+. This component of adsorption is expressed by coulombic (Boltzmann) term K_{coul},

$$K_{coul} = \exp\frac{-\Delta ZF\Psi}{RT} \tag{3.26}$$

where ΔZ is change of surface charge, *F* is Faraday constant, *Ψ* is surface potential, R is universal gas constant, and T is temperature. Bulk adsorption constant is a product of intrinsic (chemical) and coulombic constant:

$$K_{bulk} = K_{int} \times K_{coul} \tag{3.27}$$

At pH_{ZPC} the numbers of positively and negatively charged sites are identical, bulk surface charge is equal to zero, and, thus, $K_{bulk} = K_{int}$. When pH increases, negatively charged sites start to predominate, more cations are adsorbed and anions are desorbed (Fig. 3.7). This behavior is called *adsorption edge.*

However, it has to be emphasized that even at $pH < pH_{ZPC}$ some negatively charged sites exist, but they are less abundant than positively charges sites. Cations like Pb^{2+} are already adsorbed at pH much lower than pH_{ZPC} (for $Fe(OH)_3$ about 8.3), usually at $pH < 6.5$ because their concentrations in water are generally small and they have strong affinity for adsorption.

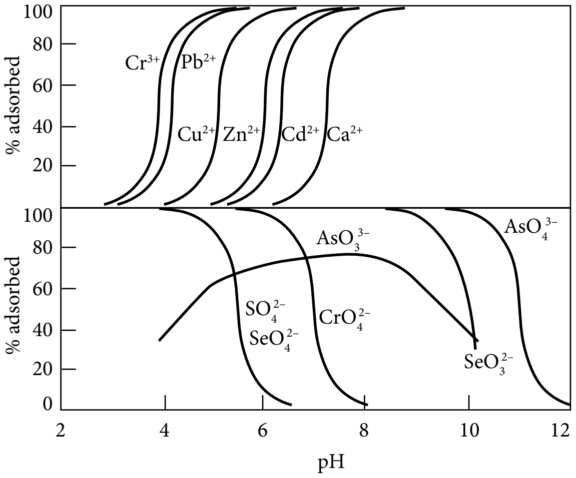

Fig. 3.7 Adsorption behavior of cations and anions (after Drever, 1997).

Modeling of adsorption

The most common approach is based on the application of adsorption isotherms. They are empirical (not true thermodynamic constants) determined from batch experiments. In batch experiment a flask with known quantity of water and solid phace is spiked with known concentration of contaminant and after equilibration (usually 24 hours) the partitioning between solid phase and water is determined. Adsorbed amount of contaminant (generally in mg/g) is plotted as a function of water concentration (usually in mg/L). Adsorbed amount is calculated as

$$S = \frac{\left(C_{equil} - C_{init}\right)V}{M} \tag{3.28}$$

where C_{equil} is equilibrium concentration, C_{init} is initial concentration, *V* is volume of water and *M* is mass of solid phase adsorbent.

Linear distribution coefficient K_d is determined as a slope in the graph $S = f(C)$.

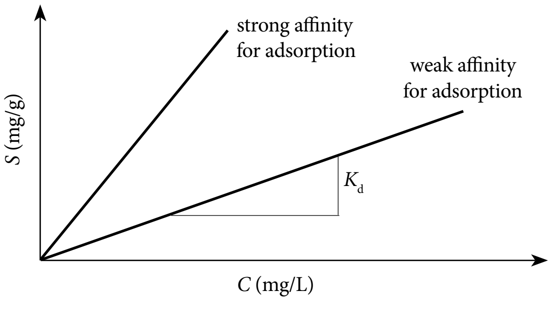

Fig. 3.8 Concept of linear adsorption isotherm K_d.

Principal problem of linear adsorption isotherm is related to the lack of limit for adsorption with increasing concentration in water. This is not correct because number of adsorption sites is limited and there is saturation of adsorption sites when concentration in water becomes too high.

Adsorption isotherm of Freundlich, expressed as

$$S = K_F \cdot C^N \qquad 3.29$$

takes into account decreasing adsorption with increasing concentration in water. The exponent N, which is generally < 1.0, changes the slope of straight line at higher concentrations in water. However, there is no maximum adsorption limit either. *Linear distribution coefficient* K_d is special case of the isotherm for $N = 1.0$.

Finally, *adsorption isotherm of Langmuir*, expressed as

$$S = \frac{S_{\max} K_L C}{1 + K_L C} \qquad 3.30$$

where $S_{\max}$ is maximum amount of contaminant which can be adsorbed. When concentration in water is high, the product $K_L \times C >> 1$, we obtain $S = S_{\max}$, which is asymptote of the graph $S = f(C)$ or adsorption limit.

Adsorption isotherms can be implemented into advection-dispersion equation (ADR) (see Chapter 7.7) and used to calculate *retardation factor* R (see section on transport), which is defined as

$$R = \frac{v_{\text{water}}}{v_{\text{contam}}} = 1 + \left(\frac{\rho_b}{n}\right)\frac{\mathrm{d}S}{\mathrm{d}C} \qquad 3.31$$

where v_{water} is velocity of ground water flow (or a conservative, non-adsorbed tracer migration) and $v_{\text{contaminant}}$ is velocity of adsorbed contaminant migration. Retardation factor for different isotherms is (Fetter, 1999):

a) linear isotherm:

$$R = 1 + \left(\frac{\rho_b}{n}\right) K_d \qquad 3.32$$

b) Freundlich isotherm

$$R = 1 + \left(\frac{\rho_b}{n}\right) K_F N C^{N-1} \qquad 3.33$$

c) Langmuir isotherm:

$$R = 1 + \left(\frac{\rho_b}{n}\right) \frac{K_L S_{\max}}{(1 + K_L C)^2} \qquad 3.34$$

Note in the equations above that retardation factor R is constant for linear isotherm, but it is function of concentration for Freundlich and Langmuir isotherms! This behavior has very serious consequences for remediation of contaminated soils (see later).

We have discussed so far isotherms describing adsorption of only one ion on solid phase. *Selectivity coefficient* describes exchange between two ions in reaction expressed, for example, as

$$2\ \text{A-clay} + \text{B}^{2+} \longleftrightarrow \text{B-clay} + 2\ \text{A}^{+} \qquad 3.35$$

with selectivity coefficient (equilibrium constant) $K_{\text{A-B}}$. Selectivity coefficient $K_{\text{A-B}}$ just like adsorption isotherms is not a real thermodynamic constant because there is no thermodynamic description of adsorbed ions behavior. Values are also valid for specified pH and water chemistry.

Problem: Calculate fractions of adsorption sites occupied by Na^+ and Ca^{2+}, when concentrations in water are for both species 10^{-3} mol/L and $K_{\text{Na-Ca}}$ is equal to 1.0.

Solution: equation of reaction is

$$2\ \text{Na-clay} + \text{Ca}^{2+} = \text{Ca-clay} + 2\text{Na}^{+} \qquad K_{\text{Na-Ca}} = 1.0$$

then

$$\frac{X_{\text{Ca-clay}}}{X^2_{\text{Na-clay}}} = K_{\text{Na-Ca}} \frac{m_{\text{Ca}^{2+}}}{m^2_{\text{Na}^+}}$$

where X is molar fraction adsorbed on clay, for example

$$X_{\text{Ca-clay}} = \frac{\text{Ca-clay}}{\text{Ca-clay} + \text{Na-clay}}$$

and $X_{\text{Ca-clay}} + X_{\text{Na-clay}} = 1.0$, after substitution

$$\frac{1 - X_{\text{Na-clay}}}{X^2_{\text{Na-clay}}} = 1 \times \frac{10^{-3}}{10^{-6}}$$

which results in quadratic equation with solution $X_{\text{Na-clay}} = 0.03$, $X_{\text{Ca-clay}} = 0.97$.

In the problem above we can see that in the case of the same concentrations in water Ca^{2+} is preferentially adsorbed. However, in water with high Na^+ concentrations there is much more Na^+ adsorbed on solid phase than Ca^{2+}. Applications of selectivity coefficient are disscused in Appelo and Postma, (1999). In Table 3.2, there are selectivity coefficients for cation exchange with Na^+,

$$Na^+ + 1/i\ I\text{-}X_i = Na\text{-}X + 1/i\ I^{i+} \qquad 3.36$$

where X represents X fraction of ion I on adsorption sites, and i is charge of the ion.

The notation in the Equation 3.36. is called Gaines-Thomas notation. There are other types of notation (Gapon, Vanselow), discussed in Appelo and Postma, (1999).

Table 3.2 Selectivity coefficients (Appelo and Postma, 1999) .

Ion I^+	$K_{Na/I}$	Ion I^{2+}	$K_{Na/I}$
Li^+	1.2 (0.95–1.2)	Mg^{2+}	0.50 (0.4–0.6)
K^+	0.2 (0.15–0.25)	Ca^{2+}	0.40 (0.3–0.6)
NH_4^+	0.25 (0.2–0.3)	Sr^{2+}	0.35 (0.3–0.6)
Rb^+	0.10	Ba^{2+}	0.35 (0.3–0.6)
Cs^+	0.08	Fe^{2+}	0.6
		Cu^{2+}	0.5
		Zn^{2+}	0.4 (0.3–0.6)
Ion I^{3+}	$K_{Na/I}$	Cd^{2+}	0.4 (0.3–0.6)
Al^{3+}	0.6(0.5–0.9)	Pb^{2+}	0.3

Modeling of surface complexation, which takes into account changes in surface layer of adsorbent due to changes of pH and water chemistry, is beyond the scope of this text. We will mention briefly double diffuse layer (DDL) model as it is used in code MINTEQA2 (Allison et al., 1991). The model is based on adsorption on hydrous ferric hydroxide (HFO) with composition of goethite, molecular weight of 89 g/mol, surface area of 600 m²/g, and number of adsorption sites 0.2mol/mol HFO. It is possible to change these parameters. In some cases (adsorption of trace metals) second type of adsorption sites with number of 0.005 mol/mol HFO is included.

The following procedure is used:

a) After water chemistry input open adsorption menu and choose diffuse double layer model. Enter concentration of Fe^{3+} converted to HFO as Fe^{3+} [g/L] × 1.589.
b) Enter specific surface in [m²/g], which is 600 m²/g for freshly precipitated HFO, but is lower for older precipitates.
c) Enter concentration of adsorption sites in [mol of sites/L], which is 0.2 mol sites/mol HFO × concentration of HFO [mol HFO/L].
d) Then append file feo-dlm.dbs, which is data base including chemical adsorption constants and run the program.

It is possible to use so called sweep option in MINTEQA2 with step-wise change of pH to determine adsorption edge for a metal.

Problem: (from Langmuir, 1997): Calculate using sweep option adsorption of zinc in pH interval 4.0–8.5 with step 0.5. Concentration of HFO is $C_s = 8.9\times10^{-2}$ g/L, concentration of zinc is 10^{-6} mol/L, surface area of HFO = 600 m²/g, and adsorption sites density is $\Gamma = 2\times10^{-4}$ activ. sites/L.

Solution: See table of surface speciation and adsorption of Zn. It is evident that surface charge (second column) becomes negative between pH 8.0 and 8.5, but adsorption of zinc is already finished below pH of 7.0, where bulk surface charge is still positive.

Table 3.3 Surface speciation of HFO and adsorption of zinc (from Langmuir, 1997).

	ψ	σ	($FeOH_2^+$)	(FeOH)	(FeO^-)	($FeOZn^+$)	% Zn
pH	volts	C/m²	M	M	M	M	adsorbed
4.0	0.184	0.212	−3.93	−4.10	−5.9	−8.43	0.4
4.5	0.169	0.158	−4.04	−3.97	−5.54	−7.56	2.8
5.0	0.152	0.112	−4.14	−3.90	−5.26	−6.76	17.5
5.5	0.132	0.0763	−4.30	−3.85	−5.05.	−6.21	61.4
6.0	0.110	0.0496	−4.41	−3.83	−4.90	−6.03	92.5
6.5	0.0865	0.0305	−4.49	−3.82	−4.79	−6.00	99.0
7.0	0.0609	0.0174	−4.56	−3.82	−4.72	−6.00	99.9
7.5	0.0341	0.0084	−4.60	−3.82	4.67	−6.00	100.0
8.0	0.00066	0.0015	−4.64	−3.82	−4.63	−6.00	100.0
8.5	−0.02100	−0.0049	−4.67	−3.82	−4.60	−6.00	100.0

Note: Listed are the surface potential (ψ) and surface charge (σ), and molar concentrations of surface species.

References.

Allison J. D. D., Brown S., Novo-Gradac K. J., 1991: MINTEQA2, *A Geochemical Assesment Data Base and Test Cases for Environmental Systems*. Athens, U.S. EPA.

Appelo C.A.J., Postma D., 1999: *Geochemistry, groundwater and pollution*, Revised edition. A.A. Balkema, Rotterdam/Brookfield.

Deutsch W. J., 1997: *Groundwater Geochemistry, Fundamentals and Applications to Contamination*. Lewis Publishers, Boca Raton, New York.

Drever J.I., 1997: *The Geochemistry of Natural Waters, Surface and Groundwater Environments*. 3rd Edition, Prentice Hall, Upper Saddle River.

Domenico P., Schwartz F.W., 1990: *Physical and Chemical Hydrogeology*. John Wiley & Sons, New York.

Fetter C.W., 1999: *Contaminant Hydrogeology*. Prentice Hall, New York.

Freeze R.A., Cherry J.A., 1979: *Groundwater*. John Wiley&Sons

Langmuir D., 1997: *Aqueous Environmental Geochemistry*. Prentice Hall, Upper Saddle River.

Nikolaidis N.P., Robbins G.A., Scherer M., McAninch B., Binkhorst G., Asikainen J., Snib S., 1994: Vertical distribution and partitioning of chromium in a galci-fluvial aquifer. *Ground Water Monitor. and Rem.*, Summer 1994, pp. 150–159.

Palmer C.D., Cherry J.A., 1984: Geochemical evolution of groundwater in sequences of sedimentary rocks. *J. Hydrol.*, 75, pp. 27–65.

Parkhurst, D. L., 1995: *Users Guide to* PHREEQC-*A Computer Program for Speciation, Reaction-Path, Advective-Transport, and Inverse Geochemical Calculations*. U.S. Geological Survey Water-Resources Investigation Report 95–4227.

Stumm W., Morgan J. J., 1996: *Aquatic Chemistry*. 3rd Edition, John Wiley & Sons, Inc.

Chapter 4: Carbonate System

4.1 Introduction

Water continually transforms the surface of the Earth, through interaction with the solid surface and transport of dissolved and suspended matter. One of the most important systems, which affect water quality, is carbonate system. Beyond that, carbonate system represents tight interconnection between inorganic and organic systems, and ensure the stable conditions for the latter. Aquatic carbonate geochemistry is therefore the principal concern of many geochemists and geologist.

In this chapter, the tools of thermodynamics will be applied to water carbonate systems. There will be developed methods for predicting the carbonate species present in water at equilibrium. Then there will be examined the interactions of solutions with solids through precipitation and dissolution.

Most reactions of carbonate system in aqueous solutions can be placed in one of the following categories:

- Acid-base reactions (e.g. dissociation of carbonic acid)

  $H_2CO_3 \longleftrightarrow H+ + HCO_3^-$
- Dissolution/Precipitation (e.g. dissolution of calcite)

  $CaCO_3(\text{calcite}) \longleftrightarrow Ca^{2+} + CO_3^{2-}$
- Adsorption/Desorption (e.g. adsorption of metal on a carbonate surface)

  $\equiv S + M^{2+} \longleftrightarrow =S\text{–}Mn$

  (where ≡S indicates the surface of the carbonate).
- Complexation (e.g. complexation of uranyl ion):

  $UO_2^{2+} + 2\ CO_3^{2-} \longleftrightarrow [UO_2(CO_3)_2]^{2-}$

In this chapter, we will consider the first two reactions in detail. Basic principles of adsorption/desorption were already introduced in Chapter 3.5.

4.2 Acid-base Reactions in Carbonate System

The hydrogen and hydroxide ions often participate in all the foregoing reactions. As a result, many of these reactions are pH dependent. In order to characterize the state of an aqueous solution, e.g., to determine how much $CaCO_3$ a solution will dissolve, the first step is usually to determine pH. On a larger scale, weathering of limestone and precipitation of carbonates in sediments depend critically on pH. Thus pH is sometimes called the master variable. While pH represents the hydrogen ion activity, or proton concentration, the hydroxide ion concentration can be easily calculated from pH since the proton and hydroxide concentrations are related by the dissociation constant for water, i.e., by:

$$H_2O \longleftrightarrow H^+ + OH^- \qquad K_W = a_H\, a_{OH} \qquad 4.1$$

The value of K_W, like all equilibrium constants, depends on temperature, but is about 10^{-14} at 25°C.

The strength of an acid or base is measured by its tendency to donate or accept protons. The dissociation constant for an acid or base is the quantitative measure of this tendency and thus is a good indication of its strength. For example, dissociation of HCl:

$$HCl \longleftrightarrow H^+ + Cl^-$$

has a dissociation constant

$$K_{HCl} = \frac{a_{H^+} a_{Cl^-}}{a_{HCl}} = 10^3$$

HCl is a strong acid because only about 3% of the HCl molecules added will remain undissociated. The equilibrium constant for dissociation of hydrogen sulfide:

$H_2CO_3 \longleftrightarrow H^+ + HCO_3^-$

is

$$K_{H_2CO_3} = \frac{a_{H^+} a_{HCO_3^-}}{a_{H_2CO_3}} = 10^{-6.35}$$

Thus H_2CO_3 is a weak acid because very few of the H_2CO_3 molecules actually dissociate except at high pH.

Most protons released by an acid will complex with water molecules to form hydronium ions, H_3O^+ or even $H_5O_2^+$. However, in almost all cases we need not concern ourselves with this and we can treat the H^+ ion as if it were a free species. Thus we will use $[H^+]$ to indicate the concentration of $H^+ + H_3O^+ + H_5O_2^+$.

4.2.1 Proton Accounting, Charge Balance, and Conservation Equations

4.2.1.1 Proton Accounting

Knowing the pH of an aqueous system is the key to understanding it and predicting its behavior. This requires a system of accounting for the H^+ and OH^- in the system. One approach is the Proton Balance Equation. In this system, both H^+ and OH^- are considered components of the system, and the proton balance equation is written such that the concentration of all species whose formation through reaction with water caused the production of OH^- are written on one side, and the concentration of all species whose formation through reactions with water caused the production of H^+ are written on the other side. Because water dissociates to form H^+ and OH^-, $[H^+]$ always appears on the left side (because one OH^- will have been produced for every H^+ produced by dissociation of water) and OH^- always appears on the right side of the proton balance equation (because one $H^+$is produced for every OH^- produced). The proton balance equation for pure water is thus:

$$[H^+] = [OH^-] \qquad 4.2$$

In pure water the concentrations of H^+ and OH^- are equal.

Now, consider the example of a carbonic acid solution. H^+ will be generated both by dissociation of water and dissociation of carbonic acid:

$H_2CO_3 \longleftrightarrow H^+ + HCO_3^-$

Since one HCO_3^- ion is generated for every H^+, and one CO_3^{2-} ion is generated for two H^+ ions, the proton balance equation becomes:

$$[H^+] = [OH^-] + [HCO_3^-] + 2\,[CO_3^{2-}] \qquad 4.3$$

An alternative approach to the proton balance equation is the TOT_H proton mole balance equation. In this system, H^+ and H_2O are always chosen as components of the system but OH^- is not. The species OH^- is the algebraic sum of H_2O less H^+:

$$[OH^-] = [H_2O] - [H^+] \qquad 4.4$$

Because aquatic chemistry almost always deals with dilute solutions, the concentration of H_2O may be considered fixed at a mole fraction of 1, or 55.4 M. Thus H_2O is made an implicit component, i.e., its presence is assumed by not written, so that equation 4.4 becomes:

$$[OH^-] = -\,[H^+] \qquad 4.5$$

The variable TOT_H is the total amount of component H^+, rather than the total of species H^+. Because we create the species OH^- by subtracting component H^+ from component H_2O, the total of component H^+ for pure water will be:

$TOT_H = [H^+] - [OH^-]$

The TOT_H in this case is the difference between the concentrations of H^+ and OH^-. Now consider the dissolution of CO_2 in water to form carbonic acid:

$$CO_2 + H_2O \longleftrightarrow H_2CO_3 \qquad 4.6$$

Under the normal conditions of pH, this carbonic acid will dissociate to form bicarbonate ion:

$$H_2CO_3 \longleftrightarrow H^+ + HCO_3^- \qquad 4.7$$

In our system of accounting, we would choose CO_2 as a component. The carbonic acid species would then be made from:

$H_2CO_3 = H_2O + CO_2$

The bicarbonate ion would be made from components CO_2, H_2O, and H^+:

$HCO_3^- = CO_2 + H_2O - H^+$

Thus in the proton mole balance equation, bicarbonate ion would count negatively, so TOT_H is:

$TOT_H = [H^+] - [OH^-] - [HCO_3^-]$ 4.8

We could have combined reactions 4.6 and 4.7 to write:

$CO_2 + H_2O \longleftrightarrow H^+ + HCO_3^-$

4.2.1.2 Charge Balance

Solutions are electrically neutral. This means that the number of positive and negative charges must balance:

$\Sigma\, m_i z_i = 0$ 4.9

where m_i is the number of moles of ionic species *i* and z_i is the charge of species *i*. Equation 4.9 is known as the charge balance equation. This equation provides an important constraint on the composition of a system. In some cases, the proton balance and charge balance equations are identical.

For each acid-base reaction an equilibrium constant expression may be written. By manipulating these equilibrium constant expressions as well proton balance, charge balance, and mass balance equations, it is possible to predict the pH of any solution. In natural systems where there are many species present, however, solving these equations can be a complex task. An important step in their solution is to decide which reactions have an insignificant effect on pH and can be neglected.

4.2.1.3 Conservation Equations

A further constraint on the composition of a system is provided by mass balance. Acid-base reactions will not affect the total concentration of a substance. Regardless of reactions 4.6 and 4.7, and any other reactions, the total concentration of carbonate species remains constant. Thus we may write:

$\Sigma\, c_T = [CO_2] + [H_2CO_3] + [HCO_3^-] + [CO_3^{2-}] + \ldots$

We can write one mass balance, or conservation, equation for each component in solution. Mass balance equations are useful for those components forming more than one species.

While the charge balance constraint is an absolute one and always holds, mass balance equations can be trickier because other processes, such a redox, precipitation, and adsorption, can affect the concentration of a species. We sometimes can get around this problem by writing the mass balance equation for an element, since an elemental concentration is not changed by redox processes. We might also define our system such that it is closed to get around the other problems. Despite these restrictions, mass balance often provides a useful additional constraint on a system.

Problem: Write the proton, proton mass balance, and charge balance, and carbonate conservation equations for a solution prepared by dissolving Na_2CO_3 in water. Assume that Na_2CO_3 dissociates completely and that the system is closed.

Answer: We begin with the proton balance equation. From the dissociation of water we have:

$[H^+] = [OH^-]$

In addition to this, hydroxide ions will also be generated by reaction between CO_3^{2-} and water:

$CO_3^{2-} + H_2O \longleftrightarrow HCO_3^- + OH^-$

$HCO_3^- + H_2O \longleftrightarrow H_2CO_3 + OH^-$

Since for each HCO_3^- formed, one OH^- must have formed and for each H_2CO_3 present two OH^- must have formed, the proton balance equation is:

$[H^+] + [HCO_3^-] + 2[H_2CO_3] = [OH^-]$

Choosing the carbonate and sodium ions as components (in addition to H^+ and H_2O), the bicarbonate and carbonic acid species are combinations of carbonate and one and two, respectively, protons, so that the proton mole balance equation is:

$TOT_H = [H^+] + [HCO_3^-] + 2[H_2CO_3] - [OH^-]$

Alternatively, we could chose CO_2 (in addition to H^+, H_2O and Na^+) as our forth component, rather than carbonate ion. In this case, the three carbonate species are made from components as follows:

$H_2CO_3 = H_2O + CO_2$
$HCO_3^- = H_2O + CO_2 - H^+$
$CO_3^{2-} = H_2O + CO_2 - 2H^+$

In this case, the proton mole balance equation is:

$TOT_H = [H^+] - [HCO_3^-] - 2\,[CO_3^{2-}] - [OH^-]$

Here we see that TOT_H depends on how we define our components. The charge balance equation is:

$[H^+] + [Na^+] = [OH^-] + [HCO_3^-] + 2[CO_3^{2-}]$

The conservation equation for carbonate species is:

$\Sigma\, CO_3 = [CO_3^{2-}] + [HCO_3^-] + [H_2CO_3]$

4.2.3 The Carbonate System

Water at the surface of the Earth inevitably contains dissolved CO_2, either as a result of equilibration with the atmosphere or because of respiration by organisms. CO_2 reacts with water to form carbonic acid:

$$CO_2 + H_2O \longleftrightarrow H_2CO_3 \qquad 4.10$$

Some of the carbonic acid dissociates to form bicarbonate and hydrogen ions:

$$H_2CO_3 \longleftrightarrow H^+ + HCO_3^- \qquad 4.11$$

Some of the bicarbonate will dissociate to an additional hydrogen ion and a carbonate ion:

$$HCO_3^- \longleftrightarrow H^+ + CO_3^{2-} \qquad 4.12$$

We can write three equilibrium constant expressions for these reactions:

$$K_{sp} = \frac{a_{H_2CO_3}}{p_{CO_2}} \qquad 4.13$$

$$K_1 = \frac{a_{H^+} a_{HCO_3^-}}{a_{H_2CO_3}} \qquad 4.14$$

$$K_2 = \frac{a_{H^+} a_{CO_3^{2-}}}{a_{HCO_3^-}} \qquad 4.14$$

The equilibrium constants for these reactions are given in Table 4.1 as a function of temperature.

In the above series of reactions, we have assumed that dissolved CO_2 reacts completely with water to form H_2CO_3. This is actually not the case, and much of the dissolved CO_2 will actually be present as distinct molecular species, $CO_2(aq)$. Thus reaction 4.10 actually consists of the two reactions:

$$CO_2(g) + H_2O \longleftrightarrow CO_2(aq) \qquad 4.10a$$

$$CO_2(aq) + H_2O \longleftrightarrow H_2CO_3 \qquad 4.10b$$

The equilibrium for the second reaction favors $CO_2(aq)$. However, it is analytically difficult to distinguish between the species $CO_2(aq)$ and H_2CO_3. For this reason, $CO_2(aq)$ is often combined with H_2CO_3 when representing the aqueous species. The combined total concentration of $CO_2(aq) + H_2CO_3$ is written as $H_2CO_3^*$. We will write it simply as H_2CO_3.

The importance of the carbonate system is that by dissociating and providing hydrogen ions to solution, or associating and taking up free hydrogen ions, it controls the pH of many natural waters. *Problem* shows that pure water in equilibrium with atmospheric

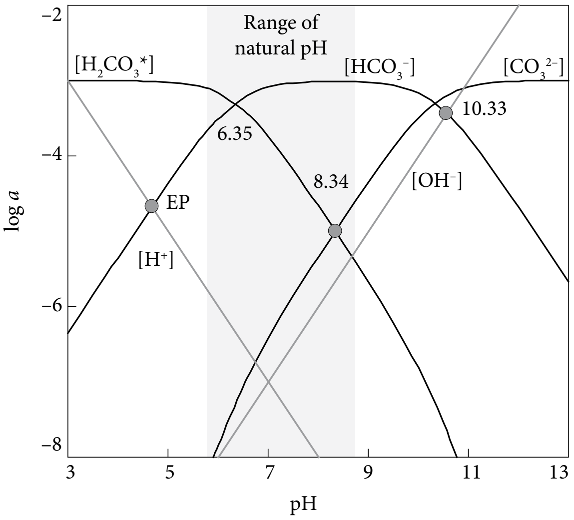

Figure 4.1. Activities of different species in the carbonate system as a function of pH assuming $\Sigma\ CO_2 = 10^{-3}$.

Table 4.1. Equilibrium constants for the carbonate system.

T (°C)	pK_{CO2}	pK_1	pK_2	pK_{cal}	pK_{arag}	$K_{CaHCO3+}$*	pK_{CaCO30}†
0	1.11	6.58	10.63	8.38	8.22	−0.82	−3.13
5	1.19	6.52	10.55	8.39	8.24	−0.90	−3.13
10	1.27	6.46	10.49	8.41	8.26	−0.97	−3.13
15	1.34	6.42	10.43	8.43	8.28	−1.02	−3.15
20	1.41	6.38	10.38	8.45	8.31	−1.07	−3.18
25	1.47	6.35	10.33	8.48	8.34	−1.11	−3.22
30	1.52	6.33	10.29	8.51	8.37	−1.14	−3.27
45	1.67	6.29	10.20	8.62	8.49	−1.19	−3.45
60	1.78	6.29	10.14	8.76	8.64	−1.23	−3.65
80	1.90	6.34	10.13	8.99	8.88	−1.28	−3.92
90	1.94	6.38	10.14	9.12	9.02	−1.31	−4.05

* $K_{CaHCO3+} = a_{CaHCO3+} / (a_{Ca2+}\, a_{HCO3-})$
† $K_{CaCO30} = a_{CaCO30} / (a_{Ca2+}\, a_{CO32-})$

CO_2 will be slightly acidic. The production of free H^+ ions as a result of the dissolution of CO_2 and dissociation of carbonic acid plays an extremely important role is weathering. Natural waters with a pH equal to or greater than 7 must contain cations other than H^+.

Problem: What is the pH of water in equilibrium with the atmospheric CO_2 at 25°C, assuming ideal behavior and no other dissolved solids or gases present? The partial pressure of CO_2 in the atmosphere is 3.5×10^{-4}.

Solution: In this case, the proton balance and charge balance equations are identical:

$$[H^+] = [OH^-] + [HCO_3^-] + [CO_3^{2-}]$$

We might guess that the pH of this solution will be less than 7 (i.e., $[H^+] \geq 10^{-7}$). Under those circumstances, the concentrations of the hydroxyl and carbonate ions will be much lower than that of the hydrogen and bicarbonate ions. Assuming we can neglect them, our equation then becomes simply:

$$[H^+] = [HCO_3^-]$$

We can combine equations 4.13 and 4.14 to obtain an expression for bicarbonate ion in terms of the partial pressure of CO_2:

$$[HCO_3^-] = K_1 K_{CO2} p_{CO2} / [H^+]$$

Substituting this into previous equation and rearranging, we have:

$$[H^+]^2 \longleftrightarrow K_1 K_2 K_{CO2} p_{CO2}$$

Taking the negative log of this expression and again rearranging, we obtain:

$$pH = (-\log K_1 - \log K_2 - \log p_{CO2}) / 2$$

Substituting values from Table 4.1, we calculate pH = 5.64. Looking at Figure 4.1, we can be assured that our assumption that carbonate and hydroxyl ion abundances are valid. Indeed, an exact solution using the Solver in Excel™ differs from the approximate one by less than 0.0001 pH units.

Ground water may not be in equilibrium with the atmosphere, but will nonetheless contain some dissolved CO_2. Because of respiration of organisms in soil (mainly plant roots and bacteria) through which they pass before penetrating deeper, ground water often contains more CO_2 than water in equilibrium with the atmosphere. In addition, calcite and other carbonates are common minerals in soils and in sedimentary, metamorphic, and altered igneous rocks. Ground water will tend to approach equilibrium with calcite by either dissolving it or precipitating it:

$$CaCO_3 \longleftrightarrow Ca^{2+} + CO_3^{2-} \qquad 4.16$$

Carbonate ions produced in this way will associate with hydrogen ions to form bicarbonate as in reaction 4.12, increasing the pH of the solution. Water containing high concentrations of calcium (and magnesium) carbonate is referred to as 'hard water'. Such waters are generally somewhat alkaline.

Now suppose we have a known activity of all carbonate species in solution, say for example 10^{-2}:

$$a_{H_2CO_3} + a_{HCO_3^-} + a_{CO_3^{2-}} = \sum CO_2 = 10^{-2} \qquad 4.17$$

From this, and the dissociation constants, we can calculate the amount of each species present as a function of pH and temperature. For example, we can use the equilibrium constant expressions to obtain substitutions for the carbonic acid and carbonate ion activities in equation 4.17 that are functions of bicarbonate ion activity and pH. We then solve Equation 4.17 to obtain an expression for the activity of the bicarbonate ion as a function of total CO_2 and hydrogen ion activity:

$$a_{HCO_3^-} = \frac{\sum CO_2}{\frac{a_{H^+}}{K_1} + 1 + \frac{K_2}{a_{H^+}}} \qquad 4.18$$

Similar equations may be found for carbonic acid and carbonate ion. Carrying out these calculations at various pH, we can construct the graph shown in Figure 4.1. In this figure, we see that carbonic acid is the dominant species at low pH, bicarbonate at intermediate pH, and carbonate at high pH.

Particularly simple relationships occur when the activities of two species are equal. For example, choosing pH to be 4.35 (at 25°C) we can rearrange equation 4.14 and substitute to obtain:

$$\frac{a_{H^+}}{K_1} = \frac{a_{H_2CO_3}}{a_{HCO_3^-}} = \frac{10^{-6.35}}{10^{-6.35}} = 1 \qquad 4.19$$

The activity of the carbonate ion will be very low at this pH. If we ignore it, equ. 4.17 becomes:

$$a_{H_2CO_3} + a_{HCO_3^-} \cong 10^{-2}$$

According to Equation 4.19, the activities of both species are equal, so each must be 5×10^{-3}.

Now consider the point where the hydrogen ion concentration equals the bicarbonate ion concentration. At this point, the concentration of the carbonate ion is extremely low, and there is exactly enough H^+ to convert all HCO_3^- to H_2CO_3. From the perspective of the proton balance then, the HCO_3^- concentration is equivalent to the same concentration of H_2CO_3. This point, labeled EP on Figure 4.1, is called the CO_2 equivalence point. In a similar way, the point where the carbonic acid and carbonate ion concentrations are equal is called the bicarbonate equivalence point, and that where bicarbonate and hydroxyl concentrations are equal is called the carbonate equivalence point. The pH of these equivalence points depends, among other things, on the $\Sigma\ CO_2$ concentration.

The exact concentrations of carbonate species depends on total carbonate concentration as well as the concentration of other ions in solution. Thus the distribution shown in Figure 4.1 is unique to the conditions specified ($c_T = 10^{-2}$, no other ions present). Nevertheless, the distribution will be qualitatively similar for other conditions.

Problem: A groundwater moving through soil into a deep aquifer acquires a total dissolved CO_2 concentration of 10^{-2} M. Assuming the water does not exchange with surrounding rock, ideal behavior and no other dissolved solids or gases, what is the pH of the water?

Solution: In this case, our charge and proton balance equations are the same as in Example 4.2, i.e., Equation 4.26. Since the solution does not exchange with surrounding rock, it can be considered a closed system and we can write the following mass balance equation:

$$\Sigma\ CO_2 = [H_2CO_3] + [HCO_3^-] + [CO_3^{2-}] = 10^{-2}$$

Simultaneously solving the change balance and mass balance equations, and using equilibrium constant expressions to eliminate carbonate and OH^- species, we obtain:

$$[H^+]^4 + K_1 [H^+]^3 + \{K_1 K_2 - K_W - K_1 \Sigma\ CO_2\}[H^+]^2$$
$$- \{K_W + 2 K_2 \Sigma\ CO_2\}K_1 [H^+] - K_1 K_2 K_W = 0$$

We might again guess that the concentration of the carbonate ion will be very low, and that we can therefore neglect all terms in which K_2 occurs. We might also guess that pH will be acidic so that $[H^+] \gg [OH^-]$, and therefore that we can neglect terms containing K_W. Our equation becomes:

$$K_1^{-1}[H^+]^2 + [H^+] = \Sigma\ CO_2$$

Solving this quadratic equation, we find that pH = 4.18.

4.2.4 Conservative and Non-Conservative Ions

We can divide dissolved ions into conservative and non-conservative ones. The conservative ions are those whose concentrations are not affected by changes in pH, temperature, and pressure, assuming no precipitation or dissolution. In natural waters, the principal conservative ions are Na^+, K^+, Ca^{2+}, Mg^{2+}, Cl^-, SO_4^{2-} and NO_3^-. These ions are conservative because they are fully dissociated from their conjugate acids and bases over the normal range of pH of natural waters. Non-conservative ions are those that will undergo association and dissociation reactions in this pH range. These include the proton, hydroxide ion, and carbonate species as well as many inorganic and organic anions. Variations in the concentrations of non-conservative ions result from reactions between them, and these reactions can occur in the absence of precipitation or dissolution. For example, reaction of the carbonate and hydrogen ion to form bicarbonate will affect the concentrations of all three ions. Of course, if the system is at equilibrium, this reaction will not occur in the absence of an external disturbance, such as a change in temperature.

4.2.5 Total Alkalinity and Carbonate Alkalinity

Alkalinity is a measure of acid-neutralizing capacity of a solution and is defined as the sum of the concentration (in equivalents) of bases that are titratable with strong acid. Mathematically, we define alkalinity as the negative of TOT_H when the components are the principal components of the solution at the CO_2 equivalence point. The acidity can be defined as the negative of alkalinity, and hence equal to TOT_H.

Let us consider a solution containing a fixed total dissolved concentration of $CaCO_3$. At the CO_2 equivalence point, H_2CO_3 (or $CO_2(aq)$) is the principal carbonate species, so we chose our components as H^+, H_2O, CO_2, and Ca^{2+}. Species HCO_3^- and CO_3^{2-} are made by combining these components as follows:

$$HCO_3^- = H_2O + CO_2 - H^+$$

$$CO_3^{2-} = H_2O + CO_2 - 2H^+$$

The proton mole balance equation is then:

$$TOT_H = [H^+] - [HCO_3^-] - 2[CO_3^{2-}] - [OH^-] \tag{4.20}$$

The alkalinity is then:

$$Alk = -\,TOT_H = -\,[H^+] + [HCO_3^-] + 2[CO_3^{2-}] + [OH^-] \tag{4.21}$$

This sum, $-\,[H^+] + [HCO_3^-] + 2[CO_3^{2-}] - [OH^-]$, is called the carbonate alkalinity. In this example, carbonate alkalinity and alkalinity are equal since there are no other ions in solution. To avoid confusion with carbonate alkalinity, alkalinity is sometimes called total alkalinity.

Now let's consider a somewhat more complex example, a solution that contains $H_3SiO_4^-$, $B(OH)_4^-$, and HS^-, and phosphoric acid (H_3PO_4 and dissociated species). This solution is similar to seawater. The corresponding components, the species actually present at the CO_2 equivalence point, are H_4SiO_4, $B(OH)_3$, H_2S, and $H_2PO_4^-$. Our expression for alkalinity is then (assuming negligible concentrations of S^{2-} and PO_4^{3-}):

$$Alk = -\,[H^+] + [HCO_3^-] + 2[CO_3^{2-}] + [OH^-] + [B(OH)_4^-]$$

$$+\,[H_3SiO_4^-] + [HS^-] + [H_2PO_4^-] + 2[HPO_4^{2-}] \tag{4.22}$$

An analytical definition of alkalinity is that it is the quantity of acid that must be added to the solution to bring the pH to the CO_2 equivalence point.

We can also express alkalinity in terms of conservative and non-conservative ions. The charge balance equation, equation 4.9, could be written as:

$$\Sigma \text{ cations (in equivalents)} - \Sigma \text{ anions (in equivalents)} = 0 \tag{4.23}$$

This can the be expanded to:

$$\Sigma \text{ conserv.cat} - \Sigma \text{ conserv.an} + \Sigma \text{ non-conserv.cat} - \Sigma \text{ non-conserv.an} = 0$$

all in units of equivalents)*. Rearranging, we have:

$$\Sigma \text{ conserv.cat} - \Sigma \text{ conserv.an} = -\,\Sigma \text{ non-conserv.cat} + \Sigma \text{ non-conserv.an} \tag{4.24}$$

The right hand side of equation 4.20 is equal to the alkalinity. Hence we may write:

$$Alk = \Sigma \text{ conserv.cat} - \Sigma \text{ conserv.an} = -\,\Sigma \text{ non-conserv.cat} + \Sigma \text{ non-conserv.an} \tag{4.25}$$

This equation emphasizes an important point. The difference of the sum of conservative anions and cations is clearly a conservative property, i.e., they cannot be changed except by the addition or removal of components. Since alkalinity is equal to this difference, alkalinity is also a conservative quantity (i.e., independent of pH, pressure and temperature). Thus total alkalinity is conservative, though concentrations of individual species are not.

Problem: Calculate the alkalinity of spring water from Thonon, France, whose analysis is given in table.

Anions	mM	Cations	mM
HCO_3^-	5.436	Ca^{2+}	2.475
SO_4^{2-}	0.146	Mg^{2+}	0.663
NO_3^-	0.226	K^+	0.036
Cl^-	0.231	Na^+	0.223

Solution: We can use equation 4.22 to calculate alkalinity. All the ions listed here are conservative with the exception of HCO_3^-. To calculate alkalinity, we first need to convert the molar concentrations to equivalents; we do so by multiplying the concentration of each species by its charge. We find the sum of conservative anion concentrations to be 0.749 meq (milliequivalents), and that of the conservative cation concentrations to be 6.535 meq. The alkalinity is the difference, 5.786 meq.

4.2.5.1 *Alkalinity Determination and Titration Curves*

If the concentrations of all major conservative ions in a solution are known, the alkalinity can be simply calculated from equation 4.23. It is often useful, however, to determine this independently. This is done, as the definition of alkalinity suggests, through titration. Titration is the process of progressively adding a strong acid or base to a solution until a specified pH, known as an endpoint, is reached. In the case of the determination of alkalinity, this end point is the CO_2 equivalence point.

Consider a solution containing a certain concentration of sodium bicarbonate (Na_2CO_3). Because the carbonate ion can act as a proton acceptor, $NaCO_3^-$ is a base. We can determine both the alkalinity and the total carbonate concentration of this solution by titrating with a strong acid, such as HCl.

For simple solution, we make several simplifying assumptions. First, we assume ideal behavior. Second,

---

* One equivalent of a species is defined as the number of moles multiplied by the charge of the species. Thus one equivalent of CO_3^{2-} is equal to 0.5 moles of CO_3^{2-}, but one equivalent of Cl^- is equal to 1 mole of Cl^-. For an acid or base, an equivalent is the number moles of the substance divided by the number of hydrogen or hydroxide ions that can be potentially produced by dissociation of the substance. Thus there are 2 equivalents per mole of H_2CO_3, but 1 equivalent per mole of Na(OH).

we assume the system is closed, so that all components are conserved, except for $[H^+]$ and $[Cl^-]$, which we progressively add. Third, we assume that the volume of our Na_2CO_3 solution is sufficiently large and our HCl sufficiently concentrated that there is no significant dilution of the original solution. Finally, we assume both Na_2CO_3 and HCl dissociate completely.

The charge balance equation during the titration is:

$$[Na^+] + [H^+] = [Cl^-] + [HCO_3^-] + 2[CO_3^{2-}] + [OH^-] \qquad 4.26$$

Since the Cl^- concentration is conservative, it will be equal to the total amount of HCl added. Into Equation 4.26, we can substitute the following:

$$\left[HCO_3^-\right] = \frac{K_1\left[H_2CO_3\right]}{\left[H^+\right]} \qquad 4.27a$$

$$\left[CO_3^{2-}\right] = \frac{K_2K_1\left[H_2CO_3\right]}{\left[H^+\right]^2} \qquad 4.27b$$

$$\left[OH^-\right] = \frac{K_W}{\left[H^+\right]} \qquad 4.27c$$

Doing so and rearranging yields:

$$\left[Cl^-\right] = \left[Na^+\right] + \left[H^+\right] - \frac{K_1\left[H_2CO_3\right]}{\left[H^+\right]} - \frac{K_2K_1\left[H_2CO_3\right]}{\left[H^+\right]^2} - \frac{K_W}{\left[H^+\right]} \qquad 4.28$$

We may also write a conservation equation for carbonate species, which is the same as last equation in first Chapter 4 problem. Substituting Equations 4.27a and 4.27b into

$$\Sigma CO_3 = [CO_3^{2-}] + [HCO_3^-] + [H_2CO_3]$$

and rearranging, we have:

$$\left[H_2CO_3\right] = \frac{\sum CO_2}{1 + \frac{K_1}{\left[H^+\right]} + \frac{K_1K_2}{\left[H^+\right]^2}} \qquad 4.29$$

Substituting this expression into 4.28, we obtain:

$$\left[Cl^-\right] = \left[Na^+\right] + \left[H^+\right] - \frac{\sum CO_2}{\left[H^+\right] + K_1 + \frac{K_1K_2}{\left[H^+\right]}}\left\{K_1 - \frac{K_1K_2}{\left[H^+\right]}\right\} - \frac{K_W}{\left[H^+\right]} \qquad 4.30$$

From stoichiometry, we also know that $\Sigma CO_2 = [Na^+]$. From this equation we can construct a plot showing how many moles of HCl we must add to achieve a certain pH. We can also use Equation 4.27 and similar ones expressing the bicarbonate and carbonate ions as functions of pH to plot the change in the carbonate speciation during the titration. Figure 4.2 shows such a plot for a 0.005 M Na_2CO_3 solution. There are two regions where pH changes rapidly with small additions of HCl. These are the two end-points of the titration. Comparing the titration curve with the speciation curves, we see that the two end-points correspond to the CO_2 and bicarbonate equivalence points.

An analytical definition of alkalinity is its acid neutralizing capacity when the end-point of the titration is the CO_2 equivalence point (Morel and Hering, 1993). We had previously defined alkalinity as the negative of TOT_H when the principal components are those at the CO_2 equivalence point. Now let's show that these definitions are equivalent.

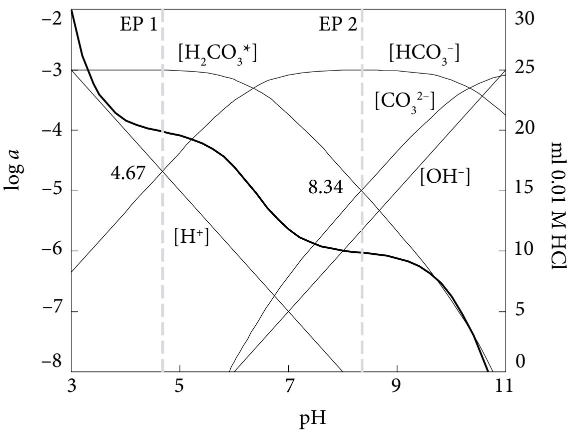

Figure 4.2. Titration curve (bold line) for 100 militer 0.001 M Na_2CO_3 solution titrated with 0.01 M HCl. Right axis shows the number of ml of HCl to be added to obtain a given pH. Also shown are the concentrations of carbonate species, H^+, and OH^- (thin lines, left axis gives scale).

Our TOT_H expression, written in terms of components at the CO_2 equivalence point, is identical to 4.20:

$$TOT_H = [H^+] - [HCO_3^-] - 2\,[CO_3^{2-}] - [OH^-] \qquad 4.20$$

and the charge balance equation (before any HCl is added) is:

$$[Na^+] + [H^+] = [HCO_3^-] + 2\,[CO_3^{2-}] + [OH^-] \qquad 4.9$$

Combining the two we have: $TOT_H = -\,[Na^+]$

Since the alkalinity is the negative of TOT_H, it follows that (before the addition of HCl):

$$Alk = [Na^+] \qquad 4.31$$

We obtain exactly the same result from Equation 4.25. It is easy to show that after titrating to the CO_2 equivalence point, the alkalinity is 0. The change in alkalinity is thus equal to the number of equivalents, or moles, of H^+ we have added to the solution.

Since at the end point, $[H^+] = [HCO_3^-]$ and the concentrations of CO_3^{2-} and OH^- are negligible, our charge balance equation, 4.26, reduces to:

$$[Na^+] = [Cl^-]$$

Comparing this with 4.29, we see that the alkalinity is equal to the amount of HCl added. In the example in Figure 4.2, the equivalence point occurs after the addition of 10 ml of 1M HCl, or a total of 0.01 moles of Cl^-. Notice that since at the end points, small additions of acid result in large changes in pH, we do not have to determine pH particularly accurately during the titration for an accurate determination of alkalinity. So the alkalinity is 0.01 equivalents. This is exactly the answer we obtain from 4.29 for 1 liter of 0.005 M Na_2CO_3 since there are 2 moles of Na^+ for each mole of Na_2CO_3.

By assuming that the concentration of H^+ contributes negligibly to charge balance, it is also easily shown (Example 4.2) that at the bicarbonate equivalence point:

$$\Sigma CO_2 = [Cl^-] + [OH^-] \tag{4.32}$$

Thus total carbonate is obtained by titrating to the bicarbonate equivalence point (knowing the pH of the end-point allows us to determine the ΣCO_2 exactly; however neglecting the $[OH^-]$ term in 4.30 results in only a 1% error in the example shown. In Figure 4.2, this occurs after the addition of 5 ml 1M HCl.

4.2.6 Buffer Intensity

The buffer intensity of a solution is defined as the inverse of change in pH per amount of strong base (or acid) added:

$$\beta = \frac{dc_B}{dpH} = -\frac{dc_A}{dpH} \tag{4.33}$$

where c_B and c_A are the concentrations, in equivalents, of strong base or acid respectively. The greater the buffer capacity of a solution, the less change in its pH as an acid or base is added. The buffer capacity of a solution can be calculated by differentiation of the equation relating base (or acid) concentration to pH, as is illustrated in following *Problem*.

In nature, a pH buffer acts to control pH within a narrow range as H^+ ions are added or removed from solution by other reactions. To understand how this works, imagine a solution containing carbonic acid, CO_3^{2-}, HCO_3^-, and H^+ ions in equilibrium concentrations. Now imagine that additional H^+ ions are added (for example, by addition of rain water containing HNO_3). In order for the right hand side of equation 4.19 to remain equal to K_1 despite an increase in the activity of H^+ (which it must at constant temperature and pressure), the bicarbonate activity must decrease and the carbonic acid activity increase. It is apparent then that reaction 4.11 must be driven to the left, taking free hydrogen ions from solution, hence driving the pH back toward its original value. Similarly, reaction 4.12, the dissociation of bicarbonate, will also be driven to the left, increasing the bicarbonate concentration and decreasing the hydrogen and carbonate ion concentrations.

The buffer capacity of the carbonate system depends strongly on pH and also on the concentration of the carbonate species and the concentration of other ions in solution. In pure water containing no other ions and only carbonate in amounts in equilibrium with the atmosphere, the buffering capacity is negligible near neutral pH, as is shown in Figure 4.4. Natural solutions, however, can have substantial buffering capacity. Figure 4.3 illustrates three examples of natural pH buffers. "Hard water" is an example of water with a substantial buffering capacity due to the presence of dissolved carbonates. How adversely lakes and streams are impacted by "acid rain" depends on their buffering intensity.

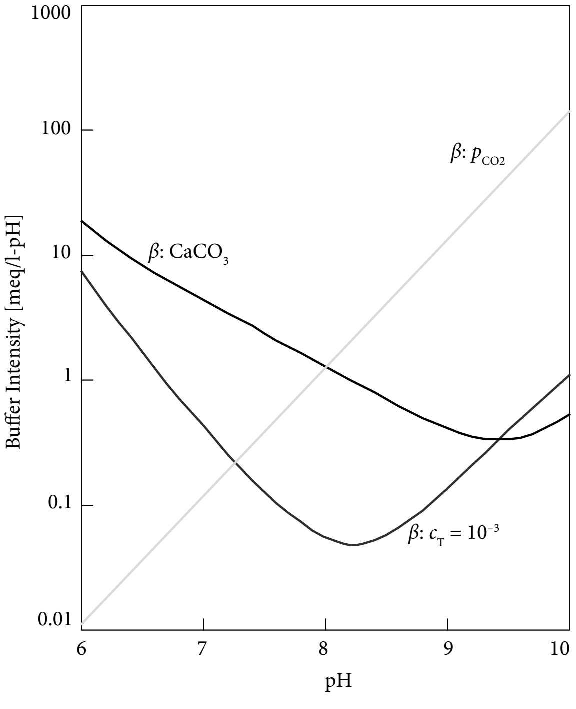

Figure 4.3. Buffer intensity as a function of pH for several ideal natural systems: β_{cT} fixed total dissolved CO_2, β_{pCO2} water in equilibrium with atmospheric CO_2, $\beta_{CaCO3(s)}$ water in equilibrium with calcite.

Problem: How will pH change for given addition of a strong base such as NaOH for a solution of pure water in equilibrium with atmospheric CO_2? Calculate the buffer intensity of this solution as a function of pH. Assume that NaOH completely dissociates and ideal behavior.

Solution: We want to begin with the charge balance equation in this case because it relates the two quantities of interest in this case, $[Na^+]$ and $[H^+]$. The charge balance equation is the same as in first Example:

$$[Na^+] + [H^+] = [OH^-] + [HCO_3^-] + 2[CO_3^{2-}]$$

Since Na^+ is a conservative ion, its concentration will depend only on the amount of NaOH added, so that $c_B = [Na^+]$. Substituting this into equation 4.9 and rearranging, we have:

$$c_B = [OH^-] + [HCO_3^-] + 2\,[CO_3^{2-}] - [H^+]$$

We can now use the equilibrium constant relations to substitute for the first three terms of the right hand side and obtain:

$$c_B = \frac{K_W + K_1 K_{sp} p_{CO_2}}{\left[H^+\right]} + 2\frac{K_2 K_1 K_{sp} p_{CO_2}}{\left[H^+\right]^2} - \left[H^+\right]$$

Using the relation pH = – log $[H^+]$ to replace $[H^+]$ in this equation with pH, we have:

$$c_B = \frac{K_W + K_1 K_{sp} p_{CO_2}}{10^{-pH}} + 2\frac{K_2 K_1 K_{sp} p_{CO_2}}{10^{-2pH}} - 10^{-pH}$$

Now differentiating with respect to pH, we obtain:

$$\frac{d c_B}{d pH} = \beta = \log\left\{\left(K_W + K_1 K_{sp} p_{CO_2}\right)\times 10^{pH} + \right.$$
$$\left. + \; 4K_2 K_1 K_{sp} p_{CO_2} 10^{2pH} + 10^{-pH}\right\}$$

Figure 4.4 shows a plot of this equation using the values in Table 4.1. Buffer intensity is negligible in neutral to slightly acidic conditions, but increases rapidly with pH.

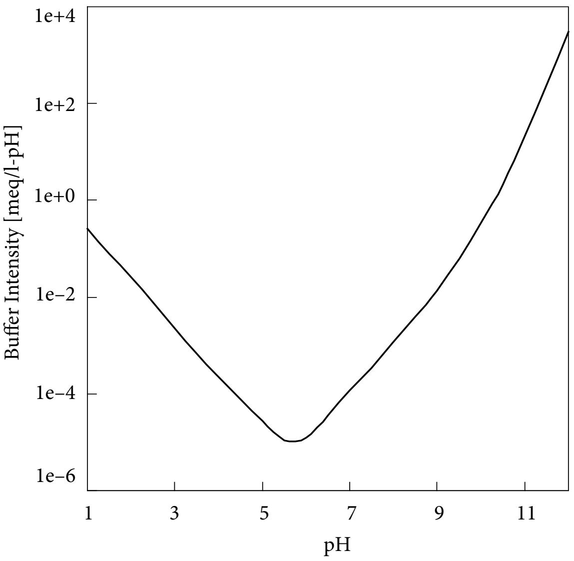

Figure 4.4. Buffer capacity of a carbonate solution in equilibrium with atmospheric CO_2.

4.3 Dissolution and Precipitation Reactions

4.3.1 Calcium Carbonate in Ground and Surface Waters

Calcium carbonate is a common component of sedimentary rocks and is found present in weathered igneous and metamorphic rocks. It is also a common constituent of many soils. Water passing through such soils and rocks will precipitate or dissolve calcite until equilibrium is achieved. This process has a strong influence on carbonate concentrations, hardness, and pH as well as dissolved calcium ion concentrations.

The solubility product of calcite is:

$$K_{sp\text{-}Cal} = a_{Ca^{2+}} a_{CO_3^{2-}} \qquad 4.34$$

This can be combined with Equations 4.13–15 to obtain the calcium concentration water in equilibrium with calcite as a function of p_{CO2}:

$$\left[Ca^{2+}\right] = p_{CO_2}\,\frac{K_1 K_{sp\text{-}Cal} K_{sp\text{-}CO_2}}{4K_2 \gamma_{Ca^{2+}} \gamma_{HCO_3^-}^2 \left[HCO_3^-\right]^2} \qquad 4.35$$

In a solution in equilibrium with calcite and a CO_2 gas phase and containing no other dissolved species, it is easy to modify equation 4.35 so that the calcium ion concentration is a function of p_{CO2} only. A glance at Figure 4.1 shows that we can neglect OH^-, H^+, and CO_3^{2-} if the final pH is less than about 9. The charge balance equation in this case reduces to:

$$2\,[Ca^{2+}] = [HCO_3^-] \qquad 4.36$$

Substituting this into 4.35, we obtain:

$$\left[\mathrm{Ca}^{2+}\right] = p_{\mathrm{CO}_2} \frac{K_1 K_{\text{sp-Cal}} K_{\text{sp-CO}_2}}{4K_2 \gamma_{\mathrm{Ca}^{2+}} \gamma^2_{\mathrm{HCO}_3^-} \left[\mathrm{Ca}^{2+}\right]^2} \tag{4.37}$$

or

$$\left[\mathrm{Ca}^{2+}\right] = \left\{ p_{\mathrm{CO}_2} \frac{K_1 K_{\text{sp-Cal}} K_{\text{sp-CO}_2}}{4K_2 \gamma_{\mathrm{Ca}^{2+}} \gamma^2_{\mathrm{HCO}_3^-}} \right\}^{1/3} \tag{4.38}$$

There are two interesting aspects to this equation. First, the calcium ion concentration, and therefore calcite solubility, increases with increasing p_{CO2}. This might seem counter-intuitive at first, as one might think that increasing p_{CO2} should produce an increase the carbonate ion concentration and therefore drive the reaction toward precipitation. However, increasing p_{CO2} decreases pH, which decreases CO_3^{2-} concentration, and therefore drives the reaction towards dissolution. Second, calcium ion concentration varies with the one-third power of p_{CO2} (Figure 4.5). Because of this nonlinearity, mixing of two solutions, both of which are saturated in Ca^{2+} with respect to calcite, can result in the mixture being undersaturated with respect to Ca^{2+}. For example, consider the mixing of stream and ground water. Stream water is in equilibrium with the atmosphere for which p_{CO2} is $10^{-3.5}$. On the other hand, p_{CO2} in soils is often as high as 10^{-2}. So mixing between calcite-saturated groundwater and calcite-saturated surface water would produce a solution that is undersaturated with calcite.

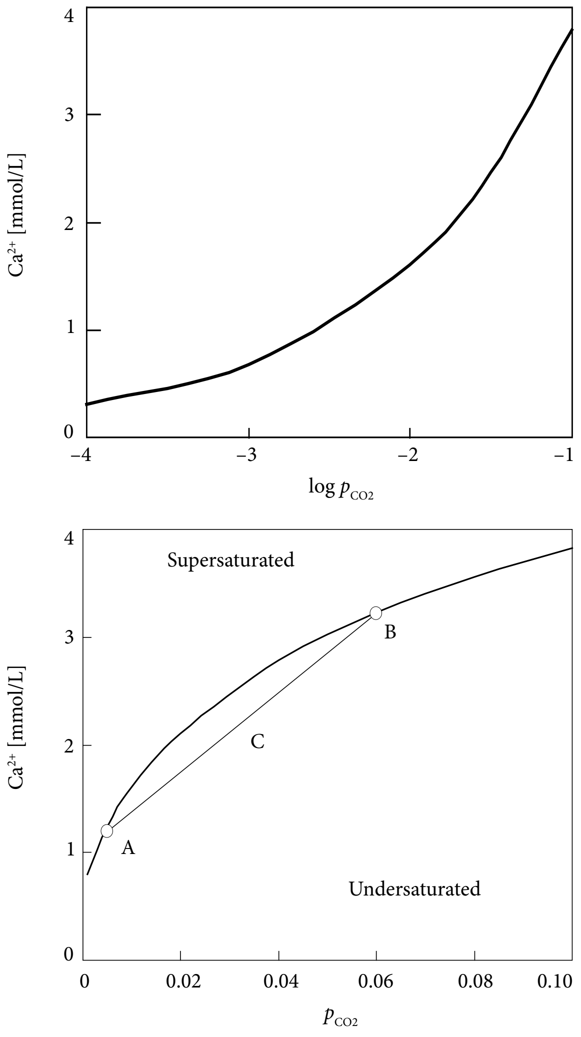

Figure 4.5. Concentration of calcium ion in equilibrium with calcite at 25°C and 1 atm as a function of p_{CO2}. After Drever (1988).

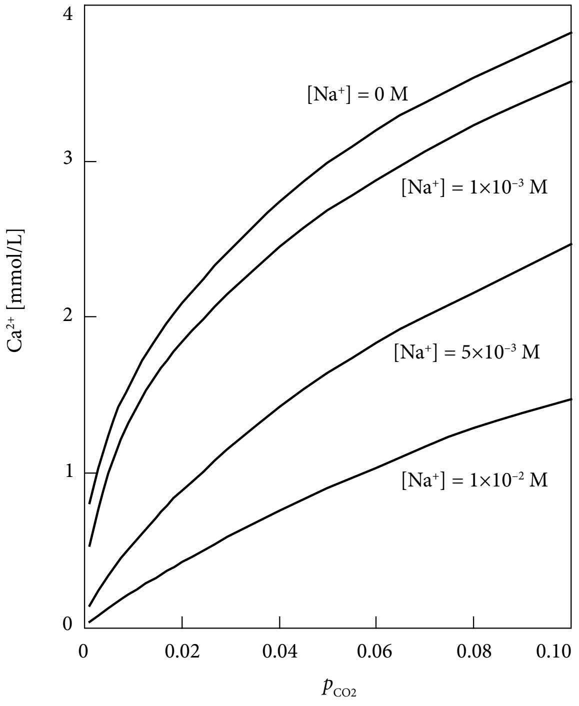

Figure 4.6. Concentration of calcium ion in a solution containing $\mathrm{Na_2CO_3}$ in equilibrium with calcite at 25 °C and 0,1 MPa as a function of p_{CO2} and sodium concentration. After Drever (1988).

Calcite solubility is also affected by the presence of other ions in solution. Figure 4.6 illustrates the effect of sodium ion concentration on calcite solubility.

Equation 4.38 describes calcite solubility for a system open to exchange with gaseous CO_2. For a p_{CO2} of $10^{-3.5}$ (i.e., the atmosphere), this equation yields a calcium concentration of 1.39 mM. Water in pores and fractures in rocks does not exchange with a gas phase. Second *Problem* in this chapter shows that under those circumstances, less calcite will dissolve; in the case of $p_{\mathrm{CO2}} = 10^{-2}$, calcite saturation is reached at only 0.33 mM, or about a fourth as much. The difference is illustrated in Figure 4.7, which is a plot of $[\mathrm{HCO}_3^-]$ vs. pH. Systems in equilibrium with constant p_{CO2} (open systems) evolve along straight lines on this plot and ultimately reach calcite saturation at higher pH and lower $[\mathrm{HCO}_3^-]$ (and $[\mathrm{Ca}^{2+}]$) than closed systems that initially equilibrate with the same p_{CO2}.

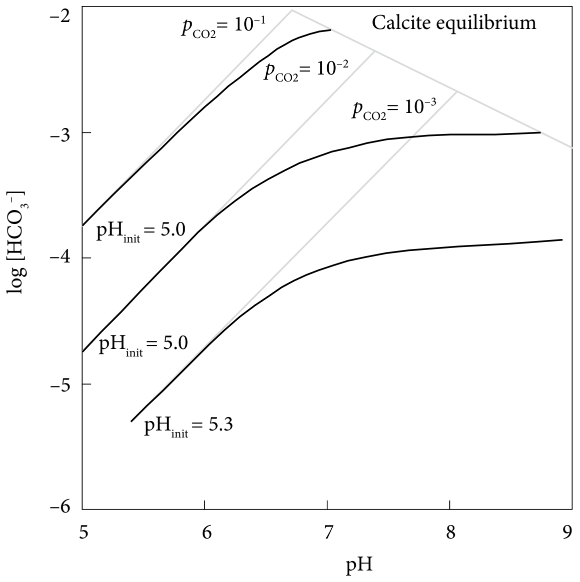

Figure 4.7. Comparison of the evolution of systems with constant p_{CO2} (open systems) with those closed to gas exchange. After Stumm and Morgan (1996) and Deines et al. (1974).

Problem: Using the water and stability constants given in the adjacent tables, calculate the activities of the major species in this water.

Analysis of Stream Water (mM):

Na$^+$	0.32	Cl$^-$	0.22
K$^+$	0. 06	SO$_4^{2-}$	0.12
Mg^{2+}	0.18	ΣCO$_2$	1.0
Ca^{2+}	0. 36	pH	8.0

Log of Stability Constants:

	OH$^-$	HCO$_3^-$	CO$_3^{2-}$	SO$_4^{2-}$	Cl$^-$
H$^+$	14	6.35	10.33	1.99	–
Na$^+$	–	−0.25	1.27	1.06	–
K$^+$	–	–	–	0.96	–
Mg^{2+}	2.56	1.16	3.4	2.36	–
Ca^{2+}	1.15	1.26	3.2	2.31	–

Solution: The first two problems we need to address are the nature of the carbonate species and activity coefficients. At this pH, we can see from Figure 4.1 that bicarbonate will be the dominant carbonate species. Making the initial assumption that all carbonate is bicarbonate, we can calculate ionic strength and activity coefficients using the Debye-Hückel Law. These are shown in the table below. Having the activity coefficients, we calculate the approximate abundance of the carbonate ion by assuming all carbonate is bicarbonate:

$$\left[\mathrm{CO}_3^{2-}\right] = \frac{\gamma_{\mathrm{HCO}_3^-}\sum \mathrm{CO}_2}{\beta\, a_{\mathrm{H}^+}\,\gamma_{\mathrm{CO}_3^{2-}}}$$

where β is the stability constant for the complexation reaction:

$$\mathrm{CO}_3^{2-} + \mathrm{H}^+ \longleftrightarrow \mathrm{HCO}_3^-$$

The "corrected" bicarbonate ion is then calculated as:

$$[\mathrm{HCO}_3^-] = \Sigma\, \mathrm{CO}_2 - [\mathrm{CO}_3^{2-}]$$

The result confirms our initial first order assumption that all carbonate is present as bicarbonate. Using the concentrations and stability constants given as well as the activity coefficients we calculated, we can them make a first pass at calculating the concentrations of the complexes. For example, $\mathrm{MgCO_3}$ is calculated as

$$a_{\mathrm{MgCO}_3} = \beta_{\mathrm{MgCO}_3}\, a_{\mathrm{Mg}^{2+}}\, a_{\mathrm{CO}_3^{2-}}$$

The results of this first iteration are shown in a matrix. Chlorine does not complex with any of the major ions to any significant degree, so we can neglect it in our calculations. We then correct the free ion activities by subtracting the activities of the complexes they form. Thus for example, the corrected free ion activity of Mg^{2+} is calculated as:

$$a^{\mathrm{corr}}_{\mathrm{Mg}^{2+}} = a^{\mathrm{init}}_{\mathrm{Mg}^{2+}} - a_{\mathrm{MgOH}^+} - a_{\mathrm{MgHCO}_3^+} - a_{\mathrm{MgCO}_3} - a_{\mathrm{MgSO}_4}$$

We then repeat the calculation of the activities of the complexes using these corrected free ion activities. A second matrix shows the results of this second iteration. In fresh waters such as this one, most of the metals are present as free ions, the alkaline earths being 5% complexed by sulfate and carbonate.

Ion Activities: Iteration 1

	free ion	OH$^-$	HCO$_3^-$	CO$_3^{2-}$	SO$_4^{2-}$
free ion		1×10−06	9.17×10−04	6.79×10−07	1.62×10−04
H$^+$	1×10−08	–	2.12×10−05	9.46×10−04	1.75×10−10
Na$^+$	3.03×10−04	–	1.62×10−07	2.51×10−08	6.27×10−07
K$^+$	5.69×10−05	–	–	–	9.33×10−08
Mg^{2+}	1.39×10−04	5.09×10−08	2.03×10−06	1.65×10−06	6.10×10−06
Ca^{2+}	2.77×10−04	4.29×10−09	5.08×10−06	2.07×10−06	1.08×10−05

Ion Activities: Iteration 2

	free ion	OH$^-$	HCO$_3^-$	CO$_3^{2-}$	SO$_4^{2-}$
free ion		1×10−06	9.12×10−0	41.1×10−06	1.65×10−04
H$^+$	1×10−08	–	2.06×10−05	9.12×10−04	1.58×10−10
Na$^+$	3.03×10−04	–	1.57×10−07	2.35×10−08	5.64×10−07
K$^+$	5.69×10−05	–	–	–	8.40×10−08
Mg^{2+}	1.40×10−04	5.03×10−08	1.84×10−06	1.45×10−06	5.14×10−06
Ca^{2+}	2.80×10−04	3.92×10−09	4.64×10−06	1.83×10−06	9.16×10−06

Problem: Suppose ground water initially equilibrates with a p_{CO2} of 10^{-2} and thereafter is closed to gas exchange, so that there is a fixed $\Sigma\ CO_2^{initial}$. The water then equilibrates with calcite until saturation is reached. What will be the final concentration of calcium in the water? Assume ideal behavior and an initial calcium concentration of 0.

Solution: Since the system is closed, a conservation equation is a good place to start. We can write the following conservation equation for total carbonate:

$$\Sigma\ CO_2 = \Sigma\ CO_2^{initial} + \Sigma\ CO_2^{from\ calcite}$$

Since dissolution of one mole of calcite adds one mole of Σ CO2 for each mole of Ca^{2+}, this equation may be rewritten as:

$$\Sigma\ CO_2 = \Sigma\ CO_2^{initial} + [Ca^{2+}]$$

Neglecting the contribution of the carbonate ion to total carbonate, this equation becomes:

$$[H_2CO_3] + [HCO_3^-] = ([H_2CO_3]^{initial}) + [Ca^{2+}]$$

where $([H_2CO_3]^{initial})$ denotes that amount of H_2CO_3 calculated from Equation E 4.1.1 for equilibrium with CO_2 gas; in this case a partial pressure of 10^{-2}. This can be rearranged to obtain:

$$([H_2CO_3]^{initial}) = [H_2CO_3] + [HCO_3^-] - [Ca^{2+}]$$

Further constraints are provided by the three carbonate equilibrium product expressions (E 4.1.1–4.1.3) as well as the solubility product for calcite (4.34), and the charge balance equation. We assume a final pH less than 9 and no other ions present, so the charge balance equation reduces to equation 4.36. From equation 4.13 and the value of K_{CO2} in Table 4.1, $[H_2CO_3]^{initial} = 10^{-2} \times 10^{-1.47}$ M. Dividing equation 4.14 by 4.15 yields:

$$\frac{K_1}{K_2} = \frac{\left[HCO_3^-\right]^2}{\left[H_2CO_3\right]\left[CO_3^{2-}\right]}$$

Then substituting Equations 4.34 and 4.36 gives:

$$\frac{K_1}{K_2} = \frac{4\left[Ca^{2+}\right]^3}{K_{sp\text{-}Cal}\left\{\left[H_2CO_3\right]_{init} - \left[Ca^{2+}\right]\right\}}$$

Into this equation we substitute $p_{CO2}\, K_{CO2} = [H_2CO_3]$ and rearrange to obtain:

$$\left[Ca^{2+}\right]^3 + \frac{K_1 K_{Cal}}{4K_2}\left[Ca^{2+}\right] - \frac{K_1 K_{Cal} K_{CO_2}}{4K_2}\, p_{CO_2^{init}} = 0$$

This is a cubic that is readily solved for $[Ca^{2+}]$. For an initial p_{CO2} of 10^{-2}, we calculate a calcium concentration of 0.334 mM

4.3.2 Solubility of Mg

There are a number of compounds that can precipitate from Mg-bearing aqueous solutions, including brucite ($Mg(OH)_2$), magnesite ($MgCO_3$), dolomite ($CaMg(CO_3)_2$), as well as hydrated carbonates such as hydromagnesite ($MgCO_3(OH)_2 \times 3H_2O$). The stability of these compounds may be described by the following reactions:

$$Mg(OH)_2 \longleftrightarrow Mg^{2+} + 2OH^- \qquad K_{bru} = 10^{-11.6} \qquad 4.39$$

$$MgCO_3 \longleftrightarrow Mg^{2+} + CO_3^{2-} \qquad K_{mag} = 10^{-7.5} \qquad 4.40$$

$$CaMg(CO_3)_2 \longleftrightarrow Mg^{2+} + Ca^{2+} + 2CO_3^{2-} \qquad K_{dol} = 10^{-17\,\dagger} \qquad 4.41$$

†The solubility of dolomite is poorly known; values for this equilibrium constant vary between $10^{-16.5}$ and 10^{-20}.

We can use these reactions and their equilibrium constants, together with the reactions for the carbonate system (Equations 4.10–4.12) to construct predominance diagrams for Mg-bearing solutions in equilibrium with these phases. For example, for reaction 4.39 we may derive the following relationship (assuming ideal solution):

$$\log\frac{\left[Mg(OH)_2\right]}{\left[Mg^{2+}\right]} = \qquad 4.42$$

$$= pK_{Bru} + 2pK_W + 2pH = -16.4 + 2pH$$

where we use the notation pK = – log K. For reaction 4.61, we can derive the following:

$$\log\frac{\left[MgCO_3\right]}{\left[Mg^{2+}\right]} = \qquad 4.43$$

$$= pK_{Mag} + \log\sum CO_2 + \frac{1}{\frac{\left[H^+\right]^2}{K_1K_2} + \frac{\left[H^+\right]}{K_2} + 1}$$

Assuming the solid is a pure phase, the term on the left of each equation is then just – log $[Mg^{2+}]$. We can use these equations to construct stability, or predominance diagrams. For example, on a plot of log $[Mg^{2+}]$ vs. pH, the predominance boundary between Mg^{2+}_{aq} and brucite plots as a line with a slope of –2 and an intercept of +16.4. Figure 4.8 shows two predominance diagrams derived from these equations. Brucite is the stable phase at high pH and low p_{CO2}.

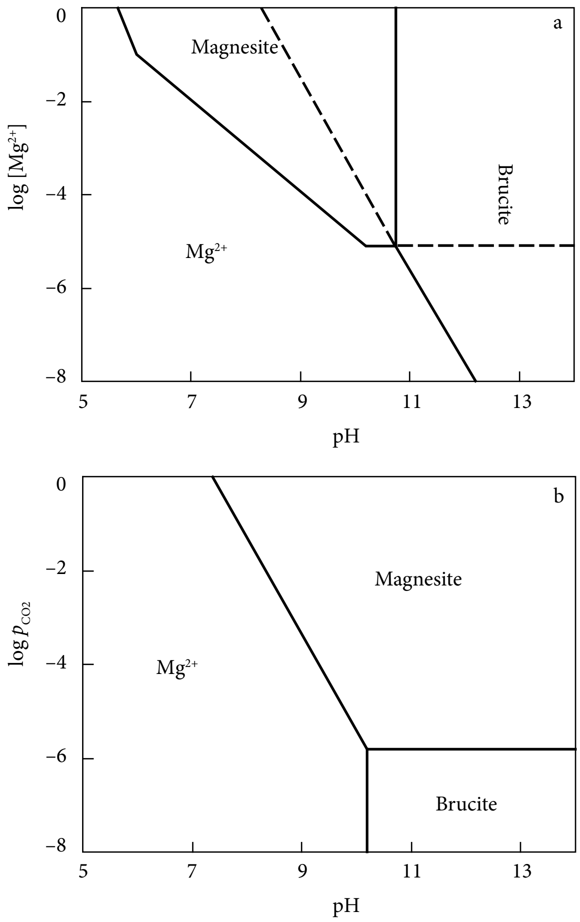

Figure 4.8. Predominance diagrams for Mg-bearing phases in equilibrium with aqueous solution. Total CO_2 is fixed at $10^{-2.5}$ M in 4.14a. The concentration of Mg^{2+} is fixed at 10^{-4} M in 4.14b. After Stumm and Morgan (1996).

Virtually all natural solutions will contain dissolved calcium as well as magnesium. This being the case, we must also consider the stability of dolomite. We can construct similar predominance diagrams for these systems but we must add an additional variable, namely the Ca^{2+} concentration. To describe the relative stability of dolomite and calcite, it is more convenient to express the solubility of dolomite as:

$$CaMg(CO_3)_2 + Ca^{2+} \longleftrightarrow Mg^{2+} + 2\ CaCO_3 \qquad 4.44$$

because the reaction contains calcite as well as dolomite. Since this reaction can be constructed by subtracting two times the calcite dissolution (Equation 4.34) from the dolomite dissolution (4.39), the equilibrium constant for this reaction can be calculated from:

$$K = \frac{K_{Dol}}{K^2_{Cal}} \qquad 4.45$$

Figure 4.9 illustrates the stability of magnesite, dolomite, brucite and calcite as a function of p_{CO2} and the Ca^{2+} / Mg^{2+} concentration ratio. Whether any of these phases are stable relative to a Mg^{2+}-bearing solution depends on the Mg^{2+} concentration, which is not specified in the graph.

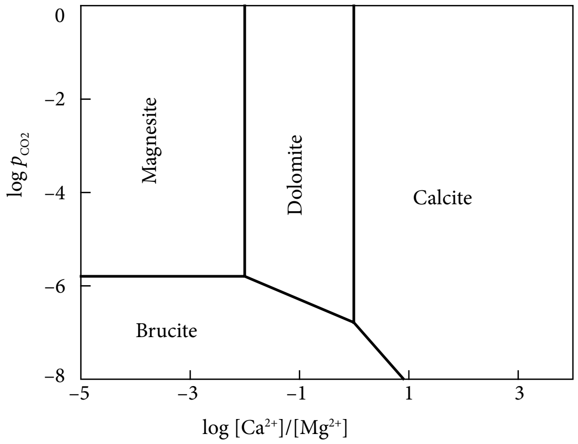

Figure 4.9. Stability of magnesite, dolomite, calcite, and brucite in equilibrium with a Mg- and Ca-bearing aqueous solution.

4.4 Regulation of Natural Waters pH by Carbonate System

The most important sources of acidity in the natural environment are: (1) Fossil-fuel combustion: Reduced sulfur contained in coal and oil is oxidized during burning to SO_2 gas which is released to the atmosphere. (2) Smelting of metal ores: Sulfide sulfur is again oxidized during ore roasting to SO_2. As a result SO_2 is dissolved in precipitation and oxidized to sulfuric acid which is deposited during rainfall. (3) Gasoline and diesel fuel combustion at temperatures when air nitrogen is oxidized to the mixture of nitrogen oxides usually denoted as NO_X. Their further oxidation in atmosphere and dissolution in rain produce nitric acid and acid rain. (4) Acid mine drainage: The waters draining from coal and ore mines are often acid because of pyrite oxidation. As will be presented in Chapter 9 the stoichiometry of this reaction can be written as

$$FeS_2 + 3.5\ O_2 + H_2O \rightarrow Fe^{2+} + 2\ SO_4^{2-} + 2\ H^+ \qquad 4.50$$

with production of acidity (presented reaction scheme does not express mechanism of this reaction). (5) Hydrolysis of Al^{3+} and Fe^{3+} released during rock weathering processes can produce quite large amount of H^+ ions according to reactions

$$Al^{3+} + H_2O \rightarrow Al(OH)_3(solid) + 3\ H^+ \qquad 4.51$$

$$Fe^{3+} + H_2O \rightarrow Fe(OH)_3(solid) + 3\ H^+ \qquad 4.52$$

(6) Decomposition of organic matter: This process produces organic acids, particularly humic/fulvic acids.

Serious environmental effects have been attributed to the acid production and acid deposition. Among others the most important damages are degradation and loss of soil (prevention of clay minerals formation), injury and death to trees, the disappearance of fish from dilute, soft-water lakes; deterioration of building stones and monuments. Probably the most serious consequence of acid rain and deposition is increased dissolution of carbonate minerals, the main component of limestone and the very important component of soil, sediment and bottom sediment of rivers, lakes and seas.

The carbonate system acts as the main regulation mechanism of natural water pH. When atmospheric carbon dioxide dissolves in rain, weak carbonic acid is formed according to equation

$$CO_2 + H_2O \longleftrightarrow H_2CO_3 \qquad 4.10$$

which dissociates and bicarbonate ion is formed.

$$H_2CO_3 \longleftrightarrow H^+ + HCO_3^- \qquad 4.11$$

The rain water in equilibrium atmospheric CO_2 contains about 1×10^{-5} M dissolved carbon dioxide and is always weakly acidic with pH value around 5.6. We can find this value as a point of intersection of $[H^+]$ and $[HCO_3^-]$ concentration lines in Figure 4.10. Dissociation of second proton from carbonic acid is negligible and according to the Equation 4.11 concentrations of protons and bicarbonate ions have to be equal.

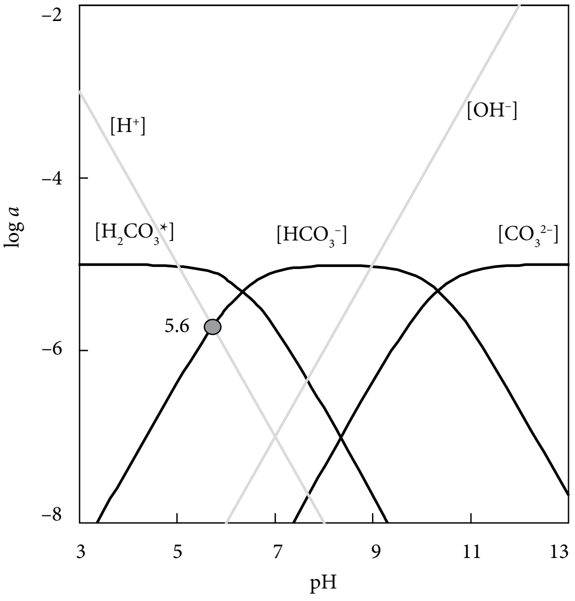

Figure 4.10 Activities of carbonate species in pure water in equilibrium with atmospheric carbon dioxide ($p_{CO2} = 10^{-3.5}$, $\Sigma\ CO_2(aq) \approx 10^{-5}$ M).Equilibrium pH is characterized by intersection of $[H^+]$ and $[HCO_3^-]$.

pH of natural water isolated from atmosphere and in contact with solid calcite can be estimated from the same diagram but for different concentration of dissolved carbonate species. Solubility product of calcite is

$$CaCO_3(Cal) \longleftrightarrow Ca^{2+} + CO_3^{2-} \qquad K_{sp\text{-}Cal} = 10^{-8.48} \qquad 4.53$$

According to the Equation 4.53 (neglecting further interactions of carbonate ion) the concentrations of Ca^{2+} and carbonate anion have to be equal and thus $[Ca^{2+}] = [CO_3^{2-}] = c_T$

$$K_{sp\text{-}Cal} = [Ca^{2+}]\ [CO_3^{2-}] = c_T^2$$

so

$$c_T = \sqrt{K_{sp\text{-}Cal}}$$

This system closed to the atmosphere (there are no additional strong acids or strong bases, $c_B - c_A = 0$) is characterized by intersection of $[OH^-]$ and $[Ca^{2+}] = c_T$. (Fig. 4.11, almost all of dissolved carbonate species is in the form of bicarbonate ion). Estimated pH value for water saturated with respect to calcite is 9.7 (exact calculation yields at 25 °C pH = 9.91).

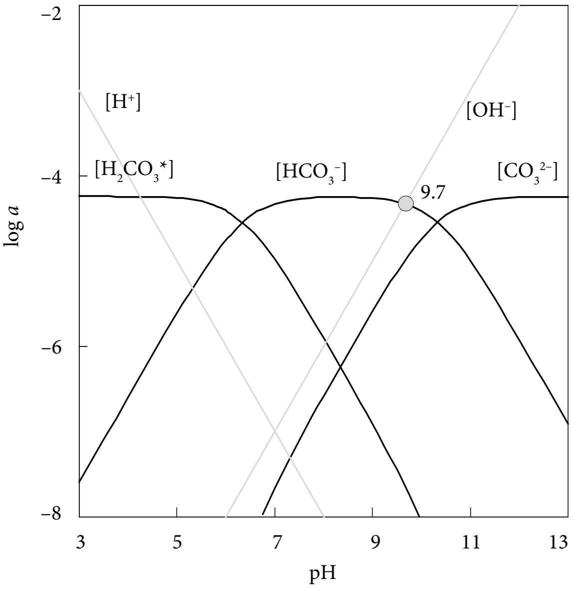

Figure 4.11 Activities of carbonate species in water in equilibrium with solid calcite. Equilibrium pH is characterized by intersection of $[OH^-]$ and $[Ca^{2+}] = c_T$. Almost all carbonate species are in the form of $[HCO_3^-]$ ($c_T \approx 6\times10^{-5}$ M).

Last system which we can usually find on surface is combination of the both previous – water in equilibrium with atmospheric carbon dioxide and solid carbonates, mostly calcite. The equilibrium composition is given by the electroneutrality condition $2\ [Ca^{2+}] \approx [HCO_3^-]$. This condition is indicated by a point on in-

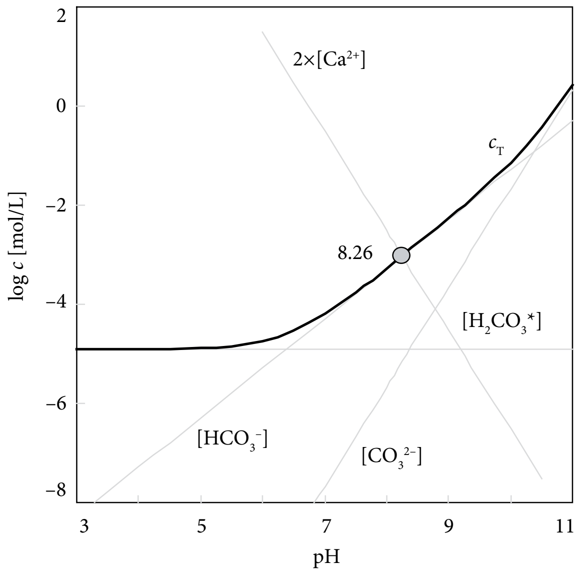

Figure 4.12 Activities of carbonate species in water in equilibrium with solid calcite and atmospheric carbon dioxide ($p_{CO2} = 10^{-3.5}$). Equilibrium pH is given by intersection of $2\times[Ca^{2+}]$ and $[HCO_3^-]$ lines. Almost all carbonate species are in the form of $[HCO_3^-]$ ($c_T \approx 6\times10^{-5}$ M). Thick curved line indicates overall concentration of dissolved carbonate species.

tersection of $2\times[Ca^{2+}]$ and $[HCO_3^-]$ lines and is reached at pH about 8.26 (Figure 4.12). The calcium concentration is determined by calcite solubility product.

Comparing this result with that of simple water equilibrium with calcite, we see that the influence of atmospheric CO_2 has depressed the pH markedly and that of $[Ca^{2+}]$ have been raised to values representative of those in natural waters. We can conclude that normal pH values of natural waters are kept by carbonate system in the range from about 5.5 (rain water, fresh water in small creeks and mountains – low amount of total dissolved species including carbonates because of short interaction time) to values about 8.3 which is characteristic for soils, waters in rivers, lakes, seas and oceans with fully developed equilibrium between water, carbon dioxide in atmosphere and solid carbonates. Note that carbonate system keeps pH values in narrow range around neutral conditions (pH ≈ 7) which is very favorable for biota.

Now we can check what will happen when some acidity enters water environment with carbonate equilibrium in the region of neutral pH. According to the Figure 4.1 the most of the carbonate species in water is in the form of bicarbonate ions. In principle, bicarbonate ions can accept proton and form carbonic acid or release proton and form carbonate ion. When some acidity enters system the protons are consumed during carbonic acid formation and thus removed from water. The pH value almost does not change. The amount of carbonic acid which is above equilibrium concentration splits to water molecule and dissolved carbon dioxide which is then released to the atmosphere. For long term functioning of this mechanism it is critically important that water is in contact and in equilibrium with solid carbonates in soils and bottom sediments of rivers and lakes.

On the other hand when some strong bases are released to water e.g. during silicate weathering when strong bases like Ca^{2+} and Mg^{2+} are released parallel with weak acids like H_4SiO_4 giving the net alkali reaction. Bicarbonate ions release proton which will react with hydroxyl anion forming neutral water molecule. Carbonate ions interact with metals in solution and are precipitated and deposited as solid carbonates. Consumed bicarbonate ions are replenished by dissolution of atmospheric carbon dioxide and carbonic acid formation. For this mechanism it is critically important that water is in contact with atmosphere.

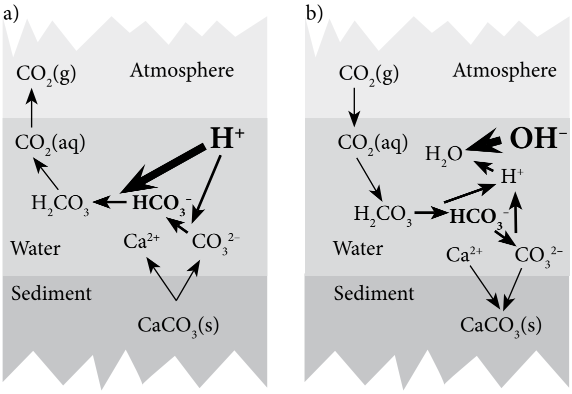

Figure 4.13 Regulation of pH in natural water by dissolved carbonate species. Addition of acidity or alkalinity is eliminated and pH value change of natural water is negligible. (a) Protons entering water system are consumed by bicarbonate ions and thus neutralized. (b) Hydroxyl ions entering water system are neutralized by protons released from bicarbonate ions.

These two mechanisms are responsible for very strong buffering action of carbonate species in natural waters. As we saw there is one important condition – in bottom sediments has to be solid carbonates present. They are normally formed during rock weathering (precipitation of solid carbonates keeps concentration of calcium and magnesium in the range of tens to hundreds milligrams per liter in fresh waters). When acid rains, acid deposition or other form of acidity enters natural waters the solid carbonates are dissolved and pH values are free to decrease. When pH decrease to values around 5, almost all carbonate species in solution are in the form of carbonic acid and no more protons can be removed by bicarbonate ions. The buffering action of carbonate species disappear and no more carbonates can be formed. At these conditions any small amount of acidity will cause large change in pH values.

There are some other not on the first sight visible consequences of carbonate system "degradation" by acid production and acid deposition. With environment acidification: (1) no heavy metal carbonates are formed (most of heavy metal carbonates are insoluble and are deposited in bottom sediments) and (2) the capacity of clay minerals and other surface active solids to catch heavy metals is decreased and originally sorbed heavy metals are again released to the water environment (metals sorbed on solid surfaces are gradually replaced by protons).

We can conclude that keeping carbonate system at "healthy" state i.e. in pH range between 5 and 9 is extremely important for maintaining stable pH water conditions in nature.

References

Deines, P., Langmuir, D., and Harmon, R.S., 1974: Stable carbon isotope ratios and the existence of a gas phase in the evolution of carbonate ground waters. *Geochim. Cosmochim. Acta*, 38, pp. 1147–1164.

Drever, J. I., 1997. *The Geochemistry of Natural Waters,* Prentice Hall, Englewood Cliffs, 437 p.

Garrels, R. M. and C. L. Christ. 1965. *Solutions, Minerals and Equilibria*. New York: Harper and Row.

Morel, F. M. M. and J. G. Hering. 1993. *Principles and Applications of Aquatic Chemistry*. New York: John Wiley and Sons.

Pankow, J. F. 1991. *Aquatic Chemistry* Concepts. Chelsea, MI: Lewis Publishers, 673 p.

Stumm, W. and J. J. Morgan. 1996. *Aquatic Chemistry,* New York: Wiley and Sons.

Chapter 5: Sampling of Water and Solids

5.1 Basic Considerations

A principal objective is to obtain a water sample with the same chemistry as those of water in its original environment (aquifer, surface water body etc.). When ground water is sampled in wells with long screen zone, then several redox zones may mix and irreversible chemical processes may occur. For example, when conditions close to water table are relatively oxic and dissolved oxygen is present, and conditions in deeper zone are reducing with dissolved iron, then there is mixing of ground water from both zones with resulting loss of both oxygen and iron in reaction like

$$Fe^{2+} + 0.25\ O_2(g) + 2.5\,H_2O = Fe(OH)_3(s) + 2H^+ \qquad 5.1$$

In that case, not only iron and oxygen are lost, but other metals like Zn and Pb may be lost too because they are adsorbed on precipitated ferric hydroxide.

However, even when no reactions occur, there still is reduction of concentration due to a conservative mixing. For example, when a plume of chloride considered as non-reactive tracer has thickness of about 4 m and thickness of screen zone is of about 10 m, then there will be lower concentration of chloride in water sample, which will not correspond to its concentration in aquifer. The only solution is the sampling with vertical resolution, using several piezometers with short screen zones open at different depths (Appelo and Postma, 1999). Piezometers are located in so called *piezometric nest.* Principal limitation is cost of such device, which is higher compared to a single well.

Another problem is related to de-gassing of CO_2. In many cases, partial pressure of CO_2 (P_{CO2}) dissolved in ground water is higher than atmospheric value of $10^{-3.5}$ atm. Thus, when a sample is equilibrated with atmosphere, the reaction

$$CaCO_3(s) + CO_2(g) + H_2O = Ca^{2+} + 2HCO_3 \qquad 5.2$$

goes to the left and calcite precipitates. Thus, a part of calcium and dissolved inorganic carbon (*DIC*) are lost. This process can be even accelerated as a consequence of increasing temperature of sample in the case of later measurement.

There is a controversy related to how many volumes of a well or piezometer should be evacuated prior to collection of sample(s). It is assumed that 3 volumes should be enough, but this requirement cannot be sometimes met in the case of large diameter domestic wells. Thus, it is recommended to pump water until parameters like pH and *EC* are stabilized and then start the sampling (Appelo and Postma, 1999). There also is requirement of low pumping rate (<1L/min) in the case of sampling of a contaminant plume because uncontaminated background water could dilute samples otherwise.

5.2 Field Parameters

Several parameters have to be measured in the field because their values based on later measurement in laboratory are almost meaningless.

Temperature: this parameter changes quickly and has an impact on other parameters such as pH and Eh. Furthermore, temperature is necessary for geochemical speciation calculation. In the ideal case, temperature should be measured directly in a well by a down-hole probe. If it is impossible, then measurement should be performed in a flow-through cell, with minimized contact with atmosphere (Fig. 5.1). Flow-through cell is a plexi-glass cylinder with slots for insertion of measurement electrodes, which is connected to a pumping device.

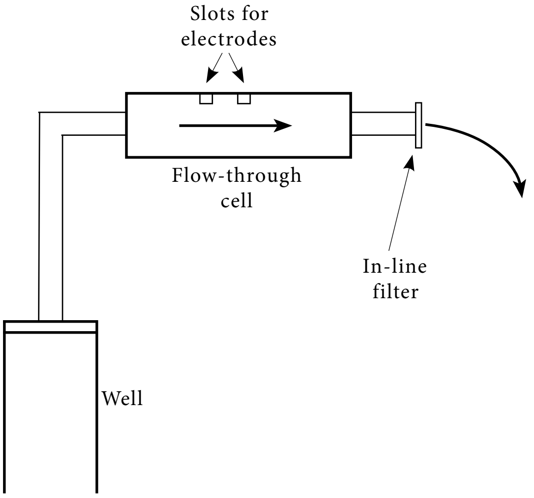

Figure 5.1 Flow though cell for measurement of temperature, pH, and Eh.

Hydrogen ion activity (pH): this is an essential parameter because most geochemical processes are pH-sensitive. The value of pH is generally determined by distribution of carbonate species in water and, thus, it is strongly affected by equilibration with atmosphere. There is de-gassing (Equation 5.2) and resulting pH is generally higher than its correct value. Thus, measurement without contact with atmosphere is required. The pH-meter has to be calibrated using standard buffers prior to measurement.

Redox potential(Eh): the Eh value is generally lower in ground water compared to surface conditions. Thus, the contact of a sample with atmosphere (log P_{O2} = –0.68 atm) causes changes in speciation such as oxidation of Fe(II) to Fe(III) (Equation 5.1). This means that any contact with atmosphere has to be avoided. Measurement is also performed in flow-through cell. The Eh value measured in field is measured with respect to Ag-AgCl or Hg-HgCl (kalomel) electrodes and the measured value has to be converted to a corresponding value for hydrogen electrode, E_{H2}:

$$E_{H2} = Eh_{field} + Eh_{correction} \qquad 5.3$$

where $Eh_{correction}$ is electrode and temperature dependent and is indicated by manufacturer for different measurement electrodes. An alternative method to obtain $Eh_{correction}$ value is based on measurement of Eh in both field sample and Zobell solution with known E_{H2} value (Kehew, 2000).

Alkalinity: it is a measure of acid-neutralizing capacity of a solution. It is generally based on carbonate species, but there can be a contribution of other species:

$$\text{Alkalinity} = HCO_3^- + 2CO_3^{2-} + H_3SiO_4^- + H_3BO_2^- \ldots \text{ etc.} \qquad 5.4$$

Especially significant can be contribution of dissolved organic matter with de-protonated carboxylic acid groups, R-COO$^-$, in the proximity of sanitary landfills. In that case, the value of alkalinity cannot be used to calculate distribution of carbonate species without corrections (Deutsch, 1997). In an ideal case, alkalinity is determined in the field by titration with acid like HCl and is reported in units like mg/L of $CaCO_3$ or mg/L of HCO_3. When field determination is impossible, then there should be collection of a special sample for later determination of alkalinity in laboratory. When a sub-sample is taken from a bigger sample later, there can be loss of alkalinity due to precipitation of calcite (Equation 5.2). Fritz (1994) concluded that most positive charge-balance errors (e.g., missing anions) were caused by errors in the measurement of alkalinity.

Dissolved oxygen (DO): this is qualitative parameter only because O_2/H_2O redox pair cannot be used for quantitative calculations. Detectable values indicate oxic environment where, for example, dissolved nitrate should be stable and ferrous iron should be unstable. Measurements are often performed by oxygen electrode, but there are more precise methods like Winkler titration.

Electrical conductivity (EC): this is semi-quantitative parameter, which roughly corresponds to total dissolved solids (*TDS*) concentration. Thus, it can be used for delimitation of inorganic contaminants plumes, salt water intrusions etc. It is measured by conductivity meter in units such as µS cm^{-1}. According to Appelo and Postma (1999), the *EC* divided by 100 gives a good estimate of the sum of anions or cations (in meq/L):

$$\Sigma \text{ anions} = \Sigma \text{ cations (meq/L)} = EC/100\ (\mu S\ cm^{-1}) \qquad 5.5$$

This relation holds up to *EC* values of about 2000 µS cm^{-1}.

5.3 Collection and Preservation of Samples

There is a controversy related to the filtration of samples. Generally, filtration is recommended in the case of samples for cation and metal analysis. The filter used is generally 0.45 μm, but filter 0.1 μm is more convenient in some cases because some colloids can pass through 0.45 μm filter. Filtering is also recommended for anion samples because organic matter and some bacteria which could participate in reactions after collection of sample like sulfate reduction are removed. Filter is generally located on the output pipe of flow-through cell (so called *on-line filter*). Samples for cation and metal analysis should be acidified by acid such as HCl to pH less than 2.0 to avoid precipitation of iron (Equation 5.1). Samples for anion analysis are unacidified, but filtration is recommended.

If we are interested in the presence of colloids, we take 2 samples: one sample filtered and acidified and second one unfiltered and acidified. In the case of the presence of colloids concentrations in second sample should be higher.

After collection, samples should be kept at low temperature (about 4°C) and analyzed as soon as possible. Conservation of samples is indicated in Table 5.1, based on Appelo and Postma (1999).

5.4 Sampling of Solids

The presence of reactive solids has a significant impact on concentration of some contaminants in water. Also, concentrations of some minerals are required in geochemical modeling.

As a general rule, contact with atmosphere should be avoided after collection of samples and samples should be deposited in tight barrels, and, if possible, in nitrogen atmosphere. For example, de-gassing of CO_2 could cause precipitation of calcite and, thus, concentration of calcite in a sample would be overestimated. There can also be oxidation of pyrite in a sample after its contact with atmospheric oxygen, with resulting precipitation of ferric hydroxide. Thus, reducing capacity of solids would be underestimated and adsorption capacity would be overestimated. Also, drying of samples should be prevented because secondary minerals previously not present in samples could be formed.

The following minerals are of interest:

Calcite: determines a neutralization capacity of a system and plays a significant role in migration of acid mine drainage. Its dissolution is generally fast. Determination is by X-ray diffraction (for content > 5.0 wt %) and by acid digestion in carbonate step of sequential extraction.

Dolomite: plays the same role as calcite, but its dissolution is slower and may be kinetically constrained. Determination is the same as for calcite.

Ferric oxides and hydroxides: they are significant adsorbents of metals and may play a role in neutralization of acid mine drainage at low pH values (above 3.0). Their adsorption capacity is strongly pH-dependent. They can be determined by X-ray diffraction or by oxalate step of sequential extraction. Ferric minerals and Mn(IV) minerals play a principal role in *oxidation capacity (OXC)* of solid phase. Methodology of the *OXC* determination is in Heron et al. (1994) and Christensen et al. (2000).

Pyrite: contributes to reducing capacity of aquifer solids and can be determined by X-ray diffraction and by SEM. Pyrite content together with organic matter content are basis for determination of *reduction capacity (RDC)* of sediments, see discussion in Christensen et al., 2000.

Organic matter: contributes to reducing capacity of aquifer solids. There is special importance of fraction of organic carbon f_{oc} in adsorption of organic contaminants (see later). Determination is based on burning of samples of solids and on detection of CO_2 released during combustion. However, there has to be removal of carbonates by acid digestion prior to analysis.

Table 5.1 Conservation of samples (based on Appelo and Postma, 1999).

Parameter	Conservation of sample
Ca, Mg, K, Na	Acidified to pH<2.0 in polyethylene
NH_4, Si, PO_4	
Heavy metals	Acidified to pH<2.0
SO_4, Cl	No conservation
NO_3, NO_2	Store at 4°C and add bactericide like thymol
H_2S	Zn-acetate conservation or spectrophotometric field measurement
TIC	Dilute sample to TIC<0.4 mmol/L to prevent CO_2 escape
Alkalinity	Field titration using Gran method
Fe^{2+}	Spectrophotometric measurement on acidified sample
pH, T, Eh, O_2	Field measurement

Clays (kaolinite, smectite): contribute to adsorption capacity of solid phase and generally represent pH-independent component of adsorption (especially smectites). They are determined by X-ray diffraction or by differential thermal analysis (DTA).

References

Appelo C.A.J., Postma D., 1999: *Geochemistry, groundwater and pollution*, Revised edition, A.A. Balkema, Rotterdam/Brookfiled.

Christensen T.H., Bjerg P.L., Banwart S.A., Jakobsen R., Heron G., Albrechtsen H.-J., 2000: Characterization of redox conditions in groundwater contaminant plumes, *J. Contam. Hydrol.* 45, pp. 165–241.

Deutsch W.J., 1997: *Groundwater Geochemistry, Fundamentals and Applications to Remediation*, Lewis Publishers, Boca Raton, New Raton.

Fritz S.J., 1994: A survey of charge-balance errors on published analyses of potable ground and surface waters, *Groundwaters* 32, pp. 539–546.

Heron G., Christensen T.H., Tjell J.C., 1994: Oxidation capacity of aquifer sediments, *Envir. Sci. Technol.* 28, pp. 153–158.

Kehew A.E., 2000: *Applied Chemical Hydrogeology*, Prentice Hall, Upper Saddle River, NJ 07458.

Chapter 6: Principles of Geochemical Modeling

6.1 Introduction

In this text we discuss geochemical models, which consider chemical reactions in the migration of contaminants. However, more sophisticated coupled transport and geochemistry models are being developed. Transport processes are discussed in Chapter 7 and there is brief discussion about coupled models at the end of this chapter.

There are geochemical equilibrium models, based on assumption of thermodynamic equilibrium reached in relatively short time (no time factor is included) and geochemical kinetic models, which include time factor. Basic division of equilibrium models is into: (a) speciation models, (b) mass balance models (also called inverse models), and (c) forward models (also called reaction path models). One of principal weaknesses of the equilibrium models is the assumption of chemical equilibrium. However, models including chemical kinetics are not common in environmental geochemistry and there still is a lack of kinetic data for many geochemical processes. There are some exceptions like the oxidation of pyrite, which has been studied extensively. Recent codes like PHREEQC-2 (Parkhurst, Appelo, 1999) include several reaction kinetics. In this text only equilibrium models are discussed.

It must be emphasized that the application of geochemical models is based on the assumption of known flow pattern. If sampling points used for the interpretation of geochemical evolution of ground water are not hydraulically connected, then the geochemical interpretation is in troubles. This means that generally we have to solve flow model prior to geochemical model. Let us look at the influence of water sampling locations on the interpretation of geochemical evolution of ground water (Fig. 6.1). This is a plan view of a simple flow system with recharge area represented by point A. From point A ground water flow is diverted in 2 directions: towards river – points B and C, and in the opposite direction, towards lake – point D. When we investigate geochemical evolution of water, we can compare points A and B (and also C), but comparison of C and D does not make much sense from the viewpoint of geochemical evolution of ground water.

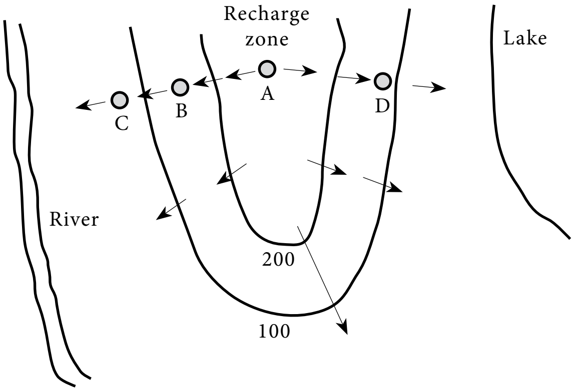

Figure 6.1 Geochemical sampling of a hypothetical flow system (adapted from Chapelle, 1993).

6.2 Speciation Models

They represent the most simple example of equilibrium models. We know chemistry of water from one sampling point (for example, from a well or piezometer) and speciation program calculates distribution of dissolved species between free ions and aqueous complexes and also saturation indexes for different minerals. Lead, for example, can be present in water as free ion Pb^{2+}, and also in the form of complexes with anions:

$$[\mathrm{Pb}]_{\mathrm{total}} = [\mathrm{Pb}^{2+}] + [\mathrm{PbSO}_4^{\,0}] + [\mathrm{PbCl}^+] + [\mathrm{PbCO}_3^{\,0}] \quad \text{etc.}$$

where $[\mathrm{Pb}]_{\mathrm{total}}$ is total lead concentration from laboratory chemical analysis.

Information about distribution of dissolved species is important for risk assessment of contamination by metals because toxicity of metals depends on their speciation in solution. Carbonate complexes of metals, for example, are less toxic than their free ions.

We will demonstrate the significance of saturation index on the example of dissolution of gypsum. The dissolution is expressed as

$$\mathrm{CaSO}_4 \cdot 2\mathrm{H}_2\mathrm{O(s)} = \mathrm{Ca}^{2+} + \mathrm{SO}_4^{\,2-} + 2\mathrm{H}_2\mathrm{O} \qquad K_{\mathrm{sp}} = 10^{-4.60} \text{ for } 25°\mathrm{C}$$

where K_{sp} is solubility product, which is equilibrium constant for this reaction from available from thermodynamic database. The value of K_{sp} is valid for a given temperature and for the reaction as it is written, e.g., for dissolution. In the case of precipitation of gypsum, the value of K_{sp} is $1/10^{-4.60}$. Ion activity product (*IAP*) for the reaction is

$$IAP = [\mathrm{Ca}^{2+}]\,[\mathrm{SO}_4^{\,2-}]$$

where terms in brackets are activities calculated by speciation program applying the Debye-Hūckel or Davies equation for calculation of activity coefficients (Drever, 1997, Langmuir, 1997). The activity α_{i} is equal to the product of activity coefficient γ_{i} and concentration m_{i}:

$$\alpha_{\mathrm{i}} = \gamma_{\mathrm{i}}\, m_{\mathrm{i}} \qquad 6.1$$

We can write, for example, for Ca^{2+} that $\alpha_{\mathrm{Ca2+}} = \gamma_{\mathrm{Ca2+}}\, m_{\mathrm{Ca2+}}$. Activity coefficients are a function of ionic strength of solution *I*, $\gamma_i = f(I)$. When ionic strength of a solution is higher than about 0.5, then the ions interaction approach based on the Pitzer's equations has to be used instead (Langmuir, 1997). Saturation index *SI* is defined as

$$SI = \log\,(IAP/K_{\mathrm{sp}}) \qquad 6.2$$

When $[\mathrm{Ca}^{2+}]\,[\mathrm{SO}_4^{\,2-}] = K_{\mathrm{sp}}$ for gypsum, then $SI = 0$ and water is at equilibrium with gypsum and gypsum in contact with the water neither dissolves nor precipitates. When $SI>0$, gypsum precipitates from the water and when $SI<0$, gypsum dissolves in contact with the water, if it is present in solid phase. Field data necessary for input of speciation program are temperature, pH, alkalinity, and results of laboratory chemical analysis. If behavior of redox-sensitive species (for example, Fe, As, U, etc.) is modeled, then field Eh value can be entered to split total concentrations on the basis of the Nernst equation. Redox couple concentrations (for example, $\mathrm{Fe}^{2+}/\mathrm{Fe}^{3+}$) can also be determined analytically or a total concentration can be split on the basis of the Eh value calculated from other redox couple (for example, $\mathrm{As}_{\mathrm{total}}$ split on the basis of the Eh value calculated from the $\mathrm{Fe}^{2+}/\mathrm{Fe}^{3+}$ couple). However, analytical determination of redox species has priority because redox equilibrium is rarely observed (Langmuir, 1997). Thus, the redox speciation based on Eh values and on other redox couples is just a rough estimate.

An example of typical speciation model output is shown in Fig. 6.2.

Common problems solved using speciation programs are: (a) there is a sample with high concentration of dissolved aluminum and we need to know distribution of aluminum between Al^{3+} and different complexes

Figure 6.2 Output of speciation in program SIMUL (Reardon, 1992).

Species	Conc	log Conc mmol/kg	Gamma mol/kg
H+	3.023E-05	-7.5196	0.5310
OH-	4.911E-04	-5.3089	0.8103
Ca2+	4.17	-2.3798	0.4452
Mg2+	1.32	-2.8794	0.4455
MgOH+	4.414E-05	-7.3552	0.8254
Na+	11.7	-1.9318	0.8365
Fe3+	1.238E-12	-14.9073	0.1796
FeOH2+	1.343E-07	-9.8721	0.4454
Fe(OH)2+	2.872E-05	-7.5418	0.8284
F e(OH)30	2.844E-04	0.5451	1.0054
Fe(OH)4-	1.969E-02	-4.1058	0.8546
Cl-	0.157	-3.8053	0.8497
SO42-	5.49	-2.2504	0.4322
HSO4-	6.660E-06	-8.1765	0.8547
CO2aq	0.531	-3.2750	1.0054
HCO3-	11.4	-1.9425	0.8503
CO32-	5.410E-02	-4.2668	0.3255

Phase	Log SI	
PCO2	-1.79	
Brucite	-5.15	
Portlandite	-10.34	
Calcite	0.93	NOTE: Supersalurated
Aragonite	0.74	NOTE: Supersaturaled
Valerile	0.42	NOTE: Supersalurated
Gypsum	-0.78	
Bassanite	-1.65	
Nesquehonite	-2.88	
Mg-oxychloride	-13.57	
Ca-oxychloride	-41.83	
Ca~monochlorid	-24.55	
Halite	-7,46	
Nahcolite	-3.52	
Dolomite	1.62	NOTE: Supersaturated
Fe{OH)3	5.38	NOTE: Supersaturated

(for example, $Al(OH)_4^-$, $AlSO_4^+$ etc.) because different forms of aluminum have different toxicity, (b) there are ground water samples from contaminant plume downgradient from mine tailing impoundment and we want to verify the possibility of precipitation of minerals like gypsum, $CaSO_4.2H_2O$, and jarosite, $KFe_3(SO_4)_2(OH)_6$. An example of speciation program is WATEQ4F (Plummer et al., 1976). However, more advanced programs like PHREEQC (Parkhurst, 1995) also include speciation modul. There are countless examples of speciation modeling applications in geochemical and hydrogeological literature (for example, Blowes, Jambor, 1990, Robertson et al., 1991, etc.).

Principal difficulties related to the application of speciation models are:

(1) Calculations are based on assumption of thermodynamic equilibrium and do not include a time factor. This means that the *SI* values just determine the direction of a reaction, but not how long time it takes to complete the reaction. There are so called reactive minerals with fast dissolution/precipitation rate (however, expressions ”fast” and ”slow” depend on the velocity of ground water flow and on time scale of investigation). Examples of reactive minerals are (Deutsch, 1997): Carbonates: calcite $CaCO_3$, dolomite, $CaMg(CO_3)_2$, siderite, $FeCO_3$, rodochozite, $MnCO_3$; Sulfates: gypsum, $CaSO_4.2H_2O$, jarosite, $KFe_3(SO_4)_2(OH)_6$, melanterite, $FeSO_4.7H_2O$, basaluminite, $AlOHSO_4$; Oxides and hydroxides: ferrihydrite, $Fe(OH)_3$, goethite, FeOOH, gibbsite, $Al(OH)_3$, manganite, MnOOH, and amorphous silica, SiO_2(am).

On the other hand, dissolution of silicates like feldspares is slow and can be made even slower by the formation of secondary products layers on their surfaces. This type of reactions requires kinetic descriptions with a time factor. There are other reactions which never reach equilibrium, and in which reactants are gradually transformed into products. An example is the oxidation of organic matter by oxygen. Another example is the oxidation of pyrite because pyrite does not precipitate in oxidizing environment even when concentrations of Fe^{2+} and SO_4^{2-} increase.

(2) Equilibrium constants are defined for pure mineral phases, which seldom occur in nature. For example, there can be a gradual transition between K-jarosite $KFe_3(SO_4)_2(OH)_6$ and natro-jarosit $NaFe_3(SO_4)_2(OH)_6$ with changing value of equilibrium constant. A notorious example is ferric hydroxide because the value of equilibrium constant for the mineral phase changes several orders of magnitude depending on the degree of crystallization (Langmuir, 1997).

(3) Complexation with organic matter can highly increase concentrations of dissolved metals. In ground water without organic matter metals would precipitate as minerals. Most of modeling codes do not have data base of equilibrium constants for complexation with organic matter. Furthermore, the characterization of organic matter composition is complicated and expensive problem. Terms like humic and fulvic acids describe groups of organic acids with several hundred of members and only for some of them equilibrium constants are available.

6.3 Mass Balance Models

This type of models (also called inverse models) is used in cases, when we already know chemistry of ground water and solid phase composition, and we want to determine which reactions have already happened between hydraulically connected sampling points. There are two types of the mass balance modeling: evolution of ground water chemistry between 2 sampling points and mixing problem. In the case of chemical evolution, the input includes ground water chemistry of 2 samples located on the same flowline and composition of solid phase in the aquifer between these 2 points. In the case of mixing problem, the required input are 3 (or more) samples, which represent chemistry of 2 waters prior to mixing and chemistry of final water after mixing and completion of geochemical reactions. Typical model of the type is NETPATH (Plummer et al., 1994). Program is based on mass balance equation:

$$\Delta m_{T,k} = \Sigma \alpha_p b_{p,k} \qquad k = 1, j \tag{6.3}$$

where $\Delta m_{T,k}$ is change of total dissolved concentration of k^{th} component between sampling points, α_p is the quantity of component p (for example, in mol/kg of water) which dissolved or precipitated and $b_{p,k}$ is stechiometric coefficient of k^{th} component in p^{th} mineral. For example, for dissolved inorganic carbon change along flowpath with reacting phases including calcite, dolomite and CO_2(g), we can write

$$\Delta m_{T,C} = \alpha_{\text{calcite}} + 2\alpha_{\text{dolomite}} + \alpha_{\text{CO2}} \tag{6.4}$$

Then the program solves a set of equations for specified components and the goal is to calculate mass transfer coefficient α for each phase. Similar equations are solved for mass balance of electrons and isotopes.

The output has the following form:

$$\text{Water A + Reactants = Water B + Products} \tag{6.5}$$

Example of mass balance model output is the interpretation of water chemistry in the Madison Aquifer in Wisconsin, USA (Plummer et al., 1984):

Recharge water +2 0.15 gypsum + 3.54 dolomite + 0.87 CH_2O +15.31 NaCl + 2.52 KCl + 0.09FeOOH+8.28 Na_2-X = Mysse water + 5.33 calcite + 0.09 pyrite + 8.28 Ca-X

where mass transfer coefficients are in mmol/L and X indicates exchange sites on clays. The type of model is often used for the interpretation of regional water chemistry evolution, but it has also been used for interpretation of reactions in contaminated aquifers. An example of contaminated site data interpretation is the interpretation of geochemical reaction in a shallow aquifer contaminated by crude oil near Bemidji, Minnesota, USA (Baedecker et al., 1993). Selected ground water chemistry data are in Table 6.1. Site B, far from the oil plume, is located about 40 m downgradient from Site A, at the margin of the plum with free phase.

The interpreted geochemical reactions related to the degradation of dissolved organic carbon released from the oil spill were: - methanogenesis of DOC, degassing of CO_2 and CH_4 from the water table into the unsaturated zone, - dissolution of calcite, MnO_2, and goethite in solid phase, and precipitation Ca-siderite with 20 % of Ca. Values of $\delta^{13}C$ for carbon species in liquid and solid phases were also used for interpretation. Elements (constraints) used in modeling were: C, Ca, Fe, Mn, N, Redox (includes electron mass balance in redox reactions). Minerals (phases) used in model were: MnO_2, goethite, siderite, adsorption of NH_4^+, mixture CO_2-CH_4 with CO_2 fraction 0.14, and calcite (Plummer et al., 1994). Resulting ground water evolution model was

Water A + 0.111 MnO_2 + 6.488 goethite + NH_4^+-X = Water B + 7.464 siderite + 2.476 CO_2-CH_4 + 0.276 calcite

The calculated isotopic values of $\delta^{13}C$ were relatively close to the values of samples from the field.

Difficulties related to the application of mass balance models are: (1) results are non-unique and the same water chemistry evolution can be explained by several models, (2) there are no thermodynamic constraints in mass balance models and program may suggest impossible reactions. This means that the type of models has to be used in conjunction with speciation model. If, for example, the mass balance model suggests dissolution of gypsum as a possible reaction, then saturation index SI_{gypsum} has to be less than 0 and gypsum has to be present in solid phase. However, principal proof of dissolution/precipitation of a mineral is its mineralogical evidence using methods like X-ray diffraction and scanning electron microscope (SEM). (3) There is a problem related to the definition of solid phase composition because in the case of silicates their composition may be quite complex.

Table 6.1 Water chemistry at the Bemidji site [in mmol/L, unless stated otherwise].

Property or constituent	Site A (upgradient)	Site B (downgradient)
Temperature [°C]	10	9
pH	6.78	6.93
Eh [V]	-0.15	-0.09
Dissolved O_2	0	0
Ca	3.322	3.046
Mg	1.77	1.366
Na	0.135	0.091
K	0.169	0.036
Fe	1.055	0.079
Mn	0.016	0.127
Cl	0.09	0.01
SO_4	0.005	0.012
H_2S	<0.0006	<0.0006
TDIC	17.165	10.572
DOC	4.171	1.515
CH_4(aq)	1.353	0.386
NH_4^+	0.028	0.005
SiO_2	1.018	0.508
$\delta^{13}C_{TDIC}$ [per mil]	-5.80	-5.95
$\delta^{13}C_{CH4}$ [per mil]	-56.1	-53.6

6.4 Forward Models

This type of models, also called reaction path models, is used for prediction of water chemistry evolution along a flowline. In this case, initial water chemistry is known and we try to predict water chemistry at some downgradient point along flowpath. We have to stipulate reacting mineral phases which dissolve and also mineral phases which precipitate when their SI values are more than 0. The input of model is the initial water and reacting mineral phases. This type of model also can equilibrate a water sample with a gas with specified partial pressure (for example, with P_{CO2}). The output is similar to the output of speciation model (e.g., list of dissolved species and saturation indexes), but the amount of dissolved or precipitated minerals during equilibration is also indicated (for example, 0.05 mol $Fe(OH)_3$ per 1 L of water). The concept of modeling is

$$\text{Initial water + Reacting phases =}$$
$$\text{= Predicted water + Products} \qquad 6.6$$

Let us assume dissolution of halite, NaCl, and barite, $BaSO_4$, in an initial water. Both minerals can be included in input as ”infinite phase” (which means that their amount in solid phase is large and is not influenced very much by their dissolution) and ”finite phase” (in this case we stipulate their amount in contact with 1L of water). The code will dissolve in each reaction step

$\Delta NaCl + \Delta BaSO_4$

where Δ is mass transfer coefficient in mol/L, which is a small number. In each step, the program adds into water ΔNa^+, ΔCl^-, ΔBa^{2+}, ΔSO_4^{2-}, and then there is speciation calculation. If saturation index for a dissolving phase is still negative, then dissolution continues. The transfer coefficient is kept small to avoid sudden supersaturation of water and conversion of reactants into products. In the meantime, other pre-determined reactive minerals can be precipitated if their saturation indexes values become positive.

Examples of this type of models are MINTEQA2 (Allison et al., 1991) and PHREEQC (Parkhurst, 1995). Both models include adsorption modeling using adsorption isotherms and surface complexation (Langmuir, 1997). However, in MINTEQA2 we can not mix and titrate different waters like in PHREEQC. Both codes can be used in ”batch mode”, e.g., there is equilibration of water with given phases in a closed batch. The program PHREEQC can also be used in ”column mode”, e.g., water flows through a column and is equilibrated with minerals and adsorbing phases in the column. Mass balance models and forward models are complementary because when we want to determine downgradient evolution of water chemistry, then we need to know which processes influenced water chemistry upgradient.

Typical problems solved by forward modeling are: (a) Reactions of contaminated water with aquifer solids like calcite and $Fe(OH)_3$. (b) Determination of water chemistry after mixing with water in the stream, equilibration with gases with specified partial pressures and after completion of chemical reaction. (c) Evaporation of contaminated water in discharge area with precipitation of minerals etc. Toran, (1994), used forward geochemical modeling for interpretation of data from zinc-lead mines in Schullsburg, Wisconsin, USA. Acid mine drainage produced by the oxidation of PbS and ZnS was neutralized by dissolution of calcite and dolomite and concentration of iron was lowered by precipitation of siderite and ferrihydrite. Sulfate concentration was influenced by dilution during flooding of mines, but precipitation of gypsum did not play a significant role.

Let us consider a hypothetical example of forward modeling of acid mine drainage (AMD) evolution. Ground water from mine tailings after the oxidation of pyrite with low pH, high Fe^{2+}, Fe^{3+}, and sulfate concentrations (Table 6.2) enters an aquifer with porosity 0.3, bulk density 1.8 kg/m^3, and 1.0 wt % calcite in solid phase (e.g., 0.6 mol of calcite in contact with 1 L of water). After neutralization with calcite several minerals like gypsum, siderite, and $Fe(OH)_3$ may precipitate. Finally, there is discharge of ground water to a local creek with neutral pH water (Table 6.2), where water in the creek mixes with discharging ground water in ratio 60 : 40. After the mixing, there is equilibration with atmospheric CO_2 and O_2, and there may be precipitation of calcite and $Fe(OH)_3$.

We calculate ground water chemistry (Water 2) after reaction of Water 1 with calcite in solid phase and precipitation of gypsum, siderite, and $Fe(OH)_3$ (if ground water is supersaturated with respect to them). Then water chemistry in the creek is calculated as Water 4 after mixing of original creek water (Water 3) with ground water (Water 2) in ratio 60 : 40, and after equilibration with $P_{CO2} = 10^{-3.5}$ atm, and precipitation of calcite, and $Fe(OH)_3$ (water becomes supersaturated with respect to them). Results of modeling steps are in Table 6.2. Supersaturation with respect to gypsum has never been reached and thus, there was zero amount of precipitated gypsum. Supersaturation with respect to siderite was reached only after neutralization of acid ground water by calcite, when concentration of Fe^{2+} was still high (Water 2). Concentrations of both Fe^{2+}

Table 6.2 Results of forward modeling, concentrations in mol/L (see text).

Parameter/ sample	Water 1 (acid mine drainage)	Water 2 (neutralized water)	Water 3 (original creek water)	Water 4 (mixed and equilibrated with air)
Ca	2.99×10^{-3}	2.46×10^{-2}	1.05×10^{-4}	8.75×10^{-3}
Mg	9.87×10^{-4}	9.87×10^{-4}	8.23×10^{-5}	4.44×10^{-4}
Na	2.00×10^{-3}	2.00×10^{-3}	1.44×10^{-4}	8.86×10^{-4}
C_{total}	9.83×10^{-2}	1.27×10^{-2}	2.56×10^{-4}	3.70×10^{-4}
SO_4	1.04×10^{-2}	1.04×10^{-2}	1.05×10^{-4}	4.26×10^{-3}
Fe(II)	1.00×10^{-2}	1.11×10^{-4}	-	9.91×10^{-19}
Fe(III)	5.01×10^{-3}	9.81×10^{-8}	-	2.19×10^{-8}
Cl	1.01×10^{-3}	1.01×10^{-3}	1.01×10^{-4}	4.67×10^{-4}
pH	2.7	6.26	7.6	7.77
T [°C]	22.0	22.0	25.0	23.8
$SI_{calcite}$	-8.77	0.0	-3.09	0.0
$SI_{Fe(OH)3(a)}$	-0.67	0.0	-	0.0
$SI_{siderite}$	-5.82	0.0	-	-13.54
SI_{gypsum}	-1.01	-0.05	-3.51	-0.58
log P_{CO2} [atm]	-1.57	-0.78	-3.43	-3.50
log P_{O2} [atm]	-	-	-	-0.69
Δcalcite	-	-2.16×10^{-2}	-	$+1.15\times10^{-3}$
Δ$Fe(OH)_3$(a)	-	$+5.01\times10^{-3}$	-	$+4.43\times10^{-5}$
Δsiderite	-	$+9.92\times10^{-3}$	-	-

and Fe^{3+} after mixing of acid mine drainage with water in creek dropped to almost zero because iron precipitated as ferric hydroxide (Water 4).

This reaction generated acidity and thus, resulting pH after equilibration with atmospheric CO_2 would be even higher than calculated value of 7.77 if there would have not been precipitation of dissolved iron.

There are similar problems related to the applications of forward models like in the case of speciation models. Furthermore, we have to choose reactive mineral phases which are allowed to dissolve or precipitate in the case of corresponding values of saturation index. After equilibration of water with these minerals, their SI values will be equal to zero (see, for example, SI_{calcite} in Table 6.2. for Water 4).

6.5 Coupled Transport and Geochemical Models

We have discussed so far purely geochemical models, which do not include physical processes. Now we will mention coupled models briefly. Coupled transport/chemistry models are being developed and are not available as common commercial codes so far. In this type of models, transport and chemical steps are generally separated. The advection-dispersion equation (ADE) in 1-D with chemical reactions is

$$\frac{D}{R}\frac{\partial^2 C}{\partial x^2} - \frac{v}{R}\frac{\partial C}{\partial x} - \lambda C \pm W = \frac{\partial C}{\partial t} \qquad 6.7$$

where D is hydrodynamic dispersion ($D = \alpha v + D_e$, where α is longitudinal dispersivity and D_e is effective diffusion coefficient), v is average linear velocity, R is retardation coefficient based on an adsorption isotherm like adsorption isotherm K_d, λ is 1st order decay constant, x is distance from source, t is time, and W is chemical term, which includes chemical reactions. In an iterative mode, the code solves in transport step the ADE for each of dissolved species, and then in chemical step a set of chemical reactions based on forward modeling takes place (formation of complexes, precipitation of pre-determined minerals etc.). In sequential mode the code uses the same transport parameters for all species in transport step. Some coupled codes use common forward modeling codes, for example, the code MINTRAN (Walter et al., 1994) uses MINTEQA2 (Allison et al., 1991) in its geochemical module.

We can also use transport and geochemical models separately (de-coupled approach). Migration of a conservative contaminant like chlorides can be modeled by a transport code. On the basis of transport model output we can determine the mixing factor for other, non-conservative species, and calculate concentrations of these species using mixing option in a forward geochemical model. Similar approach was used by Stollenwerk, (1994), for modeling of evolution of water chemistry in an aquifer contaminated by acid mine drainage near Globe, Arizona, USA.

References

Allison J.D., Brown S., Novo-Gradac K.J., 1991: MINTEQA2, *A Geochemical Assesment Data Base and Test Cases for Environmental Systems*, Athens, GA, U.S. EPA.

Baedecker M.J., Cozzarelli I.M., Eganhouse R.P., Siegel D.I., Bennett P.C., 1993: Crude oil in a shallow sand and gravel aquifer-III. Biogeochemical reactions and mass-balance modeling in anoxic groundwater, *Appl. Geochemistry*, 8, pp. 569–586.

Blowes D.W., Jambor J.L., 1990: The pore-water geochemistry and the mineralogy of the vadose zone of sulfide tailings, Waite Amulet, Quebec, Canada, *Appl. Geochemistry*, 5, pp. 327–346.

Chapelle F.H., 1993: *Ground Water Microbiology and Geochemistry,* John Wiley & Sons, New York.

Deutsch W.J., 1997: *Groundwater Geochemistry, Fun*damentals and Applications to Contamination, Lewis Publishers, Boca Raton, New York.

Drever J.I., 1997: *The Geochemistry of Natural Waters,* Surface and Groundwater Environments, 3rd Edition, Prentice Hall, Upper Saddle River, NJ 07458.

Domenico P., Schwartz F.W., 1998: *Physical and Chemical Hydrogeology,* 2nd Edition, John Wiley & Sons, New York.

Fetter C.W., 1999: *Contaminant Hydrogeology,* 2nd Edition, Prentice Hall, New York.

Langmuir D., 1997: A*queous Environmental Geochemistry,* Prentice Hall, Upper Saddle River, NJ 07458.

Parkhurst D.L., 1995: Users Guide to PHREEQC-A Computer Program for Speciation, Reaction-path, Advective-transport, and Inverse Geochemical Calculations, *U.S. Geological Survey Water Resources Investigations Repor*t 95–4227.

Parkhurst D.L., Appelo C.A.J., 1999: PHREEQC-2, a Hydrogeochemical Computer Program, *U.S. Geological Survey Water Res.* Inv., in press.

Plummer L.N., Jones B.F., Truesdall A.H., 1976: WATEQ4F-A Fortran IV Version of Wateq, a Computer Program for Calculating Chemical Equilibria of Natural Waters, *U.S. Geological Survey Water Resources Investigations Report* 76–13.

Plummer L.N., 1984: *Geochemical modeling: A comparison of forward and inverse methods.* First Canadian/American Conference on Hydrogeology, Eds.

B. Hitchon, E.I. Wallick, Dublin, Ohio, National Water Well Assoc., pp. 149–177.

Plummer L.N., Prestemon E.C., Parkhurst D.L., 1994: An Interactive Code (NETPATH) for Modeling Geochemical Reactions along a Flow Path, Version 2.0, *U.S. Geological Survey Water Resources Investigation Report* 94–4169.

Reardon E.J., 1992: *Aqueous geochemistry*, Course notes, University of Waterloo, Waterloo, Ontario, Canada.

Stollenwerk K.G., 1994: Geochemical Interactions between Constituents in Acidic Groundwater and Alluvium in an Aquifer near Globe, Arizona, *Appl. Geochemistry,* 9, pp. 353–369.

Robertson W.D., Cherry J.A., Sudicky E.A., 1991: Ground-Water Contamination from Two Small Septic Systems on Sand Aquifers, *Groundwater,* Vol. 29, No.1, pp. 82–92.

Toran L., 1994: Sulfate contamination in groundwater from a carbonate-hosted mine, *J. Contam. Hydrol.,* 2, pp. 1–29.

Walter A.L., Frind E.O., Blowes D.W., Ptacek C.J., Molson J.W., 1994: Modeling of Multicomponent Reactive Transport in Groundwater, I. Model Development and Evaluation, *Water Res. Research,* 30, pp. 3137–3148.

Chapter 7: Introduction to Transport Processes

7.1 Importance of Transport Processes

Our text places emphasis on geochemical processes, but a brief introduction to transport processes is also included in this chapter. The principal reason is related to the fact that all processes are coupled and there is no clear boundary between transport and geochemical processes.

In general, there is transfer of mass, but no transformation of contaminants during transport processes. Principal transport processes are diffusion, advection, dispersion, adsorption resulting in retardation, and decay.

Sources of contamination can be broadly divided on temporal basis into continuous sources (input continues for long time) and instantaneous sources (input lasts for very limited time and then stops) or on spatial basis into point sources (landfills, mine tailings and other relatively small sources), diffuse sources (there are no clear limits of a source, for example, nitrate contamination from agriculture pollution, acidification from acid deposition), and linear sources (pipelines for petrol, pollution from road salts).

7.2 Diffusion

Diffusion is transport of a contaminant based on concentration gradient. This process may take place also in stagnating water (velocity of flow $v = 0$) or even against the direction of flow. The process is described by First Fick's Law for steady-state diffusion (e.g., concentration gradient does not change in time):

$$J_D = -D_e \, \partial C/\partial x \qquad 7.1$$

where J_D is diffusive flux (kg m^2 s^{-1}), D_e (m^2 s^{-1}) is effective diffusion coefficient for porous media, C is concentration, and x is distance of transport from source of contamination. The concentration gradient $\partial C/\partial x$ can be determined relatively easily. In contrast, the value of D_e is more problematic. Generally, values of diffusion coefficient D_w for free water are in literature (they decrease with increasing molecular weight of a compound) for different ions (Table 7.1) and they have to be converted to values of D_e for porous media. There are several equations for conversion available, one of them is

$$D_e = (n/\tau) \, D_w \qquad 7.2$$

where n is porosity (or volume fraction of water in unsaturated zone) and τ is tortuosity (defined as ratio between real transport distance and straight distance in porous media, value > 1.0 is taken from literature).

When diffusion is transient, 2nd Fick's Law applies:

$$\partial C/\partial t = D_e \, \partial^2 C/\partial x^2 \qquad 7.3$$

This equation can be used, for example, to calculate diffusive flux across a clay liner for a certain period.

Table 7.1 Values of diffusion coefficient D_w for free water (from Domenico and Schwartz, 1998).

Cation	D_w [10^{-10} m^2.s^{-1}]	Anion	D_w [10^{-10} m^2.s^{-1}]
H^+	93.1	OH^-	52.7
Na^+	13.3	F^-	14.6
K^+	19.6	Cl^-	20.3
Rb^+	20.6	Br^-	20.1
Cs^+	20.7	HS^-	17.3
Mg^{2+}	7.05	HCO_3^-	11.8
Ca^{2+}	7.93	CO_3^{2-}	9.55
Sr^{2+}	7.94	SO_4^{2-}	10.7
Ba^{2+}	8.48		
Ra^{2+}	8.89		
Mn^{2+}	6.88		
Fe^{2+}	7.19		
Cr^{3+}	5.94		
Fe^{3+}	6.07		

7.3 Advection

Advection is transport with bulk motion of flowing water. Driving force of advective transport is hydraulic gradient. There are several expressions for water movement based on Darcy's Law:

$$\text{Volumetric flux } Q = k\,I\,A \qquad (\text{m}^3\ \text{s}^{-1}) \qquad 7.4$$

where k is hydraulic conductivity, I is hydraulic gradient, and A is flow cross section.

$$\text{Specific discharge } q = k\,I \qquad (\text{m s}^{-1}) \qquad 7.5$$

e.g., this is flux across a unit cross section.

$$\text{Average linear velocity } v = q/n_e = (k\,I)/n_e \qquad (\text{m s}^{-1}) \qquad 7.6$$

where n_e is effective porosity (e.g., volume of interconnected pores transmitting flow divided by total volume).

The average linear velocity is velocity of advection because advective transport takes place only within pores and not across complete profile.

Advective flux is expressed as

$$J_A = v\,n\,C = q\,C \qquad (\text{kg m}^{-2}\ \text{s}^{-1}) \qquad 7.7$$

Units for diffusive flux and advective flux are consistent because both fluxes have to be additive. Advection just moves contaminated zone downgradient and if there would not have been any other process, the interface between contaminated and uncontaminated zones would have been abrupt. Obviously, this is not a real situation and, thus, other processes are also operating.

7.4 Dispersion

Dispersion is process of contaminant spreading based on velocity variations at several scales (Fig. 7.1):

- Pore scale, where velocity is larger in the middle of a pore and zero close to contact with grains. There also is branching of particle trajectories based on different sizes of pores.
- Layer scale, where particle move larger distance in layers of higher permeability.
- Aquifer scale, where larger heterogeneity change particle trajectories.

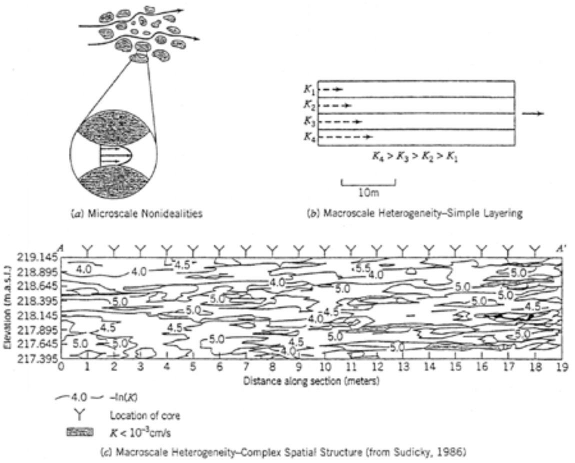

Figure 7.1 Different scales of dispersion (from Domenico and Schwartz, 1998).

Dispersion depends on advection and when advective velocity $v = 0$, there is no dispersion. Dispersion is characterized by a parameter called *dispersivity* (also characteristic length), α (m). In 3-D world, there are 3 parameters of dispersivity:

- *longitudinal dispersivity* α_L, acting in the direction of flow,
- *transverse dispersivity* α_T acting in the direction perpendicular to flow, and
- *vertical dispersivity* α_V acting in vertical direction.

In most cases, it holds that $\alpha_L > \alpha_T > \alpha_V$, e.g., longitudinal dispersivity has values in m, transverse dispersivity in dm, and vertical dispersivity in mm.

The values of effective diffusion coefficient and dispersivity are combined in parameter called hydrodynamic dispersion, D. In the direction of flow it is

$$D_L = \alpha_L\,v + D_e \qquad 7.8$$

All parameters have already been defined. When advective velocity $v \rightarrow 0$ (for example, in clay sediments of low permeability), we obtain $D_L = D_e$, e.g., hydrodynamic dispersion is equal to diffusion coefficient.

Unfortunately, the value of dispersivity is not constant. The values obtained on column tests in laboratory are generally much smaller than those obtained from field tracer tests or from calibration based on large scale contaminant plume. This is related to a higher degree of heterogeneity in the field. When a tracer fills a larger volume of an aquifer, encounters more heterogeneities and value of dispersivity increases. When a sufficient volume of an aquifer is filled, dispersivity may attain a constant value. Several empirical formulas relating dispersivity to migration distance exist. Probably the most common is the formula of Xu and Eckstein (Fetter, 1999):

$$\alpha_L = 0.83 (\log L_s)^{2.414} \qquad 7.9$$

where L_s is migration distance.

7.5 Adsorption

Adsorption is process of attachment of particles of a contaminant to the surface of solid phase. When concentration of a contaminant in water decreases, these particles are released in process called *desorption.* In classical concept, adsorption is considered fast compared to the velocity of flow and reversible.

The most common is the concept of linear adsorption isotherm K_d, defined as

$$K_d = dS/dC \ \ (\mathrm{L/kg}) \qquad 7.10$$

where S is amount of contaminant adsorbed on solid phase (mg/kg) and C is concentration of contaminant in water. The value of K_d is generally obtained from *batch test* based on addition of different amounts of contaminant into a batch with water and solid phase from investigated site. Then equilibrium concentrations of contaminant in water and in solid phase are determined and K_d is calculated as a slope of straight line in graph $S = f(C)$. There are other types of adsorption isotherms like the Freundlich isotherm and the Langmuir isotherm (see Chapter 3.5). Also, the value of K_d for organic contaminants is often determined from value of octanol-water partition coefficient K_{ow} (Chapter 11.3).

Adsorbed contaminant is retarded compared to advective flow velocity. The measure of the retardation is retardation coefficient R, linked to the K_d by equation

$$R = v_w/v_c = 1 + (\rho_b/n) K_d \qquad 7.11$$

where v_c and v_w are velocities of contaminant transport and water flow, respectively, ρ_b is bulk density of solids, and n is porosity. The term (ρ_b/n) for bulk density in kg/dm^3 indicates kg of solid phase in contact with 1 L of water. When bulk density and K_d are in consistent units, the value of R is dimensionless. For example, when $R = 4.0$, velocity of a contaminant transport is four times slower than velocity of water flow.

Problem: The hydraulic conductivity of an aquifer is 1×10^{-4} m/s, hydraulic gradient is 0.001 and effective porosity is 0.25. Calculate migration distance during 1 year for Cd^{2+} with K_d value of 0.3 L/kg. Bulk density of solid phase is 1.8 kg/dm^3 and total porosity is 0.3.

Solution: Advective velocity is
$v = (k\times I)/n_e = (1\times10^{-4})/0.25 = 4 \text{ x } 10^{-7}$ m/s,
water flow distance for 1 year is
$L_w = 4 \times 10^{-7} \times 86400 \times 365 = 12.61$ m.
Retardation factor for Cd^{2+}
$R = 1 + (\rho_b/n) = 1 + (1.8/0.3)\times0.3 = 2.8$.
Thus, migration distance of Cd^{2+} is
$L_{Cd2+} = 12.61/2.8 = 4.5$ m/year.

7.6 Decay

Decay is decomposition of a contaminant, generally accompanied with formation of daughter products. The most common description of the process is by 1st order kinetics, where decay rate depends on concentration:

$$dC/dt = - k\,C \qquad 7.12$$

where C is concentration and t is time, and k is decay konstant (day^{-1}). By integration of the equation 12 we obtain

$$C_t = C_0\, e^{-kt} \qquad 7.13$$

where C_t is concentration at time t and C_0 is initial concentration. The kinetic constant can be easily converted to half-life $t_{1/2}$,

$$t_{1/2} = 0.693/k \qquad 7.14$$

Half-life, $t_{1/2}$, (s) is the time necessary for decay of 50 % of initial concentration.

Examples of 1st order kinetics processes are radioactive decay and decay of petroleum products like benzene. However, when concentrations of benzene and other organics are too high, then 0. order kinetics with decay rate independent of concentration applies:

$$\mathrm{d}C/\mathrm{d}t = -k \qquad 7.15$$

where the value of decay constant is in $\mathrm{kg\,m^{-3}\,day^{-1}}$. By integration of equation 7.15 we obtain

$$C_t = C_0 - k\,t \qquad 7.16$$

When kinetic data are taken from literature, caution has to be used because the meanings of kinetic constant and half-life are completely opposite, e.g., large value of kinetic constant means fast decay and large value of half-life means slow decay.

7.7 Equations of Transport and their Solutions

Basic transport equation in 1-D is called the advection-dispersion equation (ADE). Its form for transport in saturated zone along x-axis is

$$D_x\, \partial^2 C/\partial x^2 - v_x\, \partial C/\partial x = \partial C/\partial t \qquad 7.17$$

where D_x is hydrodynamic dispersion, C is concentration, v_x is advection velocity and t is time. 1st term is dispersion term, 2nd term is advection term, and 3rd term is concentration term.

When adsorption/retardation are included, D_x and v_x are divided by retardation coefficient R:

$$(D_x/R)\, \partial^2 C/\partial x^2 - (\mathrm{v}_x/\mathrm{R})\, \partial C/\partial x = \partial C/\partial t \qquad 7.18$$

Finally, when decay of 1st order decay is included, the ADE has the following form:

$$(D_x/R)\, \partial^2 C/\partial x^2 - (v_x/R)\, \partial C/\partial x - kC = \partial C/\partial t \qquad 7.19$$

where k is 1st order decay constant.

A common solution of ADE in 1-D is the solution Ogata-Banks:

$$C(x,t) = (C_0/2)\,(\mathrm{erfc}[(x-v_x\,t))/2(D\,t)^{1/2}] + \\ + \exp(v_x\,x/D)\mathrm{erfc}[(x+v_x\,t))/2(D\,t)^{1/2}] \qquad 7.20$$

Short form of the equation applicable a long distance from source is

$$C(x,t) = (C_0/2)\,(\mathrm{erfc}[(x-v_x\,t))/2(D\,t)^{1/2}] \qquad 7.21$$

where C_0 is source concentration, x is distance from the source, t is time, v is advection velocity, D_x is hydrodynamic dispersion, and erfc is the complementary error function (Table 7.2). The calculations of erfc are also implemented in the spreadsheet function of Excel program. Boundary and initial conditions for semi-infinite column are $C(0, t) = C_0$ and $C(\infty, t) = 0$ for $t>0$, and $C(x, 0) = 0$. The equation 7.21. applies in farther distance from source, in the proximity of source complete version of Ogata-Banks solution (equation 7.20) has to be used (Fetter, 1999). Solution for adsorption/retardation problem is obtained by dividing D and v by retardation factor R.

When decay is implemented, the equation becomes (Domenico and Schwartz, 1998)

$$C(x,t) = (C_0/2)\,\exp((x/2\alpha_x)(1-(1+(4\lambda\alpha_x/v_x)^{1/2})) \times \\ \times\, \mathrm{erfc}((x-v_x\,t(1+4\lambda\alpha_x/v_x)^{1/2})/2(\alpha_x\,v_x\,t)^{1/2}) \qquad 7.22$$

where λ is 1st order decay constant, and α_x longitudinal dispersivity (molecular diffusion is considered negligible). For steady state (e.g., $t \rightarrow \infty$) we obtain

$$C(x,t) = C_0\,\exp((x/2\alpha_x)(1-(1+(4\lambda\alpha_x/v_x)^{1/2})) \qquad 7.23$$

The equation is used for evaluation of biodegradation in an investigation of natural attenuation.

Solution for transient diffusion equation (Second Fick's Law, Equation 7.3) is

$$C(x,\,t) = C_0[\mathrm{erfc}(x/(2(D_e\,t)^{1/2})] \qquad 7.24$$

where D_e is effective diffusion coefficient. Also diffusing contaminant can be adsorbed and solution with adsorption/retardation is obtained by dividing D_e by R.

Other solutions including 3-D solution and solutions with decay are presented in Bear (1979), Fetter (1999), and Domenico and Schwartz (1998). In that case, the shape and size of source has to be known. For example, in the case of 3-D solution it can be a plane perpendicular to ground water flow (patch source). Solution in 3-D with decay is implemented in natural attenuation codes BIOSCREEN and BIOCHLOR (Chapter 11).

Problem: Source concentration of a contaminant is 100 mg/L, flow velocity is 90 m/year, and longitudinal dispersivity is 1.0 m. Calculate concentration after 1 year at a distance of a) 92 m, and b) 85 m from source.

Solution: We use 1-D equation Ogata-Banks, assuming that molecular diffusion is negligible, e.g., $D = \alpha_L\, v$:

a) $C = (C_0/2)\,\mathrm{erfc}[(x–v\,t))/2(\alpha_L\,v\,t)^{1/2}] = (100/2)\,\mathrm{erfc}[(92–90.1)/2\,(1.90)^{1/2}$ we obtain $\mathrm{erfc}[0.1053] = 0.8815$ (erfc is available in Excel spreadsheet) and $C = C_0/2\times0.8815 = 50.8815 = 44.1$ mg/L
b) in this case, we are behind advection front and $\mathrm{erfc}[−0.26344]$, substitution $\mathrm{erfc}[−\beta] = 1 + \mathrm{erf}[\beta]$ is used, then $C = C_0/2\times1.2904 = 64.52$ mg/L

Table 7.2 Values of complementary error function erfc [erfc(−β) = 1 + erf(β)].

β	erf (β)	erfc (β)
0	0	1.0
0.05	0.056372	0.943628
0.1	0.112463	0.887537
0.15	0.167996	0.832004
0.2	0.222703	0.777297
0.25	0.276326	0.723674
0.3	0.328627	0.671373
0.35	0.379382	0.620618
0.4	0.428392	0.571608
0.45	0.475482	0.524518
0.5	0.520500	0.479500
0.55	0.563323	0.436677
0.6	0.603856	0.396144
0.65	0.642029	0.357971
0.7	0.677801	0.322199
0.75	0.711156	0.288844
0.8	0.742101	0.257899
0.85	0.770668	0.229332
0.9	0.796908	0.203092
0.95	0.820891	0.179109
1.0	0.842701	0.157299
1.1	0.880205	0.119795
1.2	0.910314	0.089686
1.3	0.934008	0.065992
1.4	0.952285	0.047715
1.5	0.966105	0.033895
1.6	0.976348	0.023652
1.7	0.983790	0.016210
1.8	0.989091	0.010909
1.9	0.992790	0.007210
2.0	0.995322	0.004678
2.1	0.997021	0.002979
2.2	0.998137	0.001863
2.3	0.998857	0.001143
2.4	0.999311	0.000689
2.5	0.999593	0.000407
2.6	0.999764	0.000236
2.7	0.999866	0.000134
2.8	0.999925	0.000075
2.9	0.999959	0.000041
3.0	0.99978	0.000022

7.8 Breakthrough Curve and Tracer Tests

When a tracer is injected into 1-D column in laboratory, the curve $C/C_0 = f(t)$ for the outlet of column is called the breakthrough curve (Fig. 7.2).

The time $t_{0.5}$ of arrival of normalized concentration $C/C_0 = 0.5$ can be used to calculate advection velocity as $v = L/t_{0.5}$, where L is length of column. When both conservative (non-adsorbed) tracer and adsorbed tracer are used, the retardation coefficient R can be calculated as

$$R = (t_{0.5})_{ads}/(t_{0.5})_{cons} \qquad 7.25$$

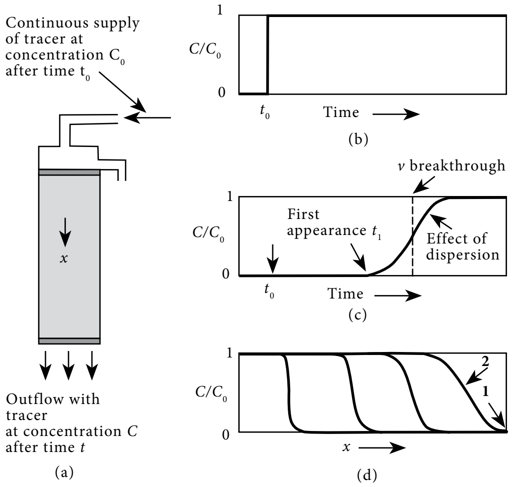

Figure 7.2 Breakthrough curve for 1-D column (after Freeze and Cherry, 1979).

The breakthrough curve can be also used to calculate longitudinal dispersivity α_L by inverse application of the Ogata-Banks solution (equation 7.21), but as we stated earlier, the dispersivity values obtained at laboratory scale have limited use at field scale. The column study can also be used to derive decay rate constant. In that case, several sampling ports across a column have to be installed and profile $C = f(x)$ in column is obtained. The concentration vs. distance curve is related to concentration vs. time curve using known velocity value:

$$C = C_0 \exp[-\lambda\,(x/v)] \qquad 7.26$$

Then the decay constant λ can be calculated easily by multiplying of slope in $\ln(C/C_0)$ vs. x graph, which is equal to $-\lambda/v$, by advective velocity of flow v. In that case, the influence of dispersion is included in decay constant and dispersion is considered as negligible.

Tracer tests in the field are performed by injection of tracer into ground water, followed by monitoring of

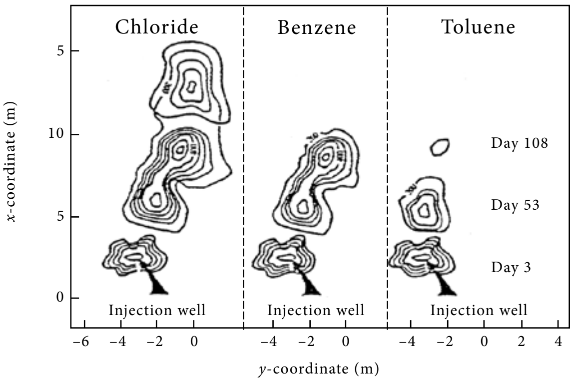

Figure 7.3 Instantaneous injection natural gradient tracer test (after Barker et al., 1987). Chloride represents conservative tracer, benzene decaying and retarded tracer and toluene represents fast-decaying tracer, which almost disappeared before last sampling campaign.

its migration in time. Mode of injection can be both instantaneous or continuous. The best data provides natural gradient test, when tracer(s) is injected into natural flow field. Results are used to calculate dispersivity values, and when comparison with a conservative tracer (chloride, bromide etc.) is available, values of retardation coefficient and decay constant can also be obtained (Mackay et al., 1986). Results of instantaneous injection, natural gradient test performed by Barker et al. (1987) are in Fig. 7.3. Forced gradient test is based on injection of tracer into injection well and its recovery from pumped well. In this case, flow field is influenced by pumping and results are less reliable than in previous case. Finally, one well tracer test is based on injection tracer into a well and recovery of tracer from the same well (Fetter, 1999). A variant of the test called push-pull test is based on injection of decaying and non-decaying tracers. It is used for determination of natural attenuation decay constant.

References

Barker J.F., Patrick G.C., Major D., 1987: Natural attenuation of aromatic hydrocarbons in shallow sand aquifer, *Ground Water Monitoring Review*, 7, pp. 64–71.

Bear J., 1979: *Hydraulics of Groundwater*, McGraw-Hill, New York.

Domenico P.A., Schwartz F.W., 1998: *Physical and Chemical Hydrogeology,* 2nd Edition, John Wiley and Sons, New York.

Fetter C.W., 1999: *Contaminant Hydrogeology*, 2nd Edition, Prentice Hall, Upper saddle River, NJ 07458.

Freeze R.A., Cherry J.A., 1979: *Groundwater*, Prentice Hall, Englewood Cliffs, New Jersey.

Mackay D., Freyberg D.L., Roberts P.V., Cherry J.A., 1986: A Natural Gradient Experiment on Solute Transport in a Sand Aquifer, I. Approach and Overview of Plume Movement, *Water Res. Research,* Vol. 22, No. 13, pp. 2017–2029.

Chapter 8: Contamination by Metals

8.1 Behavior of Metals in Water

Metals generally occur in ground water in low concentrations, less than 1 mg/L. However, it is often more than MCL (maximum contaminant level). Some metals dissolved in ground water have only one oxidation number, for example Pb^{2+}, Zn^{2+} , and Cd^{2+}. Other metals have several oxidation numbers, for example Fe^{2+} and Fe^{3+}, Mn^{2+} and Mn^{4+}, and Cr^{3+} and Cr^{6+}. Information about the oxidation state of a metal is essential for its speciation because different forms of a metal have different mobility in ground water (for example, Fe^{2+} is quite mobile and Fe^{3+} is immobile at neutral pH region), for determination of its toxicity (for example, Cr^{6+} is more toxic than Cr^{3+}), and for determination of its affinity to adsorption (for example, As^{5+} is more adsorbed than As^{3+}).

Compared to organic contaminants, there is no decay of metals during there transport and the total amount of a metal in an aquifer remains the same (of course, if there is no pumping of contaminated ground water). Metals can only change their form, for example, Cr^{6+} is reduced to Cr^{3+}, which then precipitates as $Cr(OH)_3(s)$. Total concentration of Cr in an aquifer remains the same, but Cr is immobilized in solid phase as $Cr(OH)_3(s)$. However, this solid phase may re-dissolve in future if pH and Eh change.

Concentration of metals can be limited by precipitation of their mineral phases like carbonates (for example, cerussite, $PbCO_3$, and smithsonite, $ZnCO_3$), sulfates (melanterite, $FeSO_4 \cdot 7H_2O$, chalkanthite, $CuSO_4 \cdot 5H_2O$, and anglesite, $PbSO_4$), and sulfides (secondary pyrite, FeS_2, and orpiment, As_2S_3). This means that for evaluation of the possibility of precipitation we have to determine concentrations of principal ions and not only concentrations of contaminating metals. The influence of principal ions is three-fold: 1) They contribute to ionic strength of solution, and thus, they influence activity coefficients γ_i of metals because activity coefficients are function of ionic strength I, $\gamma_i = f(I)$. 2) They increase total dissolved concentrations of metals by formation of complexes like $PbSO_4^0$. 3) They may participate in precipitation of minerals of metals. For example, precipitation of anglesite is expressed as

$$Pb^{2+} + SO_4^{2-} = PbSO_4(s) \qquad \log K_{sp} = -7.79 \text{ at } 25°C$$

where K_{sp} is the solubility product from thermodynamic database. Then ion activity product, *IAP*, is

$$[Pb^{2+}]\,[SO_4^{2-}] = IAP$$

where squared brackets indicate activities based on analytical concentrations corrected by geochemical modeling code for the influence of complexes (for example, lead in $PbSO_4^0$ is not included in Pb^{2+}) and calculated as products of activity coefficients and concentrations. Saturation index SI is defined as

$$SI = \log(IAP/K_{sp}) \qquad 8.1$$

When $IAP = K_{sp}$, ground water is at equilibrium with anglesite. When $IAP < K_{sp}$, the $SI < 0$ and anglesite should dissolve, if present in solid phase. If $IAP > K_{sp}$, the $SI > 0$ and anglesite should precipitate.

However, in many cases saturation with respect to contaminant minerals is not reached and the most important factor which controls concentrations of dissolved metals is their adsorption on oxides and hydroxides in solid phase like $Fe(OH)_3$ and MnOOH. These phases are unstable when pH and Eh conditions change and they may release adsorbed metals back to solution. Adsorption behavior of metals is a function of pH. Metals in cationic form (for example, Zn^{2+}) are more adsorbed when pH increases, and, on the other hand, metals in anionic form (for example, CrO_4^{2-}) are desorbed when pH increases (see Chapter 3). This phenomena is called adsorption edge and is related to deprotonation of adsorbent surface as a consequence of increasing pH (Langmuir, 1997). The surface charge of an adsorbent becomes more negative at higher pH values, with resulting attraction of cations and repulsion of anions. Organic matter in both solid and dissolved phase plays an important role in adsorption and complexation of metals. However, the characterization of organic matter composition is complicated and costly.

The hydroxides and organic matter play an important role in preservation of samples. If a sample has colloidal $Fe(OH)_3$ or organic matter, then there will be a significant difference in metal concentrations between filtered and unfiltered samples. Furthermore, if there is Fe^{2+} in a sample, then acidification of the sample to pH about 2.0 will prevent oxidation of Fe^{2+} to Fe^{3+} followed by precipitation of $Fe(OH)_3$, and adsorption of dissolved metals. The overall reaction is expressed as

$$Fe^{2+} + 0.25O_2(g) + 2.5H_2O + Me^{2+} \rightarrow \rightarrow Fe(OH)_3(s){\equiv}Me^{2+} + 2H^+ \qquad 8.2$$

where Me^{2+} is a metal and ≡ indicates adsorption on surface of ferric hydroxide.

This means that we have to filter and acidify samples in the field, to prevent removal of metals by adsorption before analysis.

There are three redox zones of conceptual model of migration of metals (Fig. 8.1). In the Zone 1, oxidized zone with O_2 dissolved in ground water, ferric hydroxide is stable and metals are adsorbed. In the Zone 2, intermediate zone, there is no more dissolved oxygen and $Fe(OH)_3$ becomes unstable. Its dissolution produces dissolved metals in ground water. Their is no factor controlling metal concentrations in ground water, except for precipitation of carbonate minerals like siderite, $FeCO_3$, as a sink for Fe^{2+} in some cases. However, conditions in Zone 2 are not reducing enough for sulfate reduction. In the Zone 3, reduced zone, there is reduction of sulfate and incorporation of metals in secondary sulfides like FeS, and PbS:

$$2CH_2O + SO_4^{2-} \rightarrow H_2S + 2HCO_3^- \qquad 8.2$$

$$Me^{2+} + H_2S \rightarrow MeS + 2H^+ \qquad 8.3$$

where Me^{2+} represents a metal. Reactions in Zone 3 are also a basis for remediation of contamination by metals in permeable reactive barriers (*PRB*), filled with organic matter (Chapter 12).

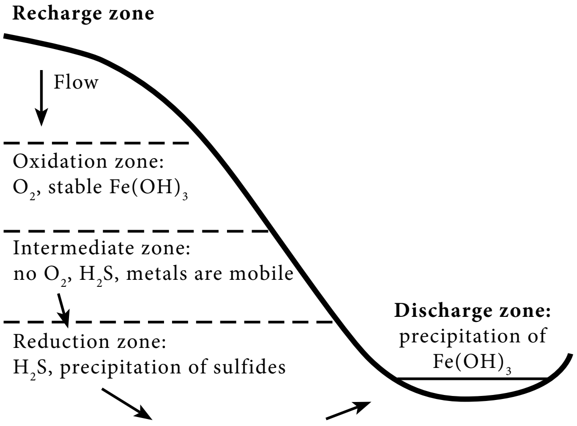

Figure 8.1 Conceptual model of redox zones in transport of metals.

In a graph of concentration in solid phase vs. concentration in water (Fig. 8.2) we can also distinguish 3 zones. In the zone A, concentration is not sufficiently high for precipitation of a mineral and concentration in water increases depending on adsorption on solid phase. The key parameter is the linear adsorption coefficient K_d (see Chapter 3.5).

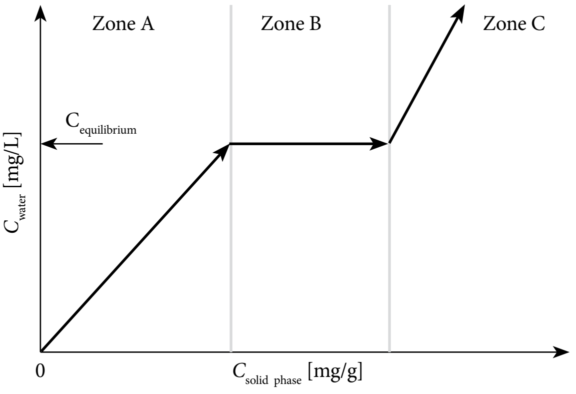

Figure 8.2 Behavior of a metal (see explanation in text).

The higher is K_d, the lower is the slope of line in Zone A of the graph.

When concentration reaches the value necessary for precipitation of a mineral of contaminant (for example, anglesite in the case of lead), then there is concentration plateau (Zone B) at equilibrium concentration because all contaminant entering water is implemented into the mineral. If the concentration of other specie(s) forming the mineral is not high enough, then there is no more limiting factor after addition of more contaminant and concentration increases without any limitation (Zone C).

8.2 Examples of Contaminants

Examples of lead, chromium and arsenic are presented in the following text.

8.2.1 Lead

Lead occurs in ground water only in one oxidation state, as Pb^{2+}. However, it can form complexes with carbonates, sulfates, and chlorides. In this case total lead concentration is

$$[Pb]_{total} = [Pb^{2+}] + [PbSO_4^0] + [PbHCO_3^+] + [PbCO_3^0] + + [PbCl^+] \qquad \text{etc.} \quad 8.4$$

In oxidized and moderately reducing environment, lead is dissolved, but can precipitate as cerussite at higher pH and dissolved inorganic carbon (*DIC*) values. Principal limiting factor for migration of lead in oxidized environment is its adsorption on $Fe(OH)_3$ and MnOOH. Adsorption begins at pH about 4.0 and adsorption intensity increases with increasing pH. At pH about 6.0, all lead is completely adsorbed. Adsorption may be prevented or shifted towards higher pH values by complexation of lead with anions like sulfate or with organic matter. In this case, there can be high concentration of lead in solution even at neutral pH region.

When an environment is reduced and sulfate reduction occurs, lead can precipitate as secondary galena, PbS. In oxidized environment with high concentrations of sulfate like acid mine drainage (*AMD*) sites, there can be precipitation of anglesite, $PbSO_4$. Inorganic speciation of lead is in Fig. 8.3.

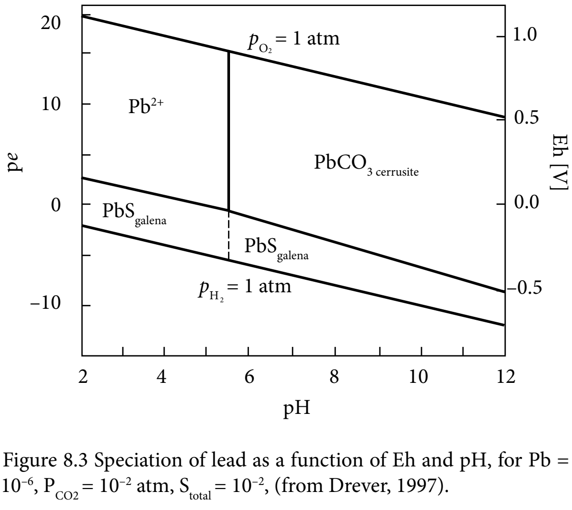

Figure 8.3 Speciation of lead as a function of Eh and pH, for Pb = 10^{-6}, $P_{CO2} = 10^{-2}$ atm, $S_{total} = 10^{-2}$, (from Drever, 1997).

8.2.2 Arsenic

Arsenic is metalloid and occurs in ground water in 3+ and 5+ forms. Oxidized arsenic (arsenate) is present as $H_2AsO_4^-$ at lower pH values and as $HAsO_4^{2-}$ at higher pH values (Fig. 8.4).

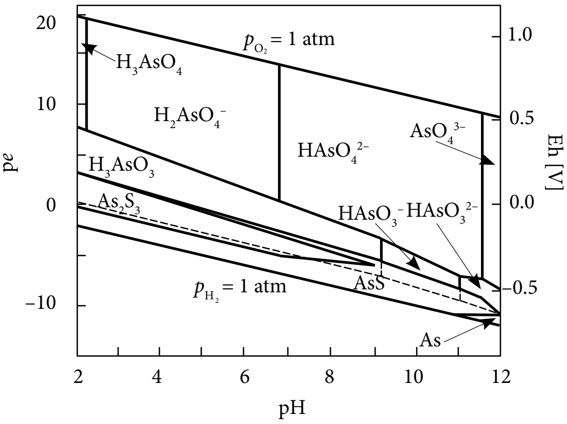

Figure 8.4 Speciation of arsenic as a function of Eh and pH, As=10^{-6}, $S_{total}=10^{-2}$, (from Drever, 1997).

Reduced arsenic (arsenite) is present as $H_3AsO_3^0$ at wide range of pH values, and only at pH above 9.0 there is formation of $H_2AsO_3^-$. The most important mineral, which can control arsenate concentration in water, is scorodite, $FeAsO_4.2H_2O$. However, the mineral is stable only at pH about 4.5, and its precipitation requires very high concentrations of dissolved As^{5+} and Fe^{3+}. Less soluble Fe(III) oxide and hydroxides generally exert more significant control on dissolved arsenic concentration. Both forms of arsenic are adsorbed on Fe(III) oxide and hydroxides, but As^{5+} has a stronger affinity for adsorption than As^{3+} (Pierce and Moore, 1982).

Adsorption of As^{5+} decreases with increasing pH due to the de-protonation of Fe(III) oxide and hydroxides surface and adsorption maximum is at pH about 4.0. Adsorption maximum for As^{3+} is at pH about 7.0, but the adsorption intensity is always lower than for As^{5+}. Some Fe(III) minerals like $Fe(OH)_3$ are unstable mineral phases, and they can dissolve when Eh and pH decrease with resulting release of adsorbed arsenic. When amorphous $Fe(OH)_3$ is aging and transformed to goethite, its specific surface decreases and this effect can also contribute to the release of adsorbed arsenic (Deutsch, 1997). Another factor, which can cause desorption of arsenic is its replacement from adsorption sites by an anion with stronger affinity for adsorption such as phosphate (Welch and Lico, 1998). This means that an application of phosphate fertilizers may cause contamination of ground water by arsenic. When an environment is strongly reduced and sulfate reduction occurs, secondary sulfides like As-pyrite and orpiment, As_2S_3, may incorporate arsenic.

8.2.3 Chromium

Chromium has 3+ and 6+ forms in ground water, and both forms have different properties and behavior. Chromium 6+ is in anionic form like $HCrO_4^-$ or CrO_4^{2-}, depending on pH (Fig. 8.5). This means that its adsorption also depends on pH, and adsorption intensity decreases with increasing pH. Reported values of distribution coefficient K_d are in the range from 0.24 to 52 mL/g (Calder 1988, in: Henderson 1995).

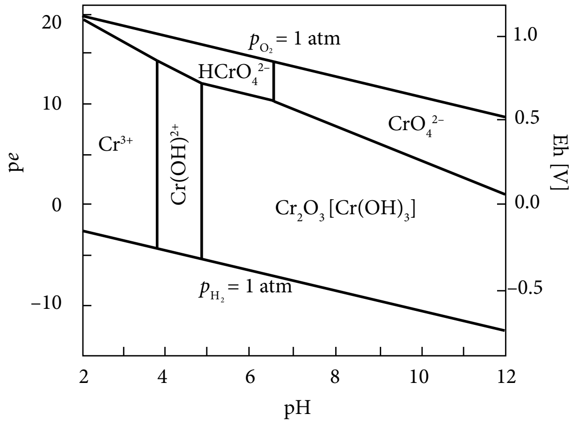

Figure 8.5 Speciation of chromium as a function of Eh and pH, $Cr_{total} = 10^{-6}$ (from Drever, 1997).

Reduced Cr^{3+} has cationic form except for pH > 12.0, where can be present as $Cr(OH)_4^-$. In the pH range from 6.0 to 12.0 (depending on concentration of Cr_{total}), Cr^{3+} precipitates as insoluble $Cr(OH)_3$. However, Cr^{6+} must be reduced to Cr^{3+} before precipitation of $Cr(OH)_3$ can take place. Reducing agents can be organic matter (both dissolved and in solid phase, but solid organic matter pool is generally much larger), and Fe^{2+} in reaction like

$$3Fe^{2+} + CrO_4^{2-} + 7H_2O = 3Fe(OH)_3 + Cr(OH)_2^+\ 3H^+ \qquad 8.6$$

In many cases Cr^{3+} co-precipitates together with Fe^{3+} in the form of $(Cr_xFe_{1.0-x})(OH)_3$ mineral.

Kinetics of Cr^{6+} to Cr^{3+} reduction is slow at neutral pH region and increases at acidic pH region. Half-life for Cr^{6+} reduction at pH 7.0 was determined as 2.5 years (Henderson, 1995). The chromium reduction and $Cr(OH)_3$ precipitation is a basis for decontamination in reactive permeable walls (PRB) filled by Fe^0 or organic matter (Chapter 12).

8.3 Investigation of Sites Contaminated by Metals

Solubility of mineral phases, which contain metals as their components, generally represent the upper limit for metal concentrations (Drever, 1997). High concentrations of metals are often related to formation of complexes with organic matter. Principal factor controlling dissolved metals concentration is their adsorption on ferric and manganese oxides and hydroxides. Intensity of adsorption increases with increasing pH for cations and decreases for anions.

The following approach can be used:

1) Determine the oxidation number of a metal, how: by analytical determination on perfectly preserved sample (preferred) or by splitting of total concentration of a metal on the basis of field Eh and the Nernst equation or on the basis of Eh calculated from other redox couple determined analytically and total concentration (questionable). These operations are implemented in geochemical programs like WATEQ4F and PHREEQC (Chapter 6).
2) Determine, if their is possibility of precipitation of a mineral containing the metal. We can use speciation program with input including temperature, pH, Eh, alkalinity, and concentration of principal ions. Negative SI value excludes precipitation of a mineral, but positive SI value does not prove precipitation! In an ideal case, precipitation of a mineral is proved by mineralogical methods such as scanning electron microscope (SEM with mocroprobe. Sequential extraction can be used to deduce a type of mineral (Tessier et al., 1996).
3) Determine, if there is a possibility of sulfate reduction, how: - from decreasing sulfate concentration and increasing alkalinity in the direction of flow, - from the absence of species which are reduced before sulfate like dissolved O_2, and NO_3^-, - from the presence of reduced sulfur species like H_2S and HS^- (warning: samples must be preserved in the field by Zn-acetate because reduced sulfur can be lost), and - from enrichment of residual sulfate in isotope ^{34}S.
4) If we can exclude the sulfate reduction, then adsorption is probable mechanism controlling dissolved metals concentrations. Determine, if there is colloidal hydroxide present (how: by comparison of filtered, acidified samples and unfiltered, acidified samples-difference is contributed to colloids), and if Fe(III) oxide and hydroxides are stable (by speciation program and redox indicators). Then determine K_d for a metal in batch experiment. If there is a significant pH change during migration, then we have to use surface

complexation modeling instead of the K_d approach. If data on metal concentration in solid phase are available, then we can calculate expected adsorbed amount $M_{adsorbed}$ [mg/in contact with 1 mL of water] using formula

$$M_{adsorbed} = (\rho_b/n)K_dC_w \qquad 8.7$$

where ρ_b is bulk density of solid phase [g/dm^3], n is porosity, K_d is linear distribution coefficient [L/g], and C_w is concentration in ground water [mg/L]. Then we compare it with M_{total} in solid phase sample. If the concentration in solid phase is higher then expected adsorbed concentration, then we have probably overlooked precipitation of a mineral. If dissolved concentration of metal is high even when water is supersaturated with respect to a reactive mineral of the metal, then there probably is complexation of the metal with organic matter.

References

Deutsch W.J., 1997: *Groundwater Geochemistry. Fundamentals and Applications to Contamination*, Lewis Publishers, Boca Raton, New York.

Drever J.I., 1997: *The Geochemistry of Natural Waters. Surface and Groundwater Environment*s, 3rd Edition, Prentice Hall, Upper Saddle River, NJ 07458.

Henderson T., 1994: Geochemical Reduction of Hexavalent Chromium in the Trinity Sand Aquifer, *Groundwater*, 33, pp. 759–768.

Langmuir D., 1997: *Aqueous Environmental Geochemistry,* Prentice Hall, Upper saddle River, NJ 07458.

Nikolaidis N.P., Robbins G.A., Scherer M., McAninch B., Binkhorst G., Asikainen J., Suib S., 1994: Vertical Distribution and Partitioning of Chromium in a Glaciofluvial Aquifer, *Ground Water Monitoring and Remediation*, Summer 1994, pp. 150–159.

Pierce M.L., Moore C.B., 1982: Adsorption of Arsenite and Arsenate on Amorphous Iron Hydroxide, *Water Res.*, 16, pp. 1247–1253.

Tessier A., Fortin D., Belzile N., Devitre R.R., Leppard G.G., 1996: Metal sorption to diagenetic iron and manganese oxyhydroxides and associated organic matter: Narrowing the gap between field and laboratory measurements, *Geochim. Cosmochim. Acta*, 60, pp. 387–404.

Welch A.H., Lico M.S., 1998: Factors Controlling As and U in Shallow Groundwater, Southern Carson Desert, Nevada, *Appl. Geochem.* 13(4), pp. 521–539.

Chapter 9: Acid Mine Drainage

9.1 Formation of Acid Mine Drainage

Term acid waters is used for waters with zero carbonate alkalinity ($pH < 4.5$) and with free ions of strong acid such as H_2SO_4. In some cases, pH is even lower than 2.0. Principal (but not the only one) source of acid waters are mining residuals and the mechanism responsible for generation of acidity is the oxidation of sulfides like pyrite, FeS_2. In the absence of mining, acid waters are not common because the oxygen supply is insufficient to oxidize enough pyrite and to produce acidity higher than alkalinity of ground water. Water generally contains less than 10 mg/L (0.33 mmol/L) of dissolved O_2.

Situation changes dramatically when mining residuals with high concentration of pyrite are dumped. There are two principal types of mining residuals. First of them is waste rock, which was removed to access ore-bearing rocks. This material is deposited in waste rock piles, generally located in the proximity of a mine. Typical feature of waste rock is very heterogeneous size of particles, from clay fraction up to large blocks. The situation results in high permeability of waste rock and water table located close to the base of a pile. Second type of mining residuals are mine tailings. They are final by-products of ore-bearing rock extraction by technologies like flotation or application of cyanides. This material is crushed and milled prior to the treatment and resulting grain size is relatively small, corresponding to silt fraction. Mine tailings are located in depressions and water table is generally close to their surface as a consequence of their low permeability.

The oxidation of sulfides like pyrite is responsible for acid generation in both environments. Conceptual model of pyrite oxidation is shown in Fig. 9.1. At the beginning, pyrite is oxidized by oxygen in the presence of water and ferrous iron, Fe^{2+}, sulfate and H^+ ions are produced:.

$$FeS_2 + 7/2O_2 + H_2O = Fe^{2+} + 2SO_4^{2-} + 2H^+ \qquad 9.1$$

Ferrous iron is then oxidized to ferric iron, Fe^{3+},

$$Fe^{2+} + 1/4O_2 + H^+ = Fe^{3+} + 1/2H_2O \qquad 9.2$$

in a relatively slow reaction which can be catalyzed by bacteria *Thiobacillus Ferooxidans*. This reaction is the principal rate-limiting step of acid drainage formation (Stumm and Morgan, 1981). Further development depends on pH of water. If pH is higher than 3.0, then there is precipitation of ferric hydroxide, $Fe(OH)_3$, in reaction described as

$$Fe^{3+} + 3H_2O = Fe(OH)_3 + 3H^+ \qquad 9.3$$

Precipitated ferric hydroxide forms typical reddish layer at the bottom of streams draining mining wastes. This layer plays an important role in adsorption of metals like Pb^{2+}, Zn^{2+} etc. On the other hand, if pH is less than 3.0 and Fe^{3+} is in contact with unoxidized pyrite, the Fe^{3+} is consumed by pyrite oxidation because Fe^{3+} ion is strong oxidant:

$$FeS_2 + 14Fe^{3+} + 8H_2O = 15Fe^{2+} + 2SO_4^{2-} + 16H^+ \qquad 9.4$$

This means that oxygen is only necessary to start the oxidation of pyrite and to recycle Fe^{2+} to Fe^{3+}. However, if an accumulation of mining residuals contains high quantity of dissolved Fe^{3+} from the previous oxidation period, then the oxidation of pyrite will continue for

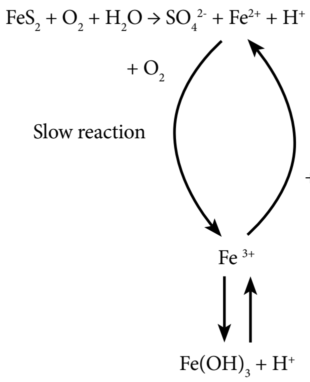

Figure 9.1 Conceptual model of oxidation of pyrite (adapted from Stumm and Morgan, 1981). Stoichiometrically balanced equations are in text.

long time even when there is no more oxygen supply. When both oxidation of ferrous iron and precipitation of ferric hydroxide take place, the coupled reaction is

$$Fe^{2+} + 1/4O_2 + 5/2H_2O = Fe(OH)_3 + 2H^+ \qquad 9.5$$

This means that there is generation of acidity in surface water bodies by the oxidation of Fe^{2+} and precipitation of ferric hydroxide even when discharging ground water originally has a neutral pH value.

9.2 Supply of Oxygen

All pyrite oxidation steps can take place in both waste rock and mine tailings. The principal difference between these two environments is in mechanism of oxygen supply and in the rate of acid generation. In fine grained mine tailings, the oxidation of pyrite takes place in relatively narrow zone (generally 0.5–5.0 m) between the surface of mine tailings and water table. The principal mechanism of the oxygen supply is diffusion in partially water filled porous media. The oxygen diffusion flux is expressed by First Fick's Law as the product of the effective diffusion coefficient for oxygen and the oxygen concentration gradient,

$$J_D = -D_{O2}\, dC_{O2}/dx \qquad 9.6$$

where J_D is diffusive oxygen flux, D_{O2} is effective coefficient of diffusion for oxygen and dC_{O2}/dx is oxygen concentration gradient in porous media. The principal problem is determination of D_{O2}, which is a function of water saturation and temperature. The following expression is applied (Reardon and Moddle, 1985)

$$D_{O2} = 3.9810^{-5}\, (\varepsilon - 0.05/0.95)^{1.7}\, T^{3.2} \qquad 9.7$$

where ε is porosity filled by air ($= n_{total} - n_{satur}$) and T is temperature.

In Fig. 9.2, we can see that D_{O2} decreases relatively slowly up to water saturation of about 60 % and then there is a sharp change about 5 orders of magnitude. The principal problem is the determination of the effective diffusion coefficient for oxygen because it decreases rapidly with increasing saturation of pore space by water.

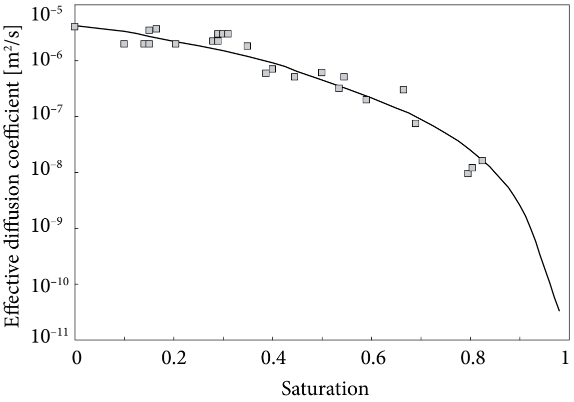

Figure 9.2 Relation between D_{O2} and water saturation (from Elberling, Nicholson, 1996).

There are 3 principal methods of *pyrite oxidation rate* (*POR*) determination:

1. Direct application of diffusive flux equation (Equation 9.6): Concentrations of O_2 are measured at different depth and then we can determine gradient of oxygen concentration. Then we need to know water saturation to determine D_{O2}. The simplest approach is to collect undisturbed mine tailings samples in vadose zone, and then calculate water saturation from weight difference before and after drying. The method is tedious and other methods from soil science like neutron probe and time-domain reflectometry can be used. However, these methods require calibration. Then the D_{O2} value is determined from water saturation-D_{O2} graph (Fig. 9.1). Under steady-state conditions, the diffusive flux of oxygen J_D can be directly converted to pyrite oxidation rate.

2. Oxygen consumption method: The method is described in detail in Elberling, Nicholson, (1996), and only brief principle is presented here. Closed vessel is located on the surface of mine tailings and oxygen concentration is measured in the headspace between surface of mine tailings and the vessel. The oxygen concentration decreases because O_2 diffuses into mine tailings. Diffusive flux is calculated as

$$J_D = C_0\, (k\, D_{O2})^{1.2} \qquad 9.8$$

where $k \times D_{O2}$ is the slope of the graph $\ln(C/C_0)$ vs. t divided by A/V, C_0 is initial oxygen concentration in the vessel and C is oxygen concentration in time t, A is cross-section of the vessel, V is volume of the vessel above mine tailings interface, and k is kinetic constant of pyrite oxidation.

3. Sulfate mass balance: Sulfate concentration in pore water are determined, for example using samples from suction lysimeters installed at different depth in unsaturated mine tailings. Regardless of pyrite oxidation mechanism, 1 mol of oxidized pyrite produces 2 moles of sulfate, and sulfate produced during a certain period is converted to the amount of oxidized pyrite. However, precipitation of secondary sulfate minerals like gypsum and jarosite decreases sulfate concentration in water, and the pyrite oxidation rate is underestimated.

In summary, the pyrite oxidation rate in mine tailings is relatively slow and generally takes place in the time scale of tens of years. On the other hand, very permeable waste rock material has very high effective diffusion coefficient for oxygen and the pyrite oxidation rate is very high. The oxidation of pyrite is exotermic reaction and strong temperature gradients can develop within a waste rock pile. Temperature close to the slope of waste rock pile at Mine Doyon site, Québec, Canada, reaches 67°C. In this case, strong temperature gradients result in pressure gradients and the air with oxygen is sucked into the pile (Sracek et al., 2004). This process, called convection, takes place close to the slope and in the upper part of a waste rock pile and can increase the pyrite oxidation rate significantly. Thus, the oxidation of pyrite in waste rock is often very fast and concentrations of species like sulfate, Fe^{2+}, and H^+ in discharging water often reach extreme values.

9.3 Neutralization of Acid Mine Drainage

In either case, there is generally acid plume with high concentrations of dissolved species in mine tailings and in later period in an aquifer, moving in the direction of hydraulic gradient towards local surface water bodies. Regardless of the acid drainage generation mechanism, several common processes take place. If solids in mine tailings and in the aquifer contain high concentrations of carbonates like calcite, $CaCO_3$, and dolomite, $CaMg(CO_3)_2$, then H^+ ions in the acid plume are consumed in relatively fast neutralization reactions taking place during dissolution of these minerals. Dissolution of calcite is expressed as

$$CaCO_3 + H^+ = Ca^{2+} + HCO_3^- \qquad 9.9$$

or at pH below 6.3 as

$$CaCO_3 + 2H^+ = Ca^{2+} + H_2CO_3^0 \qquad 9.10$$

In this case, pH in the aquifer is maintained at close to neutral region (pH 6.0–7.0). However, $H_2CO_3^0$ which forms during neutralization, can prevent later pH increase due to de-protonation of H^+ in formation of HCO_3^-. This means that the reactions above are efficient when de-gassing of CO_2 is possible, e.g. in unsaturated zone or close to water table (Webb and Sasowsky, 1994).

Movement of the acid plume is slower compared to the movement of Fe^{2+} and sulfate plumes. The movement of Fe^{2+} can also be slowed down by the formation of siderite, $FeCO_3$,

$$Fe^{2+} + CO_3^{2-} = FeCO_3 \qquad 9.11$$

If mining residuals have high content of carbonates, the acid drainage can be neutralized directly within them and low pH plume does not penetrate to the aquifer in their vicinity. After consumption of fast neutralization minerals like carbonates, several other reactions contribute to the buffering of acid drainage. Typical reactions are dissolution of previously formed siderite (pH around 5.0) and hydroxides like $Al(OH)_3$ (can maintain pH at about 4.5),

$$Al(OH)_3 + 3H^+ = Al^{3+} + 3H_2O \qquad 9.12$$

and $Fe(OH)_3$ (pH at about 3.0),

$$Fe(OH)_3 + 3H^+ = Fe^{3+} + 3H_2O \qquad 9.13$$

These buffers are generally formed during earlier, carbonate stage of the AMD buffering, and after their depletion principal buffering is related to the dissolution of silicates like muscovite and feldspars. However, kinetically constrained dissolution of silicates is slow, cannot maintain pH at neutral region, and also contributes harmful components like aluminum to water.

Concept of buffering plateaus is shown in Fig. 9.3. We can see that different types of buffering can occur in different zones of a contaminant plume. Even relatively low calcite content in solid phase (below 1.0 wt %) can slow down migration of acid plume. The retardation factor R for H^+ is calculated as

$$R = 1 + (m_{calcite}/m_{H+}) \qquad 9.14$$

where $m_{calcite}$ is the amount of calcite in contact with 1 L of water and m_{H+} is molar concentration of H^+ (e.g., 10^{-pH}).

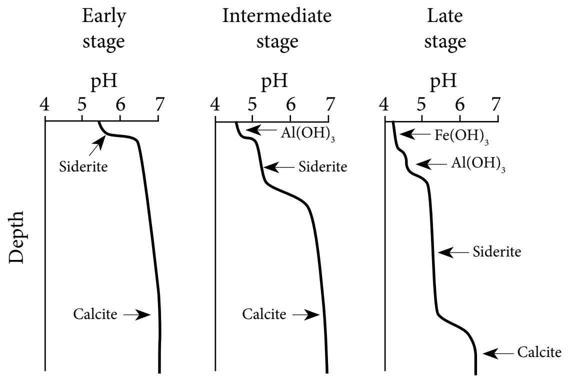

Figure 9.3 Buffering zones in the AMD plume (based on Blowes and Ptacek, 1994).

Problem: Velocity of ground water flow in an aquifer between mine tailings and a lake is 5m/day, porosity is 0.4, and bulk density of solid phase is 2.65 g/cm^3. The distance between mine tailings and lake is 100 m, pH of leachate is 2.4 and there is 1.5 wt % of calcite in solid phase. Calculate the time of acid plume migration to reach the lake.

Solution: 1m^3 of aquifer contains 600 dm^3 of solid phase and 400 dm^3 of water, thus 1 L of water is in contact with 600/400 = 1.5 dm^3 of solid phase, or with 1.5×2.65 = 4.05 kg of solid phase, which contains 4050×0.015 = 60.75 g = 0.6075 mol of calcite

1 mol of calcite neutralizes 1 mol of H^+

pH = 2.4 → $H^+ = 10^{-2.4} = 3.98\times10^{-3}$ mol

$R = [1 + (0.6075)/(3.98\times10^{-3})] = 154$

Water flows to the lake 100 m/(5 m/day) = 20 days

H^+ migration takes 20×154 = 3080 days = 8.44 years

During neutralization of AMD by carbonates there often is formation of gypsum, $CaSO_4.2H_2O$:

$$Ca^{2+} + SO_4^{2-} + 2H_2O = CaSO_4.2H_2O \qquad 9.15$$

This reaction can slow down the migration of sulfate, but to less extent than is the retardation of H^+.

After dissolution of $Fe(OH)_3$ there is dissolution of silicates. An example is dissolution of chlorite,

$$(Mg_4FeAl)(AlSi_3)O_{10}(OH)_8 + 16H^+ = \\ = 2Al^{3+} + Fe^{2+} + 4Mg^{2+} + 3H_4SiO_4 + 6H_2O \qquad 9.16$$

The reaction is kinetically constrained, and also contributes toxic aluminum to water. In this stage, there can be precipitation of jarosite,

$$K^+ + 3Fe^{3+} + 2SO_4^{2-} + 6H_2O = KFe_3(SO_4)_2(OH)_6 + 6H^+ \qquad 9.17$$

which can incorporate a large amount of dissolved sulfate.

We can summarize that if there are fast-acting neutralization minerals like carbonates in aquifer matrix, then the acid drainage can be neutralized completely. However, even if the water has neutral pH and contains high concentrations of dissolved iron and aluminum, then there is generation of acidity in surface streams during precipitation of aluminum and ferric hydroxides. The acidity in H^+ form can be only a smaller part of total potential acidity expressed as

$$\text{Potential acidity} = m_{H+} + 3m_{Al3+} + 2m_{Fe2+} + 3m_{Fe3+} \qquad 9.18$$

Coefficients are based on equations 9.12., 9.5 and 9.13 and m indicates concentrations in mol/L.

Problem: Determine total potential acidity of water sample with pH=2.4, Al^{3+} =400 mg/L, Fe^{2+} = 500 mg/L, and Fe^{3+} = 250 mg/L. Use equation 9.18.

Solution: Use equation 19. For pH = 2.4 concentration of $H^+ = 10^{-2.4} = 0.00398$ mol/L

Al^{3+} = 400 mg/L = 0.01483 mol/L×3 = 0.04449 mol/L

Fe^{2+} = 500 mg/L = 0.00895 mol/L×2 = 0.0179 mol/L

Fe^{3+} = 250 mg/L = 0.00448 mol/L×3 = 0.01344 mol/L

Total potential acidity is 0.07981 mol/L, and H^+ acidity is only of about 5 % of this value.

If there are no fast-acting neutralization minerals in an aquifer matrix and minerals like quartz and silicates predominate, then the migration of acid plume can be almost as fast as water flow.

9.4 Hydrogeology of Mining Wastes

Velocity of flow in mine tailings is generally low, of about 1 – 2 m/year. This is related to their small grain size and resulting low permeability. This means that residence period of water in mine tailings is in order of tens of years. We can use common programs for ground water flow modeling to determine flow pattern.

On the other hand, porous media in waste rock piles represents extremely heterogeneous unsaturated environment with multiple porosity, and strong temperature gradients. Furthermore, there are extremely high dissolved solids concentrations in pore water and density of water is often higher than 1.0 g/cm^3. Permeability of waste rock material is often high, with saturated hydraulic conductivity more than 10^{-3} m/s. During a rainfall event, a part of infiltrated water passes through a pile and emerges at its base in hours after the beginning of rain. However, a part of water in partially decomposed rock blocks is almost immobile. Fractures between large blocks are preferential flow zones during recharge period. During dry period, they drain first and then become barriers for water flow, which takes place mostly in fine grained material around fractures.

9.5 Prevention and Remediation of Acid Mine Drainage.

Acid drainage represents challenging problem for prevention and remediation. If mining residuals are responsible for its generation, several control and remediation options are available. Classical option is collection and treatment of leachate, but this is relatively costly. Other methods are based on the oxygen transport control.

The penetration of oxygen to mining residuals can be prevented by installation of fine-grained layer on the surface of mining residuals (Elberling, Nicholson, 1996). In this case, the effective diffusion coefficient for oxygen D_{O2} in the fine-grained material is low and so is the pyrite oxidation rate. It is related to rapid reduction of D_{O2} with increasing water saturation in fine grained material (see Fig. 9.2).

Another method is based on the application of organic material layer on the surface, in which the oxygen is consumed before its penetration to mining residuals in reaction like

$$CH_2O + O_2 \rightarrow CO_2 + H_2O \qquad 9.19$$

Potential problems are related to the formation of toxic methylated metal species under very reducing (methanogenic) conditions. The implementation of organic material cover has to be done immediately after closure of mine tailings. If the material in mine tailings is already partially oxidized, and there is large amount of $Fe(OH)_3$ in solid phase, then the implementation of organic cover could cause dissolution of $Fe(OH)_3$, and release of adsorbed metals. In some cases, mine tailings can be flooded completely to prevent contact with atmospheric oxygen. However, the flooding can decrease stability of mine tailings dams and may not be applicable in some cases.

When acid plume is already migrating in an aquifer, the situation becomes more complex. In this case, classical remediation and control technology is pump and treatment of acid water. In some situations, the volume of pumped and treated water is too large and application of this method can be inefficient. The injection of water with dissolved carbonates can be a plausible option. However, solubility of calcite under normal atmospheric pressure conditions is low and resulting bicarbonate concentration is only about 1 mmol/L (61 mg/L) with pH about 8.3. Furthermore, if water contains a significant quantity of iron, then the interaction of oxygenated alkaline water with the plume would results in precipitation of $Fe(OH)_3$ and in plugging of infiltration wells in short time period.

There are some new promising technologies for remediation of acid drainage plumes being developed. One of them is the installation of permeable reactive barrier (PRB) with crushed calcite and reducing material such as organic matter in the direction of acid plume migration. The barrier is located in the direction of the acid plume migration and must have higher permeability than the surrounding aquifer because in the opposite case it would be by-passed by the plume. There is neutralization of acid plume and reduction of sulfate within the PRB, followed by the precipitation of iron and other metals in secondary sulfides. The principal limitation of the method is the residence time requirement of 1 – 2 days within the wall to complete chemical reactions. Assuming the economically acceptable thickness of the wall of about 1 m, the maximum velocity of ground water flow for application of the method is 0.5 – 1.0 m/day.

9.6 Investigation of Acid Mine Drainage Sites

The investigation of mine tailings can be divided into investigation of unsaturated zone and saturated zone.

Common method of unsaturated zone investigation is the determination of O_2 and CO_2 concentration in pore space gas. This is done by inserting hollow needles connected to gas sensor on the ground surface. The result are O_2 and CO_2 profiles with depth, with decreasing and increasing concentrations, respectively. The O_2 profile can be used for calculation of pyrite oxidation rate. We can also use the O_2 profile to evaluate the performance of oxygen barriers. If there is high water saturation of fine grained material, then there is low O_2 concentration below the barrier (less than 2 vol %) with resulting low pyrite oxidation rate. There also is low O_2 concentration below organic matter layer.

Another important parameter is water saturation. High degree of water saturation is desirable because in this case diffusion coefficient for oxygen is low. The most common method for determination of water saturation is based on the difference of weight of sample before and after drying. The method is tedious and can be used only once with a particular sample. Other methods are the application of time domain reflectometry (TDR) and neutron probe. Both methods require calibration and are costly. Thus, the oxygen profiles are the most common method for monitoring of unsaturated zone in mine tailings. Pore water in unsaturated zone can be collected by suction lysimeters.

Piezometers located at different depth are necessary to collect water in saturated zone of mine tailings because there generally is a significant vertical zonality of water chemistry. Another important parameter gained from piezometers are hydraulic heads. There generally are strong vertical gradients in the central part of mine tailings and flow becomes more horizontal in their periphery. Piezometers are also used to run slug or bail test and resulting values of K with values of hydraulic heads are used for modeling of flow in saturated zone of mine tailings. Monitoring of chemistry should be focused on index parameters (usually pH, total iron, aluminum etc.) determined in the initial stage of project.

Problems related to the sampling of acid mine drainage are discussed in Deutsch (1997). One of advantages is that the value of redox potential Eh corresponds well to the value based on Fe^{2+}/Fe^{3+} couple. Geochemical programs such as WATEQ4F (Plummer et al., 1976) can be used to predict which minerals could control concentrations of dissolved species in ground water. Solid phase composition is generally necessary for interpretation of data (Blowes and Jambor, 1990). The most important parameter is concentration of buffers like calcite and dolomite. Interpretation of water chemistry data can be improved by the determination of quantity of secondary sulfate minerals gypsum and jarosite in solid phase.

Situation in the case of waste rock piles is more complicated. Principal method is installation of thermistors and gas sampling ports at different depth (Lefebvre et al., 1993). Zones with high pyrite oxidation rate show positive temperature anomalies and high oxygen concentrations. These zones are generally located close to slopes and at the upper boundary of a waste rock pile (Sracek et al. 2004). It is possible to sample pore water in unsaturated zone of a pile by suction lysimeters (down to depth of about 15 m), but the method is complicated and rarely used. Much more common is the monitoring of the outflow from the saturated zone at the base of waste rock pile (Ritchie, 1994). However, water chemistry of the outflow represents mixing of water from different zones of the waste rock pile and interpretation of geochemical processes on the basis of the data is complicated.

References.

Blowes D.W., Jambor J.I., 1990: The Pore-water Geochemistry and Mineralogy of the Vadose Zone of Sulfide Tailings, Waite Amulet, Québec, Canada, *Appl. Geochem.* 5, pp. 327 – 346.

Blowes D.W., Ptacek C.J., 1994: Acid-neutralization Mechanism in Inactive Mine Tailings, In: J.L. Jambor, D.W. Blowes (Editors): *Short course handbook on environmental geochemistry of sulfide mine-wastes,* Mineralogical Association of Canada, pp. 271 – 292.

Deutsch W.J., 1997: *Groundwater Geochemistry, Fundamentals and Applications to Contamination,* Lewis Publishers, Boca Raton, New York.

Elberling B., Nicholson R.V., 1996: Field determination of sulfide oxidation rates in mine tailings, *Water Res. Research*, 32, pp. 1773–1784.

Lefebvre R., Gelinas P., Isabel D., 1993: Heat Transfer during Acid Mine Drainage Production in a Waste Rock Dump, Le Mine Doyon, Québec, *Report GREGI* 93-03 for CANMET, 46 p.

Plummer L.N., Jones B.F., Truesdall A.H., 1976: WATEQ4F-A Fortran IV Version of WATEQ, a Computer Program for Calculating Chemical Equilibria of Natural Waters, *U.S. Geological Survey Water Resources Investigations Report* 76–13, 61 p.

Reardon E.J., Moddle P.M., 1985: Gas Diffusion Coefficients Measurements on Uranium Mine Tailings: Implications to Cover Layer Design, *Uranium*, Vol. 2, pp. 115–131.

Ritchie A.I.M., 1994: Sulfide Oxidation Mechanism: Controls and Rates of Oxygen Transport, In: J.L. Jambor, D.W. Blowes (Editors): *Short course handbook on environmental geochemistry of sulfide mine-wastes,* Mineralogical Association of Canada, pp. 201–245.

Sracek O., Choquette M., Gélinas P., Lefebvre R., Nicholson R.V., 2004: Geochemical characterization of acid mine drainage from a waste rock pile, Mine Doyon, Québec, Canada, *J. Contam. Hydrol.*, 69, pp. 45–71.

Stumm W., Morgan J.J., 1981: *Aquatic Chemistry*, 3rd Edition, New York, Wiley-Interscience.

Webb J.A., Sasowsky I.D., 1994: The Interaction of Acid Mine Drainage with a Carbonate Terran: Evidence from the Obey River, North-central Tennessee, *J. Hydrology* 161, pp. 327–346.

Chapter 10: Behavior of Radionuclides

10.1 Introduction

Lord Kelvin estimated the age of the solar system to be about 100 million years, based on the assumption that the energy of Sun was derived from gravitational collapse. In 1897 he revised this estimate downward to the range of 20 to 40 million years. Geologists were particularly skeptical of Kelvin's revised estimate, feeling the Earth must be older than this, but had no quantitative means of supporting their arguments. Radioactivity had been discovered about the same time (1896) by Frenchman Henri Becquerel. Only eleven years elapsed before Bertram Boltwood, an American chemist, published the first 'radiometric age'. He determined the lead concentrations in three samples of pitchblende, a uranium ore, and concluded they ranged in age from 410 to 535 million years.

Beyond providing precise ages of geologic events, radioactive decay is important because it provides natural tracers of geologic processes and because it provides information on the rates and pathways of geologic evolution. We might add dye to downwelling ocean water to trace deep ocean currents, or add a radioactive tracer to subducting lithosphere to trace mantle convection currents. In practice, however, even the contemplation of such experiments is a bit absurd. We would need far too much dye or radioactive tracer: the scales of distance and mass are simply too large for this kind of experiment. Even if we could overcome that obstacle, we would be long dead before any useful results came from our experiment: the rates of geologic processes are simply too slow. Nature, however, has provided natural tracers in the form of the radiogenic isotopes, which are products of natural radioactivity, and these tracers have been moving through the Earth since its beginning. With more quantitative observations we can use isotope ratios to estimate the rate of crustal evolution.

Two fundamental assumptions are involved in virtually all geologic uses of radiogenic isotope ratios. The first is that the rate of radioactive decay is independent of all external influences, such as temperature, pressure, etc. The second is that two isotopes of the same element are chemically identical and therefore that chemical processes cannot change, or fractionate, the ratio of two isotopes of the same elements.

10.2 The Structure of Nuclei

Nuclei are made up of various numbers of neutrons and protons. N represents the number of neutrons, the neutron number, and Z represents the number of protons, or proton number. Z is also the atomic number of the element, because the chemical properties of elements depend almost exclusively on the number of protons (since in the neutral atom the number of electrons equals the number of protons). The sum of Z and N is the mass number A.

Not all possible combinations of protons and neutrons result in stable nuclei. Typically for stable nuclei holds $N \approx Z$. Thus a significant portion of the nucleus consists of protons, which tend to repel each other. From the observation that nuclei exist at all, it is apparent that another force must exist which is stronger than coulomb repulsion at short distances. This force, called the strong force also binds quarks together to form hadrons, a class of particles that includes neutrons and protons. The intensity of the strong force decreases rapidly with distance, so that at distances more than about 10^{-14} m it is weaker than the electromagnetic force.

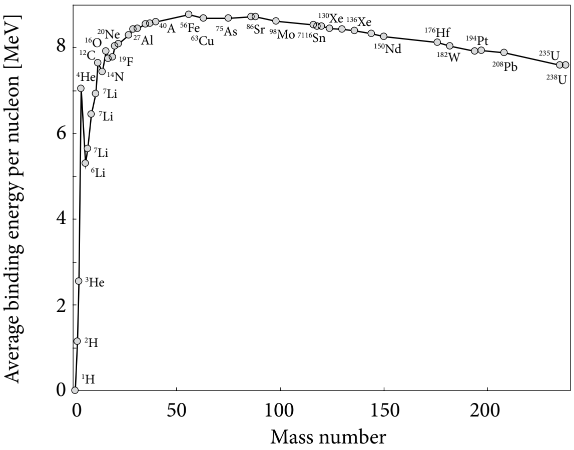

Figure 10.1 Binding energy per nucleon vs. mass number.

We expect that ^{4}He is stable relative to two free neutrons and two free protons, and then from Einstein's mass-energy equivalence

$$E = m\,c^2 \tag{10.1}$$

we can predict that the ^{4}He nucleus will have less mass that 2 free neutrons and 2 free protons. Thus we are able to predict the relative stability of various nuclei from their masses alone.

Calculation of the nominal weight of an atom from the sum of the mass of the constituent particles yields:

proton: 1.007593 daltons
(formally called amu,
atomic mass units) = $1.6726231 \text{ x } 10^{-27}$ kg
neutron: 1.008982 daltons
electron: 0.000548756 daltons = 9.10093897×10^{-31} kg

Then we define the mass decrement of an atom as:

$$\delta = W - M \tag{10.2}$$

where W is the sum of the mass of the constituent particles and M is the actual mass of the atom.

For example, W for ^{4}He is $W = 2m_p + 2m_n + 2m_e$ = 4.034248 daltons. The mass of ^{4}He is 4.003873 daltons, so δ = 0.030375 daltons. Converting this to energy using Equation 10.1 yields 28.28 MeV. This energy is known as the binding energy. Dividing by A, the mass number, or number of nucleons, gives the binding energy per nucleon, E_b:

$$E_h = \left[\frac{W - M}{A}\right] c^2 \tag{10.3}$$

E_b is a measure of nuclear stability: those nuclei with the largest binding energy per nucleon are the most stable. Figure 10.1 shows E_b as a function of mass. Note that the nucleons of intermediate mass tend to be the most stable.

Some indication of the relative strength of the nuclear binding force can be obtained by comparing the mass decrement associated with it to that associated with binding an electron to a proton in a hydrogen atom. The mass decrement above is of the order of 1%, 1 part in 10^2. The mass decrement associated with binding an electron to a nucleus of the order of 1 part in 10^8, so bonds between nucleons are about 10^6 times stronger than bonds between electrons and nuclei.

Problem: Calculate the binding energies of ^{50}V, ^{50}Cr, and ^{50}Ti. Which of these 3 nuclei is the least stable? Which is the most stable?

Solution: The nucleus of ^{50}V consists of 23 protons and 27 neutrons, that of ^{50}Cr consists of 24 protons and 26 neutrons, that of ^{50}Ti consists of 22 protons and 28 neutrons. Atoms of these elements also have, respectively 23, 24, and 22 electrons. First we calculate W for each:
W (^{50}V) = 23 × 1.007593 + 27 × 1.008982 daltons + 23 × 0.000548756 = 50.429774 daltons W (^{50}Cr) = 24 × 1.007593 + 26 × 1.008982 daltons + 24× 0.000548756 = 50.428934 daltons W (^{50}Ti) = 22 × 1.007593 + 28 × 1.008982 daltons + 22 × 0.000548756 = 50.430615 daltons The actual masses (M) of these nuclides are: ^{50}V: 49.947162 daltons; ^{50}Cr: 49.946047 daltons; ^{50}Ti: 49.944792 daltons. Using equation 10.2 we calculate the mass decrement, and then divide by 50 to calculate the mass decrement per nucleon. We convert the result to kg using the conversion factor 1 dalton = 1.66×10^{-27} kg. We then multiply by the square of the speed of light (2.998×10^8 m/sec) to obtain the binding energy in kg-m/sec or joules. We use 1 J = 6.2415×10^{12} MeV to convert our answer to MeV. The results are shown in the table below.

Nuclide	Δ	δ	δ / A	E_b	E_b
daltons		kg	kg/nucleon	J/nucleon	MeV
^{50}V	0.482612	8.011449×10^{-28}	1.60229×10^{-29}	1.4401×10^{-12}	8.9885
^{50}Cr	0.482887	8.016014×10^{-28}	1.60320×10^{-29}	1.4410×10^{-12}	8.9937
^{50}Ti	0.484568	8.043919×10^{-28}	1.60878×10^{-29}	1.4460×10^{-12}	9.0245

Our results indicate that of the three, ^{50}V is the least stable and ^{50}Ti the most stable, though the difference is not that great.

Nuclei with even number of protons and neutrons are more stable than those with odd numbers of protons or neutrons. Stable even-even configurations are most common; stable odd-odd configurations are particularly rare, as can be seen in Figure 10.2.

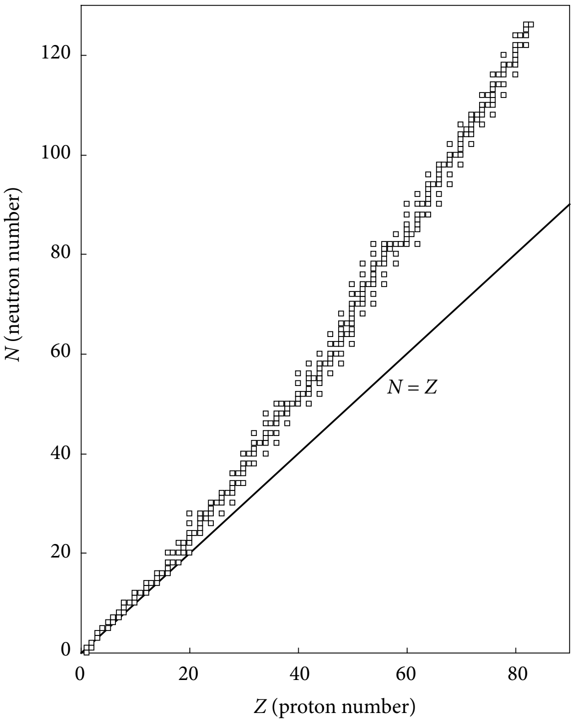

Figure 10.2. Neutron number vs. proton number for stable nuclides.

10.3 The Decay of Excited and Unstable Nuclei

Just as an atom can exist in any one of a number of excited states, so too can a nucleus have a set of discrete, quantized, excited nuclear states. The behavior of nuclei in transforming to more stable states is somewhat similar to atomic transformation from excited to more stable sites, but there are some important differences: (1) energy level spacing is much greater; (2) the time an unstable nucleus spends in an excited state can range from 10^{-14} sec to 10^{11} years, whereas atomic life times are usually about 10^{-8} sec; (3) excited atoms emit photons, but excited nuclei may emit other particles as well as photons. The photon emitted through the decay of unstable nuclei is called a gamma ray. In addition to the decay of an excited nucleus to a more stable state, it is also possible for an unstable nucleus to decay to an entirely different nucleus, through the emission or absorption of a particle of non-zero rest mass.

Nuclear decay takes place at a rate that follows the law of radioactive decay. The decay rate is dependent only on the nature and energy state of the nuclide. It is independent of the past history of the nucleus, and essentially independent of external influences such as temperature, pressure, etc. Also, it is impossible to predict when a given nucleus will decay. We can, however, predict the probability of its decay in a given time interval. The probability of decay of a nucleus in some infinitesimally small time interval, dt, is λ, where λ is called the decay constant. The probability of a decay among some number, N, of nuclides within dt is λ N. Therefore, the rate of decay of N nuclides is:

$$\frac{\mathrm{dN}}{\mathrm{d}t} = -\lambda \mathrm{N} \qquad 10.4$$

The minus sign simply indicates N decreases with time. Equation 10.4 is a first-order rate law.

10.3.1 Gamma decay

Gamma emission occurs when an excited nucleus decays to a more stable state. A gamma ray is simply a high-energy photon (i.e., electromagnetic radiation). Its frequency, v, is related to the energy difference by:

$$h\,v = E_u - E_l \qquad 10.5$$

where E_u and E_l are the energies of the upper (excited) and lower (ground) states and h is Planck's constant. The nuclear reaction is written as:

$$^{N}Z^{*} \rightarrow {}^{N}Z + \gamma \qquad 10.6$$

where Z is the element symbol, N is the mass number, and γ denotes the gamma ray.

10.3.2 Alpha decay

An α-particle is simply a helium nucleus. Since the helium nucleus is particularly stable, it is not surprising that such a group of particles might exist within the parent nucleus before α-decay. Emission of an alpha particle decreases the mass of the nucleus by the mass of the alpha particle plus a mass equivalent to the energy lost during the decay, which includes the kinetic energy of the alpha particle, and the remaining nucleus, and any gamma ray emitted. The daughter may originally be in an excited state, from which it decays by γ decay. Figure 10.3 shows an energy-level diagram for such decay.

Alpha-decay occurs in nuclei with masses above the maximum in the binding energy curve of Figure 10.1, located at ^{56}Fe. Quite possibly, all such nuclei are un-

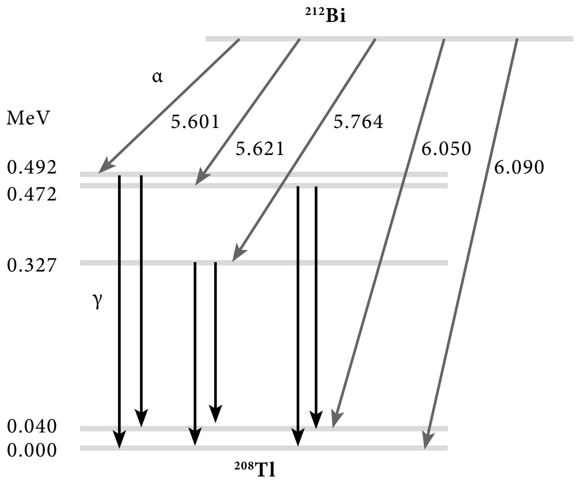

Figure 10.3 Nuclear energy-level diagram showing decay of bismuth 212 by alpha emission to the ground and excited states of thallium 208.

stable relative to alpha-decay, but the half-lives of most of them are immeasurably long.

10.3.3 Beta Decay

Beta decay is a process in which the charge of a nucleus changes, but not the number of nucleons. Beta-decay results in the emission of an electron or positron (a positively charged electron). Consider the 3 nuclei in Figure 10.4. These are known as isobars, since they have the same number of nucleons (12; isotopes have the same number of protons, isotones have the same number of neutrons). We can predict that the ^{12}C nucleus is the most stable of these three, because the spins of the neutrons and protons cancel each other. This is the case: ^{12}B decays to ^{12}C by the creation and emission of a β^- particle and the conversion of a neutron to a proton. ^{12}N decays by emission of a β^+ and conversion of a proton to a neutron. In β^- decay, a neutron is converted to a proton, giving up electron with –1 charge and leaving +1 charge in nucleus. In β^+ decay, a proton is converted to a neutron, giving up its +1 charge to a neutrino, which is converted to a positron.

10.3.4 Electron Capture

Another type of reaction is electron capture. This is sort of the reverse of beta decay and has the same effect, more or less, as β^+ decay. Interestingly, this is a process in which an electron is added to a nucleus to produce a nucleus with less mass than the parent! The missing mass is carried off as energy by an escaping neutrino, and in some cases by a γ. In some cases, a nucleus can

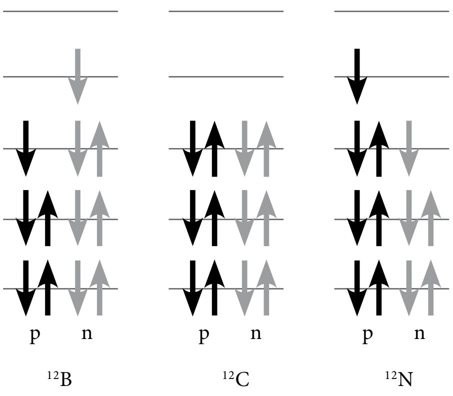

Figure 10.4 Proton and neutron occupation levels of boron 12, carbon 12 and nitrogen 12.

decay by either electron capture, β^-, or β^+ emission. An example is the decay of ^{40}K, which decays to ^{40}Ar by β^+ or electron capture and to ^{40}Ca by β^-.

β decay and electron capture often leave the daughter nucleus in an excited state. In this case, it will decay to its ground state (usually very quickly) by the emission of a γ-ray. Thus γ rays often accompany β decay.

10.3.5 Spontaneous Fission

Fission is a process in which a nucleus splits into two or more fairly heavy daughter nuclei. In nature, this is a very rare process, occurring only in the heaviest nuclei, ^{238}U, ^{235}U, and ^{232}Th (it is, however, most likely in ^{238}U). When fission occurs, some free neutrons are produced and nuclear fragments (the daughters, which may range from A = 30, zinc, to A = 64, terbium) are too rich in neutrons to be stable. The immediate daughters will decay by β^- decay until enough neutrons have been converted to protons. It is this tendency to produce unstable nuclear by-products, rather than fission itself, which makes fission in bombs and nuclear reactors such radiation hazards.

Some unstable heavy nuclei and excited heavy nuclei are particularly subjected to fission. An important example is ^{236}U. When one ^{238}U undergoes fission, some of the released neutrons are captured by ^{235}U nuclei, producing ^{236}U in an excited state. This ^{236}U then fissions producing more neutrons, etc. This is the basis of nuclear reactors and bombs (actually, most now use some other nuclei, like Pu). In general, however, the concentration of U in nature is not high enough for this reaction to happen.

Individual fission reactions are less rare. When fission occurs, there is a fair amount of kinetic energy produced, the fragments literally flying apart. These fragments damage the crystal structure through which they pass, producing 'tracks', whose visibility can be enhanced by etching. This is the basis of fission track dating.

10.4 Basics of Radiogenic Isotope Geochemistry

The basic equation of radioactive decay is:

$$\frac{dN}{dt} = -\lambda N \qquad 10.4$$

λ is the decay constant, which we defined as the probability that a given atom would decay in some time dt. It has units of time^{-1}. Let's rearrange equation 10.4 and integrate:

$$\int_{N_0}^{N} \frac{dN}{N} = \int_0^t dt \qquad 10.7$$

where N_0 is the number of atoms of the radioactive, or parent, isotope present at time t = 0. Integrating, we obtain:

$$\ln \frac{N}{N_0} = -\lambda t \qquad 10.8$$

This can be expressed as:

$$\frac{N}{N_0} = e^{-\lambda t} \qquad \text{or} \quad N = N_0\, e^{-\lambda t} \qquad 10.9$$

Suppose we want to know the amount of time for the number of parent atoms to decrease to half the original number, i.e., t when $N/N_0 = 1/2$. Setting N/N_0 to 1/2, we can rearrange 10.8 to get:

$\ln 1/2 = -\lambda\, t_{1/2}$ or $\ln 2 = \lambda\, t_{1/2}$

and finally:

$$t_{1/2} = \frac{\ln 2}{\lambda} \qquad 10.10$$

This is the definition of the half-life, $t_{1/2}$.

The decay of the parent produces some daughter, or radiogenic, nuclides. The number of daughters produced is simply the difference between the initial number of parents and the number remaining after time t:

$$D = N_0 - N \qquad 10.11$$

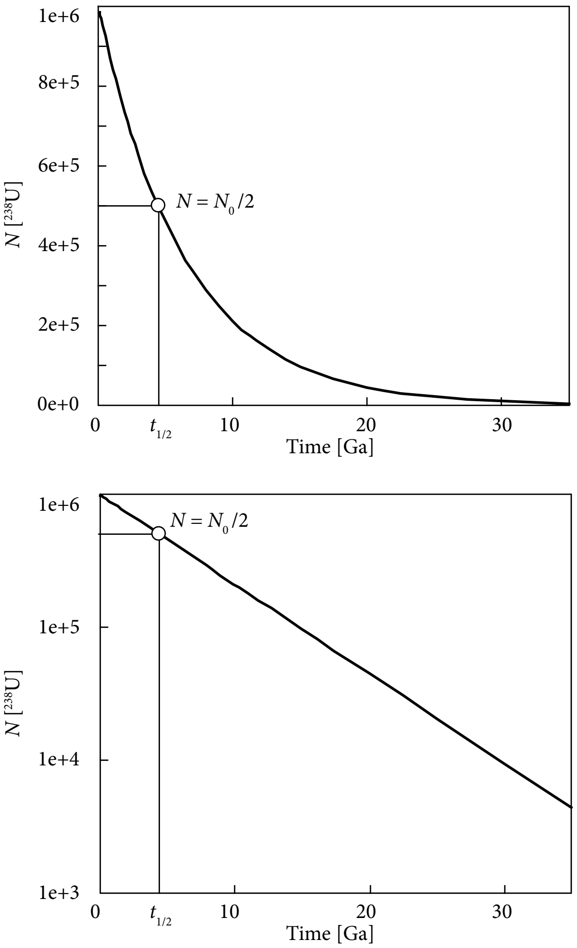

Figure 10.5 Radioactive decay is a first order reaction. Time dependence of ^{238}U atoms is on the left diagram. At half-time the number of ^{238}U is half of the original value (half-time for ^{238}U is 4.47 Ga). On logarithmic scale we get straight line (left diagram).

Rearranging 10.9 to isolate N_0 and substituting that into 10.11, we obtain:

$$D = N\, e^{\lambda t} - N = N\,(e^{\lambda t} - 1) \qquad 10.12$$

The number of daughters produced is a function of the number of parents present and time. Since in general there will be some atoms of the daughter nuclide around to begin with, i.e., when t = 0, a more general expression is:

$$D = D_0 + N\,(e^{\lambda t} - 1) \qquad 10.13$$

where D_0 is the number of daughters originally present. An exponential function can be expressed as a Taylor Series expansion:

$$e^{\lambda t} = 1 + \lambda t + \frac{(\lambda t)^2}{2!} + \frac{(\lambda t)^3}{3!} + \cdots \qquad 10.14$$

Provided $\lambda t << 1$, the higher order terms become very small and can be ignored; hence for times that are short compared to the decay constant (i.e., for $t << 1/\lambda$), equation 10.13 can be written as:

$$D \quad D_0 + N \lambda t \qquad 10.15$$

Let's now write equation 10.13 using a concrete example, such as the decay of ^{87}Rb to ^{87}Sr:

$$^{87}Sr = {}^{87}Sr_{0} + {}^{87}Rb\,(e^{\lambda t} - 1) \qquad 10.16$$

It is generally much easier, and usually more meaningful, to measure the ratio of two isotopes than the absolute abundance of one. We therefore measure the ratio of ^{87}Sr to a non-radiogenic isotope, which by convention is ^{86}Sr. Thus the useful form of 10.16 is:

$$\left(\frac{^{87}Sr}{^{86}Sr}\right) = \left(\frac{^{87}Sr}{^{86}Sr}\right)_0 + \left(\frac{^{87}Rb}{^{86}Sr}\right)\left(e^{\lambda t} - 1\right) \qquad 10.17$$

Similar expressions can be written for other decay systems.

Equation 10.17 is a concise statement of Sr isotope geochemistry: the $^{87}Sr/^{86}Sr$ ratio in a system depends on: (1) the $^{87}Sr/^{86}Sr$ at time $t = 0$, (2) the $^{87}Rb/^{86}Sr$ ratio of the system (in most cases, we can assume the $^{87}Rb/^{86}Sr$ ratio is directly proportional to the Rb/Sr ratio), and (3) the time elapsed since $t = 0$.

Table 10.1 lists the radioactive decay schemes of principal geologic interest. The usefulness and significance of each of the decay schemes are different and depend on the geochemical behavior of the parent and daughter, the half-life and the abundance of the parent.

Table 10.1 Long-Lived Radioactive Decay Systems of Geochemical Interest

Parent	Decay Mode	λ (y^{-1})	Half-life (y)	Daughter	Ratio
^{40}K	β^+, e.c., β^-	5.543×10^{-10}	1.28×10^{9}	^{40}Ar, ^{40}Ca	$^{40}Ar/^{36}Ar$
^{87}Rb	β^-	1.42×10^{-11}	4.8×10^{10}	^{87}Sr	$^{87}Sr/^{86}Sr$
^{138}La	β^-	2.67×10^{-12}	2.59×10^{11}	^{138}Ce	$^{138}Ce/^{142}Ce$, $^{138}Ce/^{136}Ce$
^{147}Sm	α	6.54×10^{-12}	1.06×10^{11}	^{143}Nd	$^{143}Nd/1^{44}Nd$
^{176}Lu	β^-	1.94×10^{-11}	3.6×10^{10}	^{176}Hf	$^{176}Hf/^{177}Hf$
^{187}Re	β^-	1.64×10^{-11}	4.23×10^{10}	^{187}Os	$^{187}Os/^{186}Os$, $^{187}Os/^{188}Os$
^{232}Th	α	4.948×10^{-11}	1.4×10^{10}	^{208}Pb, ^{4}He	$^{208}Pb/^{204}Pb$, $^{3}He/^{4}He$
^{235}U	α	9.849×10^{-10}	7.07×10^{8}	^{207}Pb, ^{4}He	$^{207}Pb/^{204}Pb$, $^{3}He/^{4}He$
^{238}U	α	1.551×10^{-10}	4.47×10^{9}	^{206}Pb, ^{4}He	$^{206}Pb/^{204}Pb$, $^{3}He/^{4}He$

Note: The branching ratio, i.e. ratios of decays to ^{40}Ar to total decays of ^{40}K is 0.117. The production of ^{4}He from ^{147}Sm decay is insignificant compared to that produced by decay of U and Th.

10.5 Geochronology

Geochronology is not our main interest here, but it is one of the most important applications of isotope geochemistry and the two are often closely intertwined. Let's rewrite equation 10.17 in more general terms:

$$R = R_0 + R_{P/D}\,(e^{\lambda t} - 1) \qquad 10.18$$

where R_0 is the initial ratio and $R_{P/D}$ is the parent/daughter ratio. Measurement of geologic time is based on this equation or various derivatives of it. Given a measurement of an isotope ratio, R, and a parent daughter ratio, $R_{P/D}$, two unknowns remain in equation 10.18: t and the initial ratio. We can calculate neither from a single pair of measurements. But if we can measure R and $R_{P/D}$ on a second system for which we believe t and R_0 are the same, we have two equations and two unknowns and subtracting the two equations yields:

$$\Delta R = \Delta R_{P/D}\,(e^{\lambda t} - 1) \qquad 10.19$$

which we can solve for t. Rearranging:

$$\frac{\Delta R}{\Delta R_{P/D}} = e^{\lambda t} - 1 \qquad 10.20$$

t may then be solved for as:

$$t = \frac{\ln\left(\dfrac{\Delta R}{\Delta R_{P/D}} + 1\right)}{\lambda} \qquad 10.21$$

We can obtain the ratio $\Delta R/\Delta R_{P/D}$ from any two data points, regardless of whether they are related or not. To overcome this problem in practice, many pairs of measurements of R and $R_{P/D}$ are made. Note that equation 10.18 has the form $y = a + b\,x$, where y is R, a is the intercept, R_0, b is the slope, $e^{\lambda t} - 1$, and x is $R_{P/D}$. An equation of this form is, of course, a straight line on a plot of R vs. $R_{P/D}$ such as Figure 10.6. The slope of the line passing through the data is thus related to the age of the system and line is called an isochron. When multiple measurements of the daughter isotope ratio and parent-daughter ratio are available, the slope, $\Delta R/\Delta R_{P/D}$, can be calculated by the statistical technique of linear regression. The age is then obtained by substituting the value of the slope into equation 10.21. Regression also yields an intercept, which is simply the initial ratio R_0 since, as may be seen from equation 10.18, $R = R_0$ when $R_{P/D} = 0$.

There are two important assumptions built into the use of equation 10.18. (1) The system of interest was at isotopic equilibrium at time $t = 0$. Isotopic equilibrium in this case means the system had a homogeneous, uniform value of R_0. (2) The system as a whole and each analyzed part of it was closed between $t = 0$ and time t (usually the present time). Violation of these conditions is the principal source of error in geochronology.

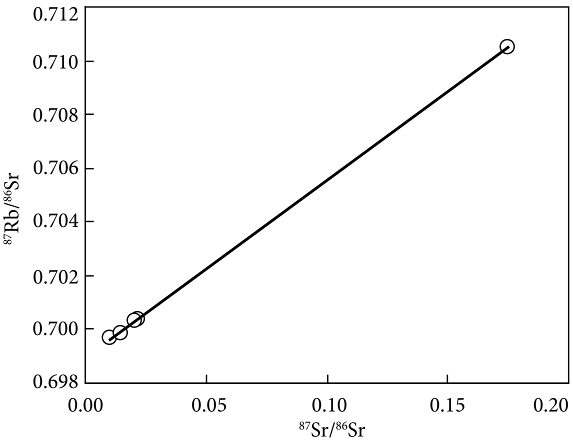

Figure 10.6 A Rb-Sr isochron. Five analyses from a clast in the Bholghati meteorite fall on an isochron, whose slope is related to the age of the system. Data from Nyquist et al. (1990).

10.6 Decay Systems and their Applications

10.6.1 Rb-Sr

This decay system was one of the first to be widely used in geochronology and remains one of the most useful geochemical tracers. An important advantage of the system is relatively large variations of the Rb/Sr ratio in rocks. Because of the difference in geochemical properties of the two elements, Rb/Sr can vary by several orders of magnitude. Since the accuracy of an age determination depends heavily on the spread of measured ratios, this makes the Rb-Sr system a useful geochronological tool. Rb is a highly soluble, highly incompatible element. Sr is also relatively soluble and is fairly incompatible in mafic and, particularly, ultramafic systems. However, it is relatively compatible in silica-rich igneous systems, partitioning preferentially into plagioclase. The result is that the mantle has a relatively uniform and low ^{87}Sr/^{86}Sr ratio, and the continental crust has a much more variable, and, on average, higher ratio.

Problem:The following ^{87}Rb/^{86}Sr-^{87}Sr/^{86}Sr data were measured by Nyquist et al. (1990) on a clast within the achondritic meteorite Bholghati. These data are plotted in Figure 10.6. What is the age and error on the age of this clast? What is the initial ^{87}Sr/^{86}Sr ratio of the clast and the error on this ratio?

^{87}Rb/^{86}Sr	^{87}Sr/^{86}Sr
0.01015	0.69966
0.17510	0.71052
0.02166	0.70035
0.02082	0.70029
0.01503	0.69988

Solution: We can calculate the age using equation 10.21 above. The value of $\Delta R/\Delta R_{P/D}$ is the 'slope' of the isochron, i.e., the slope of a line through the data on a plot of ^{87}Sr/^{86}Sr vs. ^{87}Rb/^{86}Sr. We will use simple least squares linear regression to obtain the slope and intercept; the latter will be the initial ^{87}Sr/^{86}Sr ratio.

Spreadsheet is shown below. Usually toady the spreadsheets have built in statistical functions including linear regression (something like LINREG or similar). To make it easier to read, the cells containing calculated parameters have some explanatory notes. It is fairly straightforward to calculate the slope, b, the intercept, a, and the errors on the slope and intercept. Our result is that the age of the clast is 4.51 ± 0.02 Ga (Ga is the abbreviation for gigayears, 10^9 years). At that time, the ^{87}Sr/^{86}Sr ratio of the clast was 0.69893 ± 0.00003.

	^{87}Rb/^{86}Sr	^{87}Sr/^{86}Sr		
	0.01015	0,69966		
	0.17510	0,71052		
	0.02166	0,70035		
	0.02082	0,70029		
	0.01503	0,69988		
b =	0,06619769	0,698926	= a	
se_b =	0,00031116	2,49E-05	$=se_a$	
r^2 =	0,99993372	4,41E-05	= se_y	
F =	45259,4217	3	= degree of freedom	
ss_{reg} =	8,8103E-05	5,84E-09	= ss_{resid}	
λ =	1,42E-11	y^{-1}	se_a	standard error of a
$t = \ln(b+1)/\lambda$ =	4,514E+09	y	se_b	standard error of b
t =	4,514	Ga	se_y	standard error of y estimation
$t_{er} = \ln(se_b+1)/\lambda$ =	0,022	Ga	R^2	coeficient of determination
			F	F-statistic
			ss_{reg}	sum of regresion square
			ss_{resid}	sum of residual square

Exact meaning of each statistical parameter is beyond the scope of this text and you have to look in appropriate textbook

The Sr isotopic evolution of the Earth and its major silicate reservoirs (the continental crust and mantle) is illustrated in Figure 10.7, which is a plot of ^{87}Sr/^{86}Sr vs. time (in giga-annum, or billions of years). Such a plot is called an isotope evolution diagram. A characteristic of such diagrams is that a closed reservoir will evolve along a line whose slope is proportional to the parent-daughter ratio, in this case ^{87}Rb/^{86}Sr. This is easy to show from equation 10.17. When $t << 1/\lambda$, then equation 10.17 becomes:

$$^{87}\mathrm{Sr} / {}^{86}\mathrm{Sr} = ({}^{87}\mathrm{Sr} / {}^{86}\mathrm{Sr})_0 + ({}^{87}\mathrm{Rb} / {}^{86}\mathrm{Sr})\, \lambda t \qquad 10.22$$

This equation has the form: ^{87}Sr / ^{86}Sr = a + b t (i.e., the equation of a straight line on a plot of ^{87}Sr/^{86}Sr vs. t with slope λ ^{87}Rb/^{86}Sr and intercept ^{87}Sr/^{86}Sr)$_0$ (to the degree that the Taylor Series approximation is not exact, the line will actually be curved, but the approximation is fairly good in this case). In Figure 10.7 we have plotted geologic age rather than the time since t = 0; in other words, we have transformed t to (4.55 – t), where 4.55 Ga is the assumed age of the Earth. Thus the intercept occurs at t = 4.55 rather than 0.

The initial ^{87}Sr/^{86}Sr ratio of the Earth can be estimated from the initial ratio in meteorites under the assumption that the entire solar system had a uniform ^{87}Sr/^{86}Sr at the time it was formed. Once it forms, the Earth is a closed system, so it evolves along a straight line with slope proportional to the bulk Earth ^{87}Rb/^{86}Sr. This ratio has been estimated in various ways to be about 0.085 (as we noted is the ^{87}Rb/^{86}Sr is proportional to the Rb/Sr ratio; the bulk Earth Rb/Sr is about 0.029).

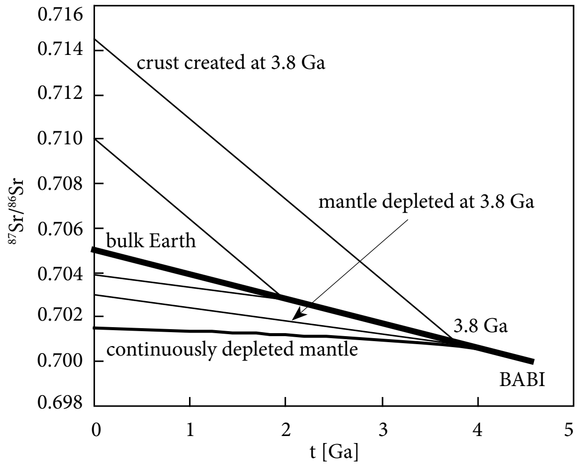

Figure 10.7 Sr isotopic evolution of the bulk Earth, evolution of high Rb/Sr crust created at 3.8 Ga, evolution of the resulting residual mantle and the evolution of a mantle being continuously depleted. 'BABI' stands for basaltic achondrite best initial, and is the assumed initial ^{87}Sr/^{86}Sr of the solar system

10.6.2 U-Th-Pb

The U-Th-Pb system is somewhat of a special case since there are 3 decay schemes producing isotopes of Pb. In particular two U isotopes decay to two Pb isotopes, and since the two parents and two daughters are chemically identical, we get two decay systems which together provide a particularly powerful tool.

Following convention, we will designate the ^{238}U/^{204}Pb ratio as μ, and the ^{232}Th/^{238}U ratio as κ. The ratio ^{238}U/^{235}U is constant in the Earth at 137.88. Now, we can write two versions of equation 10.18 as:

$$\frac{^{207}\mathrm{Pb}}{^{204}\mathrm{Pb}} = \left(\frac{^{207}\mathrm{Pb}}{^{204}\mathrm{Pb}}\right)_0 + \frac{\mu}{137.88}\left(e^{\lambda_{235}t} - 1\right) \qquad 10.23$$

and

$$\frac{^{206}\mathrm{Pb}}{^{204}\mathrm{Pb}} = \left(\frac{^{206}\mathrm{Pb}}{^{204}\mathrm{Pb}}\right)_0 + \mu\left(e^{\lambda_{238}t} - 1\right) \qquad 10.24$$

Equations 10.23 and 10.24 can be rearranged by subtracting the initial ratio from both sides. Using Δ to designate the difference between the initial and the present ratio, equation 10.24 becomes:

$$\Delta\frac{^{206}\mathrm{Pb}}{^{204}\mathrm{Pb}} = \mu\left(e^{\lambda_{238}t} - 1\right) \qquad 10.25$$

Dividing the equivalent equation for ^{235}U-^{207}Pb by equation 10.23 yields:

$$\frac{\Delta\frac{^{206}\mathrm{Pb}}{^{204}\mathrm{Pb}}}{\Delta\frac{^{207}\mathrm{Pb}}{^{204}\mathrm{Pb}}} = \frac{1}{137.88}\frac{\left(e^{\lambda_{238}t} - 1\right)}{\left(e^{\lambda_{235}t} - 1\right)} \qquad 10.26$$

The left-hand side of this equation is the slope of line on a plot of ^{207}Pb/^{204}Pb vs. ^{206}Pb/^{204}Pb such as Figure 10.8. The slope depends only on time and three constants (λ_{238}, λ_{235}, and ^{238}U/^{235}U). Because its slope depends on time, a line on a plot of ^{207}Pb/^{204}Pb vs. ^{206}Pb/^{204}Pb is an isochron, analogous to the isochrons in a plot such as Figure 10.6.

The equation 10.26 cannot be solved directly for t. However, we can guess a value of t, plug it into the equation, calculate the slope, compare the calculated slope with the observed one, revise our guess of t, calculate again, etc.

Because the half-life of ^{235}U is much shorter than that of ^{238}U, ^{235}U decays more rapidly. As a result, on a plot ^{207}Pb/^{204}Pb vs. ^{206}Pb/^{204}Pb, Pb isotopic evolution follows curved paths. The exact path that is followed depends upon μ. Three such evolution curves are shown in Figure 10.8. All systems that begin with a common initial isotopic composition at time t_0 along a straight line at some later time t.

As for Th we can combine the growth equations for ^{208}Pb/^{204}Pb and ^{206}Pb/^{204}Pb in a way similar to equation 10.26. We end with

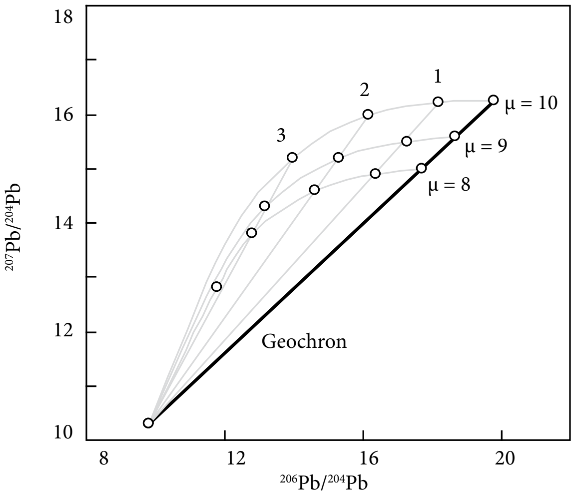

Figure 10.8 Evolution of Pb isotope ratios. The curve lines represent the evolutionary paths for systems having μ values of 8, 9, and10. The hash marks on the evolution curves mark Pb isotope compositions 1.0, 2.0, and 3.0 Ga ago.

$$\frac{\Delta \frac{^{208}\mathrm{Pb}}{^{204}\mathrm{Pb}}}{\Delta \frac{^{206}\mathrm{Pb}}{^{204}\mathrm{Pb}}} = \frac{\kappa\left(e^{\lambda_{232}t}-1\right)}{\left(e^{\lambda_{238}t}-1\right)} \qquad 10.27$$

where κ is the ^{232}Th/^{238}U ratio.

Provided κ is constant in a series of cogenetic rocks (by cogenetic we mean that at $t = 0$ they all had identical Pb isotope ratios), the slope of an array on a plot of ^{208}Pb/^{204}Pb and ^{206}Pb/^{204}Pb will depend only on t and κ, and not on the parent-daughter ratios. We can calculate κ from the slope of the data on a plot of ^{208}Pb/^{204}Pb *vs* ^{206}Pb/^{204}Pb. U and Th are both highly incompatible elements. They have similar, but not identical, partition coefficients in most minerals. It seems unlikely that they will behave identically, and hence unlikely that κ will very often be constant. It can be shown that if κ varies and is positively correlated with variations in μ then equation 10.27, when solved for κ, will actually overestimate it.

10.6.3 U and Th Decay Series

U and Th do not decay directly to Pb, rather the transition from U and Th to Pb passes through many intermediate radioactive daughters (Figure 10.9). Many of these daughters have very short half-lives, ranging from milliseconds to minutes, and are of little use to geochemists. However, a number of these intermediate daughters have half-lives ranging from days to hundreds of thousands of years and do provide useful information about geological processes. Table 10.2 lists half-lives and decay constants of some of the most useful of these nuclides.

Table 10.2 Half-lives and decay constants of long-Isotopes lived U and Th daughters

Nuclide	Half-life, yrs	Decay constant, y^{-1}	Parent
^{234}U	246,000	2.794×10^{-6}	^{238}U
^{231}Pa	32,480	2.134×10^{-5}	^{235}U
^{230}Th	75,200	9.217×10^{-6}	^{238}U
^{226}Ra	1,622	4.272×10^{-4}	^{238}U
^{228}Ra	6.7	1.06×10^{-1}	^{232}Th
^{210}Pb	22.26	3.11×10^{-2}	^{238}U

The half lives of all of these daughter isotopes are short enough so that any atoms present when the Earth formed have long since decayed (to Pb). They exist in the Earth (and in all other bodies of the solar system) only because they are continually produced by the decay of U and Th. The abundance of such an isotope depends on the balance between its own radioactive decay and its production by the decay of its parent:

$$\frac{dN_D}{dt} = \lambda_P N_P - \lambda_D N_D \qquad 10.28$$

where subscripts P and D refer to parent and daughter respectively. This equation says simply that the rate of change of the abundance of the daughter isotope is equal to the rate of production less the rate of decay. This can be integrated to give:

$$N_D = \frac{\lambda_P}{\lambda_D - \lambda_P} = N_P^0\left(e^{-\lambda_P t} - e^{-\lambda_D t}\right) +_P - N_D^0 e^{-\lambda_D t} \qquad 10.29$$

Scientists dealing with the intermediate daughters of U and Th (and it is the daughters of ^{238}U that are of the most interest), generally work with activities, measured in the number of decays per unit time, rather than atomic abundances. One reason for this is that the abundances of these isotopes are generally determined by detecting their decay. Indeed, the shorter-lived ones are so rare they cannot be detected any other way. The other reason will become apparent shortly. Activities are related to atomic (molar) abundances by the basic equation of radioactive decay:

$$\frac{dN_i}{dt} = -\lambda_i N_i \qquad 10.30$$

where d*Ni*/d*t* is the *activity* of *i*. Activity is most commonly expressed in units of disintegrations per minute (dpm) and is denoted by writing parentheses around the isotope (or the isotope ratio). Thus (^{234}U) is the activity of ^{234}U.

The radioactive equilibrium state of the daughter and the parent is the condition where their activities are equal, i.e.:

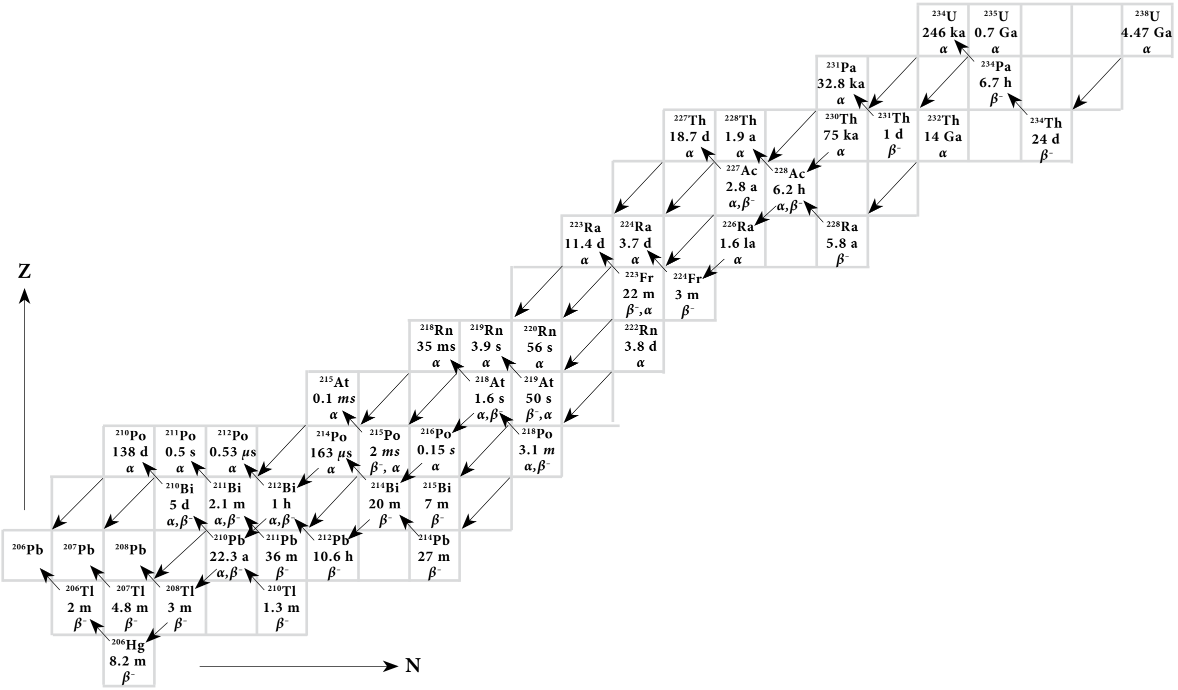

Figure 10.9 Part of the chart of the nuclides showing the series of decays that occur as ^{238}U, ^{235}U, and ^{232}Th are transformed to ^{206}Pb, ^{207}Pb, and ^{208}Pb respectively.

$$\frac{dN_D}{dt} = \frac{dN_P}{dt} \qquad 10.31$$

It shares the same fundamental characteristic as the chemical equilibrium state: it is the state that will eventually be achieved if the system is not perturbed (remains closed). We can demonstrate this is so in two ways. The first is a simple mathematical demonstration. The equilibrium state is the steady state where the abundance of the daughter does not change, i.e., where the left hand side of 10.28 is zero:

$$0 = \lambda_P N_P - \lambda_D N_D \qquad 10.32$$

We substitute the dN/dt terms for the λN terms in 10.31, rearrange, and we obtain 10.32.

Thus when a system is disturbed it will ultimately return to equilibrium. The rate at which it returns to equilibrium is determined by the decay constants of the parent and daughter. If we know how far out of equilibrium the system was when it was disturbed, we can determine the amount of time that has passed since it was disturbed by measuring the present rate of decay of the parent and daughter. Equilibrium is approached asymptotically, and these dating schemes are generally limited to time scales less than 5–10 times the half-life of the daughter. At longer times, the difference between actual activities and equilibrium ones becomes too small to measure reliably.

In most instances, the activities are measured by alpha-counting and fairly large quantities of material are necessary. But improvements in mass spectrometry have made it possible to measure the

^{230}Th/^{232}Th ratio (which is of the order of 10^{-6} in igneous rocks) in relatively small quantities of material with better precision than α counting.

10.6.4 Isotopes of He

Alpha particles are, of course, simply ^{4}He nuclei, and therefore ^{4}He is produced by alpha decay of U and Th. Thus the ratio of ^{4}He/^{3}He varies in the Earth. He is not conserved on the Earth: much of the He present when the Earth formed has been subsequently lost. Being a rare gas, He does not combine chemically with anything, and it also diffuses rapidly. Helium brought to the Earth's surface by magmatic processes eventually finds its way into the atmosphere. Once there, it can escape from the top of atmosphere because of its low mass. Since ^{4}He is continually produced and, for all practical purposes, ^{3}He is not, the ^{4}He/^{3}He ratio in the Earth is a very large number. For some reason, the He isotope ratio is generally expressed as ^{3}He/^{4}He, in contradiction to the normal convention of placing the radiogenic isotope in the numerator.

The ^{3}He/^{4}He ratio of the atmosphere is 1.384×10^{-6}. Since this ratio is uniform and atmospheric He available to all laboratories, it is a convenient standard and moreover provides the basis for a convenient normalization. He ratios are often reported and discussed relative to the atmospheric value. The units are called simply R/R_A, where R_A indicates the atmospheric ratio.

Figure 10.10 illustrates the He isotopic composition of various terrestrial reservoirs. Oceanic islands and other hotspots often have even higher ratios, up to about $R/R_A \approx 24$, though some islands, Tristan da Cunha for example, have lower ratios: $R/R_A \approx 5$ (e.g., Kurz et al., 1982). This suggests that most oceanic island basalts are derived from a less degassed, and in that sense more primordial, reservoir than MORB. This is consistent with the mantle plume hypothesis.

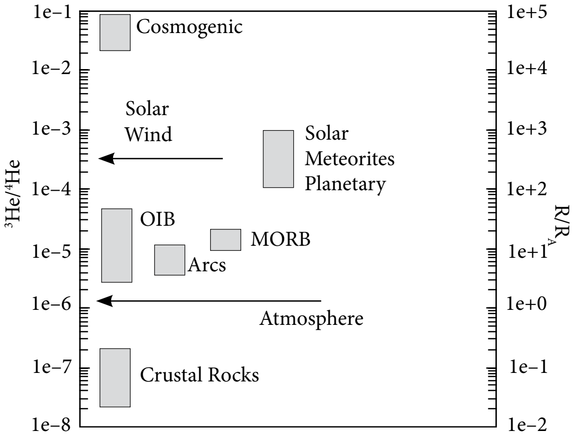

Figure 10.10 He isotope ratios in various terrestrial and solar system materials. “Solar” and “Planetary” refer to the solar and planetary components in meteorites. “Crustal rocks” shows the values expected for in situ production from α decay and neutron-induced nuclear reactions.

Island arc volcanics (IAV) seem also to be fairly uniform with $R/R_A \approx 6$ (Lupton, 1983). Ratios lower than MORB suggest the presence of a slab-derived component, but also indicate most of the He in IAV comes from the mantle wedge (a conclusion similar to the one reached from other radiogenic isotopes).

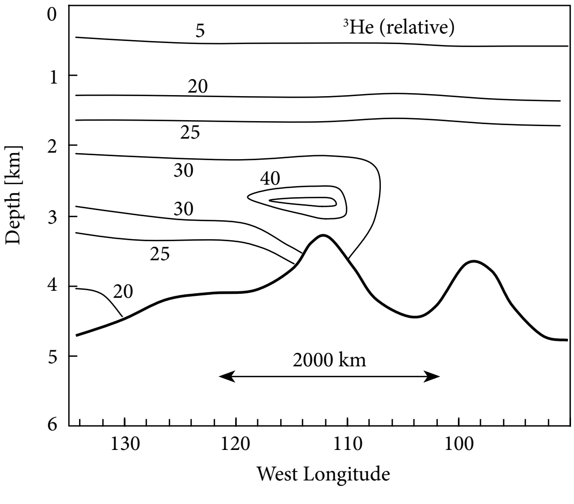

Figure 10.11 Contours of relative ^{3}He concentrations in seawater over the East Pacific Rise (Lupton and Craig, 1981).

Since He is injected at mid-ocean ridges, particularly in the Pacific, at depths of 2500–3000 meters, He isotopes can be used to trace water mass movements. Figure 10.11 shows the He plume of hydrothermal activity on the East Pacific Rise. Interestingly, the plume indicates water is flowing in the direction opposite to that which the physical oceanographers had thought. Another application is prospecting for ridge-crest hydrothermal activity. Several hydrothermal areas (including the first one) have been discovered from the He isotope anomalies in the water column. ^{4}He is also used as a tracer in U prospecting.

10.6.5 K-Ar-Ca

There are several aspects of the K-Ar system that make it particularly advantageous for some geochronological applications. First ^{40}K has one of the shortest half-lives of the decay systems in Table 10.1, making it more useful for dating young rocks than the other systems. In favorable cases, K-Ar ages on rocks as young as 50,000 yrs can be obtained with useful precision. Second, Ar is a rare gas and in most volcanic rocks and in many other rocks it is virtually totally lost when the system is reset. Thus an age can be obtained from a single K-Ar determination. Being a rare gas, Ar diffuses somewhat more readily than other elements. Further, K is concentrated in sheet silicates such as micas, which have comparatively open crystal structures. As a result, the closure temperature for the K-Ar system is low, making it a useful system for study of relatively low temperature phenomena (such as petroleum genesis). This of course, can be a disadvantage, as it means the K-Ar system is reset rather easily.

Most of ^{40}K (90%) decays to ^{40}Ca. This decay scheme has not yielded much geochemical or geochronological information so far. The reason is the low ratio of ^{40}K to ^{40}Ca in most geological materials, which in turn means the radiogenic contribution to ^{40}Ca is small and ^{40}Ca/^{42}Ca variations are very small. Also since the isotopes are rather light, they are comparatively easily fractionated.

10.6.6 Cosmogenic Isotopes

The Earth is constantly bombarded by ‘cosmic rays’ (we shouldn’t feel picked on, the entire cosmos is). These are atomic nuclei (mostly H) stripped of their electrons and traveling at relativistic velocities. Some originate in the Sun, but most originate in high-energy regions of the cosmos such as supernovae. For the most part their origin is not well understood. What is understood is that they have sufficient energy to shatter a nucleus when they collide with one. The nucleus breaks into several parts in a process called *spallation*. Spallation is the process in which a nucleus breaks into smaller nucleii as a result of a collision with a very high energy particle such as a cosmic ray.

Cosmic rays don't have much penetrating power. Thus the intensity of cosmic radiation increases with increasing altitude in the atmosphere. Most are stopped in the atmosphere, their interactions creating a cascade of lesser energy particles, or are slowed considerably. Even if they don't score a direct hit, they lose energy through electromagnetic interaction with matter (ionizing the atoms they pass by. Thus cosmic rays have their greatest effect in the atmosphere.

Nitrogen and oxygen, being the principal constituents of the atmosphere are the most common targets, yet there is no change in the isotopic abundances of these elements. Cosmic radiation is most interesting because of the production of nuclides whose half-lives are so short they would not otherwise exist. The nuclides of greatest interest are listed in Table 10.3 along with their half lives and their decay constants. These nuclides are created either directly through spallation (e.g., ^{10}Be), or by nuclear reactions with particles produced by spallation, e.g., ^{14}C: $^{14}N\ (n,p) \rightarrow {}^{14}C$.

Table 10.3 Some Cosmogenic Nuclides of Geologic Interest.

Nuclide	Half-life (y)	λ (y^{-1})
^{10}Be	1.5×10^{6}	0.462×10^{-6}
^{14}C	5730	0.1209×10^{-3}
^{26}Al	0.716×10^{6}	0.968×10^{-6}
^{36}Cl	0.308×10^{6}	2.25×10^{-6}
^{39}Ar	269	0.257×10^{-2}

10.6.6.1 ^{14}C and ^{13}C

The most well-known of the cosmogenic nuclide dating methods is based on ^{14}C. It is useful in dating archaeological, climatological, volcanological, seismological, paleontological, hydrological, etc., 'events'. Present technology utilizes accelerator mass spectrometry rather than traditional β-counting and useful information on samples as old as 40,000 years can be produced. The principle of this method is quite simple. One assumes a constant production of ^{14}C in the atmosphere. The atmosphere is well-mixed and has a uniform ^{14}C activity equal to 100 pmc (percent of modern carbon). The activity of ^{14}C isolated from atmosphere will decrease in time by decay with a half-life of 5730 years. Apparent age of a carbon sample is calculated as

$$t = -8267 \ln\left(\frac{\alpha_t\ {}^{14}C}{\alpha_0\ {}^{14}C}\right) \qquad 10.33$$

where α_t is ^{14}C activity measured in a sample and α_0 is initial ^{14}C activity (e.g., 100 pmc). In actuality, the production rate appears not to have been constant. Furthermore, the ^{14}C activity in present atmosphere is somewhat lower than it has been in the recent past due to the dilution with CO_2 released by extensive burning of fossil fuels. By comparing of ^{14}C ages with absolute ages derived from tree rings, variations in the atmospheric ^{14}C activity over the past several thousand years have been deduced. This means accurate ages ^{14}C ages can be obtained despite production rate variations. Efforts are underway to extend this calibration further by comparing ^{14}C ages with U-series disequilibrium ages.

There are some complications in the behavior of ^{14}C during recharge, so the "absolute" age of a groundwater cannot be determined reliably. These complications stem from the fact that ^{14}C is not a part of water molecule, but is only incorporated into dissolved inorganic carbon (DIC) transported by ground water flow. Then ^{14}C activity may be modified by geochemical reactions. However, if the ^{14}C activity is measured at several points along a flow line within an aquifer, the differences in age between the points and hence the flow velocity can be determined. The complications are as follows: (1) dissolution of carbonate minerals or oxidation of organic matter within the aquifer may add carbon to the water, which has no detectable amount of ^{14}C giving an erroneously old age; (2) mixing of waters. A low ^{14}C activity may mean that we have relatively old water, or a mixture of relatively young water and old water. ^{14}C measurements can be interpreted as ages only where mixing is insignificant.

There are many sophisticated methods of ^{14}C age corrections and their complete review is beyond scope of this text. Detailed treatment of this issue is, for example, in Clark and Fritz (1997), and in Kalin (2000). Correction is performed by multiplication of initial ^{14}C activity by correction factor *q*.

So called Statistical approach (STAT), when typical correction factors *q* are:
0.65 – 0.75 for karst
0.75 – 0.90 for sediments with carbonates in matrix
0,90 – 1.0 for crystalline rocks

Tamers model based on alkalinity (ALK model): This method assumes a system closed to CO_2 and generally results in $q = 0.5$.

$$q_{\mathrm{ALK}} = \frac{m_{\mathrm{H_2CO_3}} + 0.5\ m_{\mathrm{HCO_3}}}{m_{\mathrm{H_2CO_3}} + m_{\mathrm{HCO_3}}} \qquad 10.34$$

where *m* indicates concentrations of different dissolved carbon species.

Method based on the application ^{13}C: The ^{13}C is stable isotope of carbon, which does not decay, but can undergo fractionation in geochemical reactions. For example, dissolution of carbonates changes ^{13}C concentration in water (makes ^{13}C concentration higher). Concentration of ^{13}C is expressed in so called delta notation as $\delta^{13}C$. Correction factor is calculated as

$$q_{\delta^{13}C} = \frac{\delta^{13}C_{DIC} - \delta^{13}C_{carb}}{\delta^{13}C_{recharge} - \delta^{13}C_{carb}} \qquad 10.35$$

where $\delta^{13}C_{DIC}$, $\delta^{13}C_{carb}$, and $\delta^{13}C_{recharge}$ indicate values of $\delta^{13}C$ for DIC, carbonates and recharging water, respectively. Situation is complicated by the fact that value of $\delta^{13}C_{recharge}$ for recharging water in the past is not known and has to be estimated. The value depends especially on pH value and there is a possibility of significant errors (see examples in Clark and Fritz, 1997).

There are other correction methods like method of Fontes and Garnier, based on both $\delta^{13}C$ and water chemistry and mass-balance geochemical modeling (Plummer et al., 1994) based on concentration changes along flow path (Clark and Fritz, 1997).

Other interesting applications include determining the 'age' of deep water in the oceans. By comparing ^{14}C activities of benthic and planktonic foraminifera in a single sedimentary horizon, it is possible to determine bottom water ages in the past, and hence constrain 'paleocirculation' rates.

10.6.6.2 ^{36}Cl in hydrology

^{36}Cl has been applied to hydrological problems for some time. The general principle is that ^{36}Cl is produced at a constant rate in the atmosphere, carried to the surface of the Earth in rain and incorporated into hydrological systems. Cl is an excellent candidate element for such studies because it should remain in solution in most instances, and hence the only loss should be through radioactive decay. In a simple system the rainwater is incorporated into an aquifer at some unknown time in the past. In this case, if we can specify the number of ^{36}Cl atoms per liter in rain and if we can assume this value is time-invariant, then we can determine the age of water in the aquifer by measuring the number of ^{36}Cl atoms per liter since:

$$^{36}Cl = {}^{36}Cl_0\, e^{-\lambda t} \qquad 10.36$$

Determining the age of water in underground aquifers is an important problem because of the increasing demands placed in many parts of the world on limited water resources. A prudent policy for water resource management is to withdraw from a reservoir at a rate no greater than the recharge rate. Determination of recharge rate is thus prerequisite to wise management.

Dealing with just the number, or concentration, of ^{36}Cl atoms can have disadvantages, and can be misleading. Evaporation, for example, would increase the number of ^{36}Cl atoms. Thus the $^{36}Cl/Cl$ ratio (Cl has two stable isotopes: ^{35}Cl and ^{37}Cl) is often used. This also can have problems since chlorine can be leached from rocks. This chlorine will be nearly free of ^{36}Cl (some ^{36}Cl will be produced naturally by neutron capture), and hence this process will decrease the $^{36}Cl/Cl$ ratio. Further complications arise from the nuclear bomb-produced ^{36}Cl. Particularly large amounts were produced by nuclear bomb testing at sea, where bomb-produced neutrons were captured by ^{35}Cl in seawater.

In a somewhat different application, Paul et al. (1986) used ^{36}Cl to determine the accumulation time of dissolved salt in the Dead Sea. The Dead Sea is a particularly simply hydrologic system because it has no outlet. In such a simple system, we can describe the variation of the number of ^{36}Cl atoms with time as the rate of input less the rate of decay:

$$\frac{dN}{dt} = I - \lambda t \qquad 10.37$$

where I is the input rate (precipitation of chloride is assumed negligible). Integration of this equation yields:

$$N = \frac{I}{\lambda}\left(1 - e^{-\lambda t}\right) \qquad 10.38$$

Paul et al. measured $^{36}Cl/Cl$ in Mt. Hermon snow, in various rivers in the Dead Sea system, and in saline springs in the Dead Sea basin. These results are summarized in Table 10.4. Using equation 10.36, they estimated an accumulation time of 20,000 years for the salt in the Dead Sea. The Dead Sea basin has been estimated to be 15,000 years old based on ^{14}C. The difference suggests some of the Cl now in the Dead Sea was inherited from its less saline Pleistocene predecessor, Lake Lisan. The data in Table 10.4 also illustrates how a combination of Cl and ^{36}Cl data can distinguish between addition of Cl from rock leaching and evaporation, both of which are processes that will increase the concentration of Cl. Evaporation should not significantly change the $^{36}Cl/Cl$ ratio, while addition of Cl derived from rock leaching should decrease this ratio. There is a general southward (downstream) increase in Cl concentration in the Jordan River – Dead Sea system. It is apparent from the data in Table 10.4 that this is due to both addition of rock-derived Cl and evaporation.

Table 10.4 ^{36}Cl measurements in the Dead Sea system.

Site	^{36}Cl/Cl (10^{-15})mg/l	Cl 10^{6} atoms/l	^{36}Cl
Mt. Hermon Snow	1580±120	1.50	40±5
Banias River	400±60	11.9	80±15
Snir River	430±125	11.0	80±20
Dan River	725±140	10.5	129±25
Lake Kinneret	49±15	252	210±65
Jordan River	121±19	646	1,320±210
Dead Sea	17±2	2.30×10^{5}	6.6×10^{4}
Ashlag Spring (saline spring)	4±2	2.6×10^{5}	

10.6.6.3 ^{222}Rn

The decay of uranium and thorium to lead is one of the most widely used dating techniques in geology, but it is not directly applicable to hydrology. Several intermediate products in the decay scheme have been used in water studies. ^{222}Rn is produced by decay of ^{226}Ra (radium), which is itself a decay product of ^{238}U. ^{222}Rn is a gas, and when it is formed in sediment it diffuses into the overlying water. It has a half-life of 3.8 days, so that its concentration decreases with distance from the sediment. The profile of ^{222}Rn above the sediment depends on the rate at which it is transported upward in the water. If the rate is slow, the profile will be compressed close to the sediment; if it is fast, radon will be carried to greater distances from the sediment before it disappears by decay. Knowledge of transport rates near the sediment-water interface is important, because these rates determine the rate at which other species such as nutrients are transported from the sediment into the overlying water.

^{222}Rn has also attracted a great deal of attention as a potential health hazard. It is generated in rocks and soil by decay of ^{238}U and diffuses upward into the atmosphere. In the open air, rapid dilution by mixing, coupled with the short half-life of ^{222}Rn, makes it insignificant as a health hazard. When it seeps into buildings from below, however, it may build up to dangerous concentrations.

10.6.6.4 ^{3}H (Tritium)

Tritium (^{3}H or T) has a half-life of 12.43 years. It is produced naturally in atmosphere by interaction of cosmic rays with nitrogen and oxygen in the atmosphere, but by far the most important source for modern studies is thermonuclear weapons testing which took place in the atmosphere between 1952 and 1969. The natural level in rainwater was about 5–10 TU [one TU (tritium unit) = one T atom per 10^{18} ^{1}H atoms]. During the 1960s, the tritium levels in rainwater rose above 10^{3} TU (maximum in 1963), and modern values are usually between 20 and 100 TU, varying considerably with time and location.

Tritium in groundwater is not significantly affected by chemical processes because is a part of water molecule. Its most important use is in distinguishing between water that entered an aquifer prior to 1952 and water that was in contact with the atmosphere after 1952. Older water contains no tritium detectable by normal procedures; post-1952 water contains relatively high levels of tritium.

It can also be used for determination of ground water recharge. If some characteristic maximum such as a peak from 1963 can be identified, then it is assumed that all water above the peak recharged after 1963 and recharge R is calculated as

$$R = \frac{nH}{t} \qquad 10.39$$

where H is depth of the peak, t is time since 1963, and n is porosity expresed as fraction. More complicated methods are based on determination of tritium input function (TIF), which is concentration of tritium in precipitation corrected for decay. The TIF is compared with tritium values in ground water and a relative distribution of ages can be determined.

However, in some situations the methods above are not applicable. In that case, simultaneous determination of tritium and ^{3}He represents an advantage because ^{3}He is formed by decay of tritium (Clark and Fritz, 1997). Then ground water age is determined as

$$t = \frac{12.43}{\ln 2} \ln\left(1 + \frac{^{3}\mathrm{He}_t}{^{3}\mathrm{H}_t}\right) \qquad 10.40$$

where 12.43 is half-life for tritium decay and ^{3}He$_{t}$ and ^{3}H$_{t}$ are concentrations of ^{3}He and tritium at time of sampling, respectively. This method is very useful because there is no requirement of information about initial tritium activity, but is complicated by relatively difficult sampling for helium. The properties of tritium make it useful in studies of mixing in the upper layers of the ocean and mixing in lakes.

10.6.6.5 ^{10}Be in Subduction Zone Studies

One of the usual uses of cosmogenic nuclides is the use of ^{10}Be to trace sediment subduction (Tera et al., 1986). Since ^{10}Be does not exist in the Earth's interior, its presence there could result only from subduction of sediment (which concentrates cosmogenic ^{10}Be). ^{10}Be has been identified in some island arc volcanics, but not in other volcanic rocks (at least not above the background level of 10^6 atoms per gram, i.e. 1 atom in 10^{18}). This is strong evidence that subducted sediment plays a role in island arc magma genesis, something suspected on the basis of other geochemical evidence.

10.6.7 Transport of Radionuclides

There are some general rules applicable to transport of radionuclides in ground water. First of all, speciation of radionuclides is very important because often determines their behavior. For example, U(VI) is present as positively charged uranyl ion UO_2^{2+} at low pH range and is increasingly adsorbed with increasing pH. However, at neutral and alkaline pH range neutral and negatively charged carbonate complexes of U(VI) predominate and adsorption is almost negligible (Langmuir, 1997). This means that adsorption modeling based on linear adsorption isotherm K_d (see Chapter 3) is applicable only for relatively constant geochemical conditions. There also is a possibility of precipitation of minerals of radionuclides such as amorphous UO_2(am) in the case of U(IV) or co-precipitation such as incorporation of Ra into solid solution with gypsum (Ca, Ra)SO_4.2H_2O. However, concentrations of radionuclides are generally low and, thus, adsorption is much more important attenuation mechanism. Adsorption also increases residence time of radionuclides before reaching potential receptors (water supply wells, lakes etc.). This means that adsorption parameters like K_d and decay half-life are principal parameters governing transport of radionuclides and deciding about their potential threat.

References

Clark I.D., Fritz P.1997. *Environmental Isotopes in Hydrogeology*, Lewis Publishers, Boca Raton, New York.

Kalin R.M. 2000. Radiocarbon Dating of Groundwater Systems, In: Cook P.G., Herczeg A.L. (Editors): *Environmental Tracers in Subsurface Hydrology*, Kluwers Academic Publishers.

Kurz, M. D., W. J. Jenkins, and S. R. Hart. 1982. Helium isotopic systematics of oceanic islands and mantle heterogeneity, *Nature*, 297: 43–47.

Langmuir D. 1997. *Aqueous Environmental Geochemistry,* Prentice Hall, Upper Saddle River, NJ 07458.

Lupton, J. E. 1983. Terrestrial inert gases: isotopic tracer studies and clues to primordial components in the mantle, *Ann. Rev. Earth. Planet. Sci.*, 11: 371–414.

Lupton J. E. and H. Craig. 1981. A major ^{3}He source on the East Pacific Rise, *Science*, 214: 13–18.

Nyquist, L. E., D. D. Bogard, H. Wiesmann, B. M. Bansal., C.-Y. Shih and R. M. Morris. 1990. Age of a eucrite clase from the Bholghati howardite. *Geochim. Cosmochim. Acta.* 54: 2195–2206.

Paul, M., A. Kaufman, M. Magaritz, D. Fink, W. Henning, et al. 1986. A new ^{36}Cl hydrological model and ^{36}Cl systematics in the Jordan River/Dead Sea system, *Nature*, 29, 511–515.

Plummer L.N., Prestemon E.C., Parkhurst D.L. 1994. An Interactive Code (NETPATH) for Modeling Net Geochemical Reactions Along a Flow Path, Version 2.0, U.S. Geological Survey, *Water Resources Investigation Report* 94-4169.

Tera, F., L. Brown, J. Morris, I. S. Sacks, J. Klein, R. Klein and R. Middleton. 1986: Sediment incorporation in island-arc magmas: inferences from ^{10}Be, *Geochim. Cosmochim. Acta*, 50: 535–550.

Chapter 11: Organic Contamination

11.1 Types of Organic Contaminants

There are two principal groups of organic contaminants from hydrogeological viewpoint. First group includes organic contaminants lighter than water, called in LNAPLs (*l*ight *n*on-*a*queous *p*hase *l*iquids). They are represented by aromatic hydrocarbons, which float on water table. Principal subgroup are BTEX (*B*enzene, *T*oluene, *E*thylbenzene, *X*ylene) (Fig. 11.1). These organic compounds contain benzene ring, and are partially soluble in water, with maximum solubility reaching in the case of benzene 1780 mg/L.

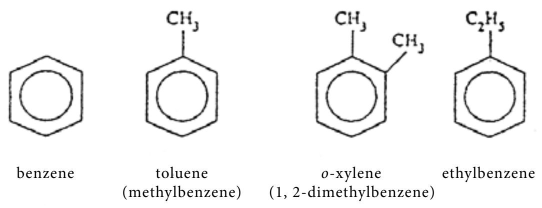

Figure 11.1 Examples of BTEX.

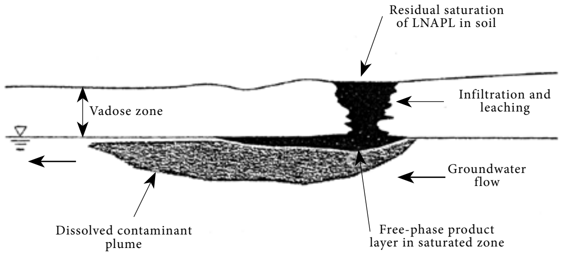

Figure 11.2 Migration of LNAPLs (after Bedient et al., 1994).

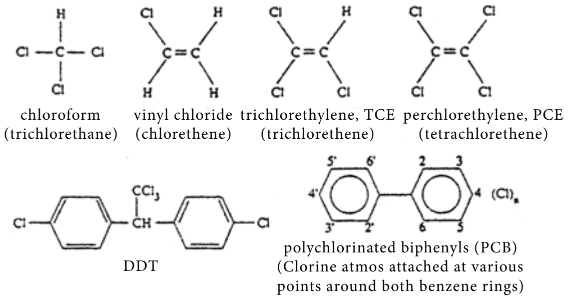

Figure 11.3 Examples of DNAPLs.

LNAPLS occur as free phase floating on water table, which is a source of dissolved plume (Fig. 11.2). Free phase may be present as *residual contamination* (free phase blobs and ganglia are disconnected and surrounded by water) or as *continuous free phase* (free phase is connected in a part of free phase zone at least). After penetration of unsaturated plume they leave behind residual free phase, which can be a source of vapor contaminant plume. Migrating dissolved contamination leaves behind contamination adsorbed on soil organic matter.

Second principal group are DNAPls (*d*ense NAPLs). Typical compounds are chlorinated solvents like trichloroethylen, TCE, and tetrachloroethylen, PCE (Fig. 11.3). These organic compounds have higher density than the density of water and they sink towards the base of an aquifer. There they form *pools* (e.g., continuous free phase accumulations) on the top of low permeability units (Fig. 11.4) and spread in the direction of the dip of aquifer basis, in some cases against the direction of ground water flow. After penetration of both unsaturated and saturated zone they leave behind

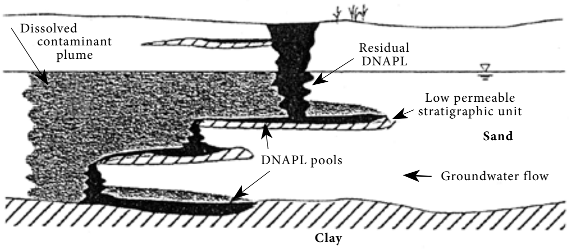

Figure 11.4 Migration of DNAPLs.

residual concentration. The residual concentration is a source of vapor plume in unsaturated zone and dissolved plume in saturated zone. A part of dissolved concentration can be adsorbed on organic matter in solid phase. Solubility of these contaminants is low, but not negligible (1100 mg/L for TCE). The maximum contaminant level (MCL) for TCE is only 5 μg/L and even small release of free phase TCE can contaminate large quantities of water.

11.2 Hydraulics of Free Phase Migration

When free phase of NAPLs penetrates porous media, its migration takes a tortuous path. NAPL is non-wetting phase which stays in the middle of large pores, and, on the other hand, water is wetting phase with respect to solid phase grains. This rule applies for majority of geological materials except for pure organic matter surfaces like peat. Degree of wettability of a fluid is estimated on the basis of contact angle (Fig. 11.5). If the contact angle is < 90°, the tested liquid is wetting, if it is > 90°, then the liquid is non-wetting.

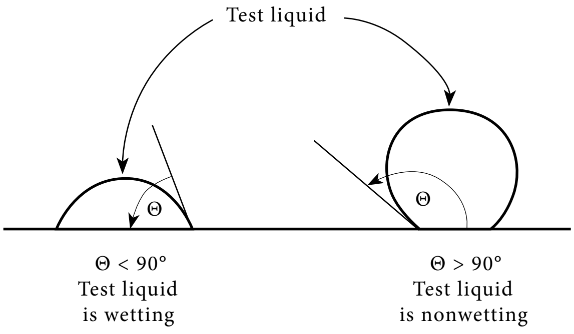

Figure 11.5 Determination of contact angle (modified from Domenico and Schwartz, 1998).

During their migration, NAPLs preferentially enters large pores. When porous media is initially saturated with water, NAPL has to exert displacement pressure P_d to push water out from a water saturated pore. Capillary pressure is defined as the difference between pressure of non-wetting fluid (NAPL) and wetting fluid (water) and is expressed as

$$P_c = P_{NW} - P_W = h_{NW}\rho_{NW}g - h_W\rho_W g \qquad 11.1$$

where P_{NW} pressure of non-wetting fluid, P_W is pressure of wetting fluid, h and ρ indicate height of columns and densities of both fluids, and g is acceleration of gravity. There are similar curves $P_c = f(S_w)$ for system NAPL-water like for unsaturated porous media. Instead of the air, the non-wetting fluid is NAPL in this case. Capillary pressure has to be equal or higher than displacement pressure for NAPL penetration to pores:

$$P_c = P_d = 2\,\delta\cos\gamma/r = h_{NW}\rho_{NW}g - h_W\rho_W g \qquad 11.2$$

After rearrangement (and substitution $h_{NW} = h_W$ because the height of both columns is the same):

$$h_{NW} = 2\,\delta\cos\gamma \,/\, [r\,g\,(\rho_{NW} - \rho_W)] \qquad 11.3$$

where δ is surface tension between water and organic contaminant [N/m], γ is contact angle and r is pore radius. The equation expresses the height of NAPL column, which has to accumulate on the top of less permeable layer to cause penetration of NAPL into the layer. The column is higher for smaller size of pores and for smaller density contrast between NAPL and water. The term ($h_W\rho_W g$) can change during pumping of underlying aquifer and in this case we can pull the contaminant into less permeable layer. There is a similar relation as equation (11.3) for penetration to a fracture. In denominator there can be 2 or other coefficient depending on fracture geometry and r indicates fracture aperture. During migration in a fracture contaminant can penetrate into surrounding blocks by diffusion and can completely disappear in blocks after long period (Parker et al., 1994).

Problem: Calculate the height of DNAPL necessary for penetration to silt (r = 0.000005 m), when δ = 0.040 N/m, ρ_{DNAPL} = is 1600 kg/m^3, and γ = 30°.

Solution: Use equation 11.3:
h = 2×0.040×cos 30° / 0.000005×9.8×(1600–1000) =
= 2.356 m

There is relation between size of pores, hydraulic conductivity, and displacement pressure. The lower is hydraulic conductivity, the higher is displacement pressure. The height of column necessary for penetration to a layer with hydraulic conductivity *k* is (McWhorter, Kueper, 1996)

$$h_{DNAPL} = 9.6\,(\rho_W/\Delta\rho)\,(\sigma/\sigma_{aw})\,(k/n)^{-0.403} \qquad 11.4$$

where $\Delta\rho$ is density difference between contaminant and water, σ is surface tension between organic contaminant and water, σ_{aw} is surface tension between water and air, and k is hydraulic conductivity.

A consequence of inverse relation between displacement pressure and pore size is that free phase of NAPL enters the largest pores by-passing small ones, and its migration often changes direction. In controlled experiments of TCE spreading in sand (Poulsen and Kueper, 1992) was found that spreading was influenced of permeability changes in the scale of mm, and residual saturation was between 2 and 18 %. It was also found that concentrated release in small drops caused penetration of TCE to greater depth than in the case of TCE spill on ground surface. This is partially related to smaller area of infiltration and thus, to more concentrated flow in the first case.

There is similar behavior of NAPLs in fractured media. In a fracture water also covers walls and a NAPL is located in the central zone. When fracture aperture is reduced, spreading of a NAPL can stop. If there is other fracture with larger aperture available, then direction of flow can be completely deflected.

11.3 Partitioning of Organics Between Phases

As stated above, in porous media free phase can be present in continuous form (pool) at the base of an aquifer or on the top of low permeability layers (in the case of DNAPL) or as a layer floating on water table (in the case of LNAPL), and as residual concentration in the form of disconnected blobs and ganglia. Organic contaminant can also be present in the form of dissolved contamination, contamination of adsorbed on solid phase, and as vapor plume in unsaturated zone. There is partitioning between free phase, water phase, solid phase, and vapor phase (in unsaturated zone) during migration of an organic contaminant. Parameters of transfer between phases are in Table 11.1.

Vapor pressure is parameter which describes volatility of organic contaminant. This parameters determines if soil vacuum extraction (SVE) can be used for remediation of a contaminant. Effective vapor pressure, P_i^{eff} in a mixture of contaminants is lower than for a single contaminant and is calculated using Raoult's Law:

Table 11.1 Partitioning parameters.

Parameter	Transfer	Indication	Units
Vapor pressure	free phase-air	P_i	atm
Solubility	free phase-water	S_i	mg/L
Henry Law's constant	water-air	H_{cc}	dimensionless
Coeff. octanol-water	water-solid phase	K_{ow}	dimensionless

$$P_i^{eff} = X P_i \qquad 11.5$$

where P_i is vapor pressure for pure organic contaminant and X_i is its molar fraction in mixture. This means that vapor pressure of a contaminant in mixture may be much lower than vapor pressure of a pure contaminant.

Solubility in water S_i [mg/L] describes dissolution of a contaminant in water and, thus, potential efficiency of pump-and-treat method of remediation. This is maximum possible dissolved concentration because analogy of Raoult's Law also applies for dissolution of a mixture of contaminants:

$$S_i^{eff} = X_i\,S_i \qquad 11.6$$

where S_i^{eff} is solubility in a mixture and X_i is its molar fraction.

Problem: Calculate molar fractions in mixture of 500 g of benzene and 500 g of toluene. Respective molecular weights are 78.1 and 92.14.

Solution:

- molar mass of benzene is 500/78.1 = 6.4, molar mass of toluene is 500/92.14 = 5.43,
- molar fraction of benzene $X_{benzene}$ = 6.4/(6.4+5.43) = 0.54, molar fraction of toluene $X_{toluene}$ = 5.43/(6.4+5.43) = 0.46.

One of consequences of Raoult's Law is that we generally find dissolved benzene concentrations about 20 mg/L in spite of its much higher solubility of 1780 mg/L. Commercial gas is a mixture of more than 100 compounds and benzene molar fraction is only about 2 %. However, in countries like Brazil at some sites concentration of benzene reach more than 50 mg/L because there is the effect of co-solvency with alcohol. Alcohol is sold at gas stations in Brazil as fuel and there often are both gas and alcohol plume present at the same site.

Another reason for much lower concentrations than theoretical solubilities is dilution by dipersion in aquifer and during sampling in a well. When free phase occurs on the top of less permeable layer as a pool, then there is saturated micro-layer close to the pool, but saturation sharply decreases with increasing height above the pool. Vertical distribution of dissolved contaminant above the pool is expressed as (Johnson and Pankow, 1996):

$$C(z) = C_{ef}.\mathrm{erfc}\{z/[2\,(D_v\,L/v)^{0.5}]\} \qquad 11.7$$

where z is height above a pool, C_{ef} is effective concentration calculated by Raoult's Law, D_v is vertical dispersion coefficient (calculated as $D_v = \alpha_v \times v + D_e$, where α_v is vertical dispersivity coefficient, v is flow velocity, and D_e is molecular diffusion coefficient), L is length of a pool in the direction of flow and erfc is complementary error function (Chapter 7.7). On the basis of the formula, we can conclude that the concentration above accumulation of free phase is higher for longer pool, higher vertical dispersivity, and lower flow velocity. On the other hand, if free phase is in the form of residual concentration, then a well in close proximity of residual concentration may show concentrations close to theoretical maximum because residual concentration has much better contact with flowing ground water than free phase in a pool. Next dilution occurs in a sampling well. For example, if thickness of dissolved plume is about 2 m and thickness of screen zone of a well is about 4 m, concentration in sampled water will be about a half of concentration in aquifer. A rule of only 1 % of theoretical maximum concentration was accepted as a possible indicator of presence of free phase (Feenstra and Cherry, 1996), but it has been questioned recently.

Partitioning between dissolved contaminant and air is described by Henry Law's coefficient, H_{cc}, which is defined as

$$H_{cc} = C_{air}/C_{water} \qquad 11.8$$

where C_{air} is concentration in air [mol/m^3], and C_{water} is concentration in water [mol/m^3]. The value of H_{cc} is dimensionless in the case above, but there can be different versions of Henry Law's constant depending on units used for concentrations and caution is necessary when we accept data from literature.

Problem: Convert Henry Law's constant for PCE equal to 0.295 in dimensionless form H_{cc} to form H_{pc} in units [atm/mol×m^3].

Solution:
$H_{pc} = p_{PCEair}/C_{PCEwater}$
$p \times v = n \times R \times T$ and $n/V = p/R \times T = C_{PCEair}$
for $T = 298.15°C$ (25°C), $R = 8.206 \times 10^{-5}$ m^3.atm/mol K
$n/V = 40.873\,p$ or $p = 2.447 \times 10^{-2}\,n/V$ for V in m^3,
then $H_{pc} = 2.447 \times 10^{-2} \times H_{cc}$ and $H_{pc} = 17.73 \times 10^{-3}$ atm/mol×m^3.

Partitioning between organic carbon in solid phase is related to the distribution coefficient octanol-water K_{ow}, defined as

$$K_{ow} = C_{octanol}/C_{water} \qquad 11.9$$

where $C_{octanol}$ and C_{water} are concentrations of organic contaminant in octanol and in water, respectively. The value of K_{ow} is generally listed in logarithmic form and increases with increasing degree of hydrophobicity of organic contaminant (e.g., with increasing tendency to partition into organic matter from water). For example, log K_{ow} for PCB is about 6.0 which means that PCB is about million times more concentrated in solid phase organic carbon than in water. Adsorption on organic matter also depends on fraction of organic matter in aquifer solids, f_{oc}. First we have to calculate distribution coefficient organic carbon-water K_{oc}, which is positively correlated to K_{ow}. Generally we use K_{ow} from tables (for example, Bedient et al., 1994, Fetter, 1999, etc.) and then we calculate K_{oc} using empirical equations. Examples are equation of Schwarzenbach and Westall,

$$\log K_{oc} = 0.49 + 0.72 \log K_{ow} \qquad 11.10$$

or equation of Karickhoff et al.,

$$\log K_{oc} = 0.088 + 0.909 \log K_{ow} \qquad 11.11$$

Sometimes the value of K_{oc} is directly indicated in literature. Distribution coefficient for adsorption of organic contaminant is calculated as

$$K_d = K_{oc} f_{oc} \qquad 11.12$$

and is used in equation for retardation coefficient R (Domenico and Schwartz, 1998):

$$R = v_{water}/v_{organic} = 1 + (\rho_b/n)\,K_d \qquad 11.13$$

where v_{water} and $v_{organic}$ are velocities of water flow and organic contaminant transport, respectively, ρ_b is bulk density of aquifer solids and n is porosity. The term (ρ_b/n) indicates the amount of solid phase in contact with 1 L of water. For $R = 4.0$, for example, transport of an organic contaminant is 4 times slower than advective velocity of water flow. Value of $R = 1.0$ means no adsorption and retardation.

Retardation coefficient R is easily implemented into both analytical and numerical models. There are, however, several problems:

- Organic matter fraction f_{oc}, which is determined in laboratory for solid samples taken out of contaminant plume should be at least 0.01 (or 1 %). For lower

values adsorption on inorganic surfaces becomes important. Considering that many plumes are in sand and gravel aquifers with low concentration of organic matter, there is a potential for significant errors.
- This method applies for hydrophobic organic compounds with solubility less than 10^{-3} mol/L.

Problem: Organic carbon fraction in aquifer solids f_{oc} is 0.01. Calculate K_d and R for 1,2-dichloroethan with $\log K_{ow} = 1.48$. Bulk density of solids is 1.9 g/cm^3 and porosity is 0.25.

Solution: Use Schwarzenbach and Westall equation to calculate K_{oc},
$\log K_{oc} = 0.49 + 0.72\times(1.48) = 1.556$
and $K_{oc} = 10^{1.556} = 35.94$
$K_d = 35.94\times0.01 = 0.359$ mL/g
finally $R = 1 + (1.9/0.25)\times0.359 = 3.731$, which means that transport of 1,2-dichloroethan is 3.731 times slower than water flow.

Both Henry Law's coefficient and distribution coefficient K_d do not depend on Raoult's Law because they describe partitioning of dissolved contaminant into other phases. On the other hand, vapor pressure and solubility depend on Raoult's Law because they describe partitioning of free phase contaminant.

11.4 Biodegradation

Biodegradation is a process that belongs to *natural attenuation* processes. Natural attenuation can be nondestructive, e.g., concentration of a contaminant is reduced by processes like dispersion and mass of a contaminant does not change ($C\downarrow$, $M = \text{const.}$) or destructive, when there is a decrease of both concentration and mass of a contaminant ($C\downarrow$, $M\downarrow$).

Biodegradation is destructive process with resulting reduction of mass of organic contaminant, which is often described as *kinetic process of 1st order* (e.g., rate of biodegradation depends on concentration) and is expressed as

$$C_t = C_0\, e^{-\lambda t} \qquad 11.14$$

where C_t is concentration at time t, C_0 is initial concentration, and λ is *decay constant* $[t^{-1}]$. Often we can found in literature *half-life* $t_{1/2}$ $[t]$ related to decay constant as $t_{1/2} = \ln 2/\lambda$. It is necessary to distinguish between half-life and decay constant because their meaning is inverse, e.g., high decay constant means fast biodegradation, and high half-life means slow biodegradation. The concept of first order biodegradation kinetics does not include any limiting factors for biodegradation (see later) and values of decay constant depends on site specific conditions (pH, redox conditions etc.) and may not be applicable for other sites. This means that decay constant for organic contaminants is not a constant in strict sense like decay constant for radionuclides. Alvarez (1996) indicates decay constant for benzen in the range from almost 0 to 0.0085 day^{-1}, with an average of 0.0046 day^{-1}.

Biodegradation of petroleum products like BTEX occurs in oxidizing environment with participation of bacteria. In the process O_2 and other oxidized species are used as electron acceptors and organic contaminants are substrate for bacterial population. For example, the reaction of benzen with O_2 is expressed as

$$C_6H_6 + 7.5\, O_2 = 6\, CO_2 + 3\, H_2O \qquad 11.15$$

Theoretical sequence of electron acceptors consumption is the same as in uncontaminated aquifers: $O_2 \rightarrow NO_3^- \rightarrow Mn^{4+} \rightarrow Fe^{3+} \rightarrow SO_4^{2-} \rightarrow$ methanogenesis (Borden et al., 1995). However, the rate of electron acceptors consumption in biodegradation of BTEX plume is much faster, and there often is an overlap between different electron acceptors zones. Resulting ground water has low redox potential (often $Eh < -200$ mV) and high concentration of dissolved metals (Baedecker et al., 1993). This is a consequence of dissolution of hydroxides such as $Fe(OH)_3$ and MnOOH in solid phase with adsorbed metals like Zn and Pb. In this process, concentration of dissolved inorganic carbon (DIC) and partial pressure of CO_2 (P_{CO2}) also increase. High P_{CO2} values and concentrations of metals represent a serious challenge during remediation because precipitation of calcite due to de-gassing of CO_2 and $Fe(OH)_3$ due to oxidation of Fe^{2+} can completely block air stripping colon for treatment of water. Thus, there is often necessary to do pre-treatment of ground water prior to air stripping. Typical geochemical zonation observed in BTEX plume at Bemidji site in Minnesota, USA, is in Fig. 11.6.

There is an important role of transverse vertical dispersion, which can supply water with electron acceptors into plume. However, most of biodegradation takes place in source zone with free product, when ground water with electron acceptors flows through it. According to Wiedermeier et al., (1995), 1 mg/L of O_2 can biodegrade 0.32 mg/L of BTEX, 1 mg/L of NO_3^- can biodegrade 0.21 mg/L of BTEX, just like biodegradation of 1 mg/L of SO_4^{2-}. Biodegradation of 1 mg/L of BTEX results in production of 21.8 mg/L of Fe^{2+} from

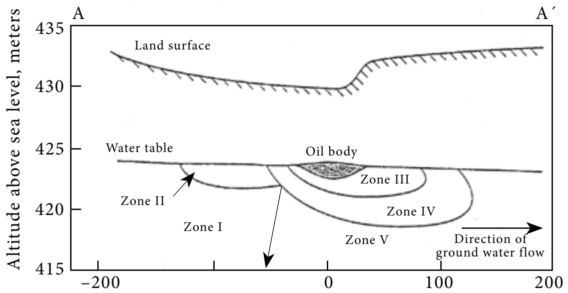

Figure 11.6 Geochemical zone at BTEX contaminated site at Bemidji, Minnesota, USA (adapted from Baedecker et al., 1993). Zone I is background water with high oxygen concentration, Zone II has low oxygen and increased Ca, Mg, and P_{CO2}, Zone III in contact with free phase has methane and high manganese and iron concentration, Zone IV has traces of oxygen and lower concentrations of metals, and Zone V is similar as Zone I.

$Fe(OH)_3$ in solid phase, and production of 0.78 mg/L of methane. Total *biodegradation capacity BC* based on instantaneous consumption of electron acceptors is

$$BC = \Sigma[(AE)_i/F_i] \qquad 11.16$$

where $(AE)_i$ is concentration of electron acceptor (O_2, NO_3^- etc.), and F_i is utilization factor equal to amount of an electron acceptor necessary for biodegradation of 1.0 mg of BTEX (for example, for O_2 it is 1/0.32 = 3.1 mg). There are generally enough electron acceptors in ground water and common length of BTEX plumes is around 100 m. When biodegradation rate is the same as the rate of contaminant input and transport, then there is formation of *steady-state plume* (plume which does not move).

Situation is more complicated in the case of chlorinated solvents. Their rate of biodegradation is often limited and biodegradation takes place in reducing environment with high concentration of H_2 generated by redox processes. Principal process is reductive dechlorination, when Cl^- in a chlorinated compound is replaced by hydrogen. In this process a contaminant is electron acceptor. Typical reductive de-chlorination sequence is PCE (tetrachloroethen) →TCE(trichloroethen) → 1,2-DCE(dichloroethen) →VC(vinylchlorid)→ ethen. If more than 80 % of DCE is in the form of cis-1,2-DCE, then there probably is reductive dechlorination (Wiedemeier et al., 1996).

Nyers and Duffin, (1997), distinguished 3 types of environments for biodegradation of chlorinated solvents (Fig. 11.7). Type 1 correspond to simultaneous occurrence of chorinated solvents with BTEX, and biodegradation of BTEX creates reducing environment necessary for reductive dechlorination. Type 2 is related by high natural concentration of organic matter, which also creates reducing environment like Type 1. Type 3 is environment with low both natural and antropogenic organic matter and with detectable O_2. In this environment there is no reductive dechlorination and principal attenuation mechanism is dispersion. Exception is biodegradation of VC and partially also 1,2-DCE, which can be biodegraded in oxidizing environment. Nyer and Duffin (1997) also present point system for evaluation of possibility of reductive dechlorination.

In the case of BTEX biodegradation, there can be application of more complicated *Monod kinetics,* which includes parameters of bacterial population in ground water. Basic equation is

$$\mu = \mu_{max} [C/(K_c + C)] \qquad 11.17$$

where μ is rate of bacteria growth $[t^{-1}]$, μ_{max} is maximum rate of bacterial growth $[t^{-1}]$, C is concentration of rate-limiting substrate [mg/L], and K_c is concentration of substrate for half-rate of maximum growth. When $K_c << C$, we obtain $\mu = \mu_{max}$ and rate of growth is at its maximum. Amount of decayed contaminant by consumption of oxygen is

$$\Delta C = M_t \, \mu_{max} [C/(K_c + C)] \, [O/(K_O + O)] \, \Delta t \qquad 11.18$$

where M_t is total microbial population, O is oxygen concentration, K_O is oxygen half saturation constant, and Δt is time period of biodegradation. However, equations above are not frequently used because there generally is lack of information about bacterial population.

Problem (from Bedient et al., 1999): There is concentration of dissolved benzene of 12 mg/L in an aquifer. Concentration of oxygen available for biodegradation is 8 mg/L, and decay constant for benzene is 0.1386 day^{-1}. Compare first-order decay, Monod kinetics, and instantaneous reaction biodegradation for period of 10 days.

Solution:

- Instantaneous reaction: 0.32 mg of benzene are biodegraded by 1 mg/L of O_2, so 3 mg/L of O_2 biodegrade 1 mg/L of benzene, final benzene concentration is 12 – (8/3) = 9.33 mg/L,
- First-order decay: final benzene concentration (equation 14) = $12\times e^{-1.386x10}$ = 3.0 mg/L
- Monod kinetic: assuming O_2 half saturation constant of 0.1 mg/L, benzene half saturation constant 22.16 mg/L, maximum utilization rate 9.3 day^{-1}, and microorganisms population of 0.05 mg/L, we substitute into equation 18: benzene reduction=9.3×[12/(12+22.16)]×[8/(8+0.1)]×10×0.05=1.59 mg/L, final benzene concentration = 12 – 1.59 = 10.41 mg/L.

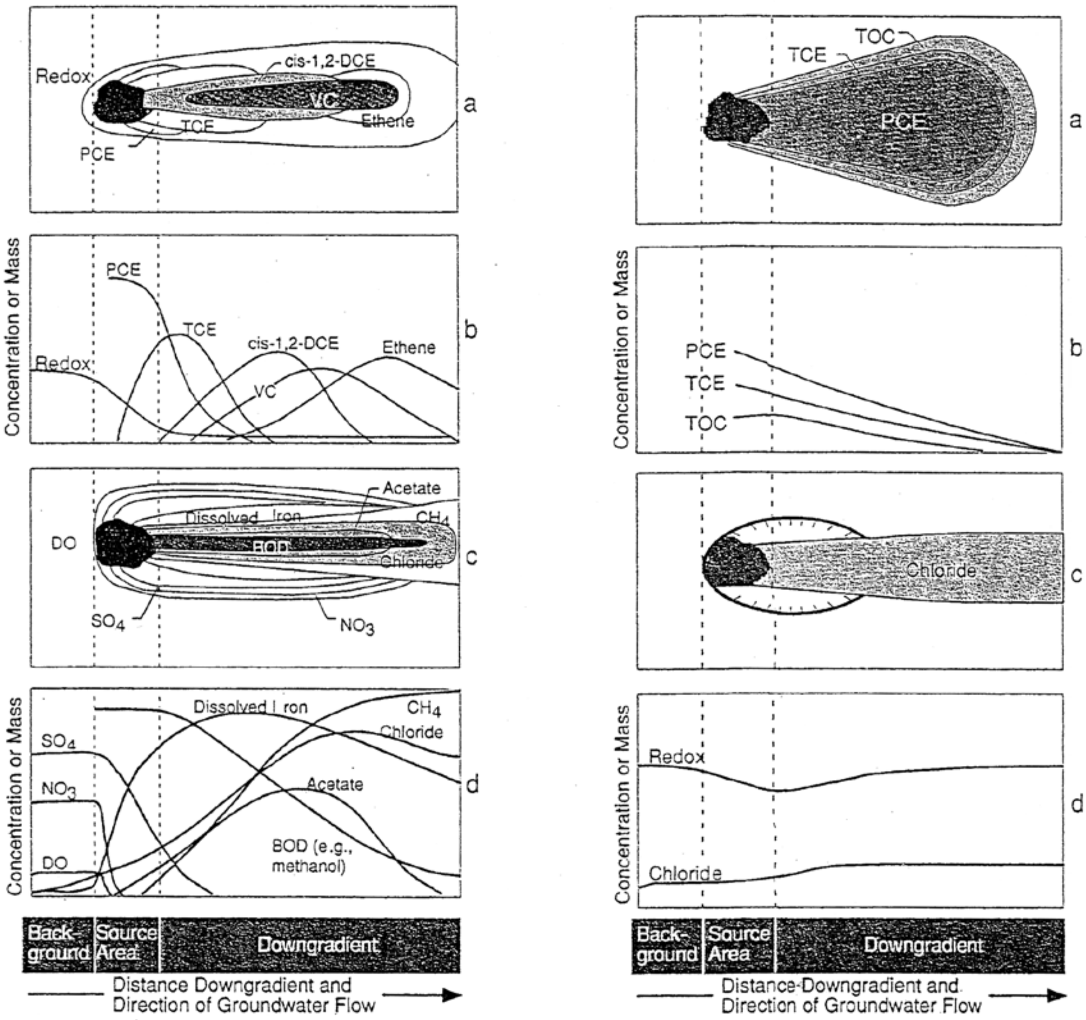

Figure 11.7 Types of environment in biodegradation of chlorinated solvents (adapted from Wiedemeier et al., 1996). Type 1 (left) and Type 3 (right).

This means that first-order decay approach may overpredict biodegradation rate because limiting factors like electron acceptors concentrations are not taken into account.

11.5 Mass Balance Calculations

Free phase localization has pivotal importance for remediation because free phase generally serves as long term source of dissolved contamination. However, in many cases we cannot make visual observation of free phase. In this case, we can evaluate the possibility of free phase presence on the basis of mass balance calculations (Feenstra et al., 1991). Mass balance for a sample from saturated zone is

$$M_{\text{total}} = C_{\text{water}}\, V_{\text{water}} + K_{\text{d}}\, \rho_{\text{solids}}\, V_{\text{solids}}\, C_{\text{water}} \qquad 11.19$$

and after rearrangement

$$C_{\text{water}} = M_{\text{total}} / (K_{\text{d}}\, \rho_{\text{solids}}\, V_{\text{solids}} + V_{\text{water}}) \qquad 11.20$$

where M_{total} is total amount of contaminant in a sample, V_{solids} and V_{water} are volumes of solid and water phase, respectively, ρ_{solids} is density of grains of solid phase, K_{d} is distribution coefficient for contaminant, and C_{water} is concentration of contaminant in water. The same equation for unsaturated zone is

$$M_{\text{total}} = C_{\text{water}}\, V_{\text{water}} + K_{\text{d}}\, \rho_{\text{solids}}\, V_{\text{solids}}\, C_{\text{water}} + H_{\text{cc}} V_{\text{air}} C_{\text{air}} \qquad 11.21$$

where H_{cc} is Henry Law's constant, V_{air} is volume of air, and C_{air} is concentration in air.

When calculated water concentration is higher than effective solubility (calculated on the basis of Raoult's Law), then we assume that there is free phase in the sample. However, when the calculated concentration is lower, we cannot exclude the possibility of free product for the following reasons: (a) there may not be equilibrium between phases in sample, and (b) it is possible that real effective solubility is lower because all compounds in mixture possibly have not been determined.

Problem: Determine if there can be free phase of TCE in a sample with total TCE 200 μg/g. Porosity is 33 %, f_{oc} = 0.02 %, ρ_s = 2.67 g/cm^3, log K_{ow} = 2.29 and solubility of pure TCE = 1100 mg/L.

Solution:

- 1 cm^3 has 0.33 cm^3 of water and 0.67 cm^3 of solids or 0.67×2.67 = 1.789 g of solids,
- TCE in 1 cm^3 = 1.789×200 μg = 357.78 μg
- K_d = 0.0002×10 exp[0.72(2.29)+0.49] = 0.0275 mL/g
- C_{water} = 357.78/(0.0275.2.67.0.67 + 0.33) = 943 μg/L = 943 mg/L, this is less than 1100 mg/L, so we cannot confirm presence of free product.

11.6 Investigation of Contaminated Sites

This is very extensive topic discussed in several publications (for example, Bedient et al., 1999, Fetter et al., 1999, etc.) and only principal points are mentioned in this text.

During investigation of contaminated sites we have to determined distribution of contaminant between phases because this information decides about the choice of remediation method. For example, highly adsorbed PCB cannot be remediated by pumping. Benzene, on the other hand, can be at least partially pumped out with ground water, and in unsaturated zone can also be remediated by soil vacuum extraction (SVE) because of its volatility.

Localization of free phase has pivotal importance because both residual concentrations and pools are long term sources of dissolved contamination. Methods for localization of free phase include:

- Direct observation: this is generally plausible in the case of LNAPLs floating on water table. On the other hand, pools of DNAPLs at the base of aquifer are difficult to find. Residual concentration of LNAPLs and especially BTEX have specific smell and color. This is not the case of DNAPLs, which often cannot be detected by senses in small concentrations.
- Application of UV light because there is fluorescence of many organic contaminants.
- Application of atmogeochemical prospection in unsaturated zone: in the proximity of free phase saturated vapor concentrations can be reached. In this case, we need to know free phase composition and calculate expected saturated concentrations by Raoult's Law. However, positive indication is a proof, negative indication is inconclusive because there are several factors which can decrease vapor concentrations. Soil gas sampling also serves to determine limits of vapor plume.
- Comparing dissolved concentrations with theoretical saturated concentrations in saturated zone: There may be saturated concentrations in close proximity of residual free phase. However, we have to include the effect of mixture by application of Raoult's Law again. Also in this case positive indication is proof, negative indication is inconclusive.
- Application of mass balance approach presented in problem above. Once more, negative results are not a proof of free phase absence.

In general, when total soil concentration, C_{org}, of organic contamination is determined, it is converted to relative saturation value:

$$S_{org}\,(\%) = \rho_b\, C_{org}/(\rho_{org}\, n\, 10^6) \qquad 11.22$$

where S_{org} is saturation of pore space by organic contaminant in %, ρ_b is bulk density of solid phase in g/cm^3, C_{org} is concentration of organic contaminant in soil sample in mg/kg, ρ_{org} is bulk density of organic contaminant in g/cm^3, and n is porosity. Mass of free phase in source zone is calculated as

$$M_{org}\,(g) = L\, W\, H\, n\, \rho_{org}\, S_{org} \qquad 11.23$$

where L, W, and H are length, width, and height of source zone, respectively.

We also need to determine limits of dissolved contamination plume. In the first phase we locate sampling wells or piezometers along direction of flow. Maximum theoretical distance of plume movement can be determined from Darcy's Law (plus some additional distance for dispersion allowed) when time of release is known. In the next phase we locate sampling points in the direction perpendicular to ground water flow to determine transversal size of plume. Finally, it is convenient to install at least one piezometric nest to determine vertical dimension of plume.

Wells for measurement of thickness of free product of LNAPLs have to be screened above maximum elevation of water table to allow the entry of free product. When there is drilling for location of DNAPLs in depressions at the base of aquifer, there has to be continuous monitoring of dissolved concentration. When the top of a pool is found, drilling has to be stopped because further drilling could contaminate underlying formations.

During sampling we should use positive pressure devices and avoid any splashing of sampled water which could cause degassing of samples. Samples should be deposited in cold environment. It is recommended to add a bactericide to avoid biodegradation of samples during deposition, especially when there is a time lag between sampling and analysis. There often is strong concentration gradient within a plume (concentration differences by several orders of magnitude), and logarithms of concentrations are recommended for plotting instead of absolute numbers.

Samples of soils for determination of soil organic matter fraction f_{oc} should be taken out of the contaminated area to avoid influence of anthropogenic carbon. Number of samples depends on financial constraints, but several samples are recommended. Equation 11.13 is used to calculate theoretical retardation factors for different contaminants.

11.7 Evaluation of Natural Attenuation

When we need to verify the possibility of natural attenuation, the following approach is used:

(1) Trends of dissolved concentrations in the plume have to be determined by several samplings. Non-parametric statistic tests (for example, Mann-Whitney test) are used to check decreasing concentrations.

(2) Background concentrations of electron acceptors (O_2, NO_3^- etc.) are determined in ground water out of plume. Then we compare background concentrations with concentrations in the plume to decide if bioremediation takes place. Products of biodegradation like Fe(II) and methane are sampled only within the plume. Equation 11.16. can be used to convert changes in concentrations of electron acceptors to the amount of biodegraded BTEX compounds. In the case of chlorinated solvents, geochemical indicators are used only as qualitative indicators of intrinsic bioremediation.

(3) Laboratory test in microcosmos with contaminated water and sediments may be run and bacterial population parameters are determined.

Last point is only optional, but first two points are necessary according to U.S. EPA methodology.

Concentration plots with time for single wells based on Equation 11.14 can be used to calculate time-based natural attenuation constants. Space-based natural attenuation constant can be determined by plotting ln (C/C_0) as a function of distance from source. From Equation 11.14. we obtain after substitution for $t = x/v$ (x is distance from source, v is advection velocity)

$$\ln (C/C_0) = -(k/v)\,x \qquad 11.24$$

which is a straight line with slope $-(k/v)$. Thus, natural attenuation constant can be calculated by multiplication of slope by advection velocity. More advanced version of this interpretation is the equation of Buscheck and Alcantar (1995).

Finally, when total mass in a plume is known from dense network of sampling points on profiles (including adsorbed contamination), Equation 11.14 can be used on mass bases and decay constant is calculated instead of natural attenuation constant:

$$\lambda = -\ln(M_2/M_1) \,/\, \Delta t \qquad 11.25$$

where λ is decay (biodegradation) constant, M_2 and M_1 are concentration in time t_2 and t_1, and Δt is time of flow between profile 1 and profile 2.

It is convenient to use analytical screening models like BIOSCREEN for BTEX and BIOCHLOR for chlorinated solvents or numerical models like RT3D to estimate natural attenuation parameters. It is always useful to have a conservative tracer like MTBE (methyl tert-butyl ether, added to gas as anti-detonator) for BTEX to separate bioremediation from other attenuation processes like dispersion. When parameters of natural attenuation are known, models can be used for prediction of concentrations in receptors (water supply wells etc.), which are necessary for risk analysis (see Chapter 13).

References

Alvarez P.J.J., 1996: Caution against the inappropriate use of analytical fate and transport models to estimate the age and risk of petroleum products releases, *Ground Water Monitor. and Rem.*, Spring 1996, pp. 72–76.

Baedecker M.J., Cozzarelli I.M., Eganhouse R.P., Siegel D.I., Bennett P.C., 1993: Crude Oil in a Shallow Sand and Gravel Aquifer-III. Biogeochemical Reactions and Mass Balance Modeling in Anoxic Groundwater, *Appl. Geochem.* 8, pp. 569–586.

Bedient P.B., Rifai H.S., Newell C.J., 1999: *Ground Water Contamination, Transport and Remediation*, 2nd Edition, Prentice Hall PTR, Upper Saddle River, NJ 07458.

Borden R.C., Gomez C.A., Becker M.T., 1995: Geochemical Indicators of Intrinsic Bioremediation, *Groundwater*, Vol. 33, No. 2, pp. 180 – 189.

Buscheck T.E.G., Alcantar C.M., 1995: Regression Techniques and Analytical Solutions to Demonstrate Intrinsic Bioremediation, In: P*roceedings of 1995 Batelle International Conference on In-Situ and On-Site Bioreclamation.*

Domenico P.A., Schwartz F.W., 1998: *Physical and Chemical Hydrogeology*, 2nd Edition, John Wiley & Sons, New York.

Feenstra S., Mackay D., Cherry J.A., 1991: A Method for Assessing residual NAPL Based on Organic Chemical Concentrations in Soil Samples, *Groundwater Mon. Rev.,* 11(2), pp. 128–136.

Feenstra S., Cherry J.A., 1996: Diagnosis and Assesment of DNAPL Sites, In: J.F.Pankow, J.A.Cherry (Editors), *Dense Chlorinated Solvents and other DNAPLs in Groundwater,* Waterloo Press, pp. 395–473.

Fetter C.W., 1999: *Contaminant Hydrogeology*, 2nd Edition, Macmillan Publishing Company, New York.

Johnson R.L., Pankow J.F., 1992: Dissolution of Dense Chlorinated Solvents in Groundwater: 2. Source Functions for Pools of Solvents, *Envir. Sci. Technol.* 26, pp. 896–901.

McWhorter D.B., Kueper B.H., 1996: Mechanics and Mathematics of the Movement of dense Non-Aqueous Phase Liquids (DNAPLs) in Porous Media, In: J.F.Pankow, J.A.Cherry (Editors), *Dense Chlorinated Solvents and other DNAPLs in Groundwater,* Waterloo Press, pp. 89–128.

Nyer E.K., Duffin M.E., 1997: The State of Art of Bioremediation, *Ground Water Monitoring and Remediation*, Spring 1997, pp. 64 – 69.

Parker B.L., Gillham R.W., Cherry J.A., 1994: Diffusive Disappearence of Immiscible-Phase Organic Liquids in Fractured Geologic Media, *Groundwater* 32(5), pp. 805–820.

Poulsen M., Kueper B.H., 1992: A Field Experiment to Study the Behavior of Tetrachloroethylene in Unsaturated Porous Media, *Envir. Sci. Technol.*, 26, pp. 889–895.

Wiedermeier T.H., Wilson J.T., Kampbell D.H., Miller R.N., Hansen J.E., 1995: *Technical Protocol for Implementing Intrinsic Remediation with Long-term Monitoring for Natural Attenuation of Fuel Contamination Dissolved in Groundwater, San Antonio, Texas*, U.S. Air Force Center for Environmental Excellence.

Wiedermeier T.H., Swanson M.A., Montoux D.E., Wilson T.J., Kampbell D.H., Hansen J.E., Hass P., 1996: Overview of the Technical Protocol for Natural Attenuation of Chlorinated Aliphatic Hydrocarbons in Ground Water under Development for the U.S. Air Center for Environmental Excellence, In: *Symposium on natural attenuation of chlorinated organics in ground water,* 540/R-96/509, pp. 35–39, Washington D.C., U.S. EPA.

Chapter 12: Geochemical Aspects of Remediation of Contaminated Aquifers

12.1 Introduction

Remediation of contaminated underground environment is complicated process. When a contaminated ground water is pumped out, there is an initial fast reduction of concentration in water, but asymptotic behavior of concentration can be observed in later phases (Fig. 12.1). The behavior is also called *tailing*. In many cases, the more or less constant concentration in late phase of pumping is higher than maximum contaminant level (MCL). Both physical and chemical processes can be responsible for this behavior.

Principal physical process is limited diffusive contaminant transport from low permeability zones (Mackay and Cherry, 1989). During pumping, the most of pumped ground water comes from high permeability preferential flow zones. Contamination from low permeability zones slowly diffuses to preferential flow zones and maintains relatively high concentration in pumped ground water. The reverse diffusion during pumping is slow process because concentration gradient dC/dx is lower than it was during contaminant migration. Thus, this behavior is related to the heterogeneity of permeability in an aquifer. This effect is even more pronounced in double porosity media. In that case, there is diffusion supply of contamination from low permeability blocs into preferential flow zones in fractures.

Another reason is related to the shape of pumping well *capture zone*. When natural flow exists, the capture zone is asymmetric and elongated upgradient. In that case, contaminant path in the middle zone of capture zone is shorter than at the periphery of capture zone. Later arrival of contamination from periphery of capture zone may also result in tailing effect (Palmer and Fish, 1994).

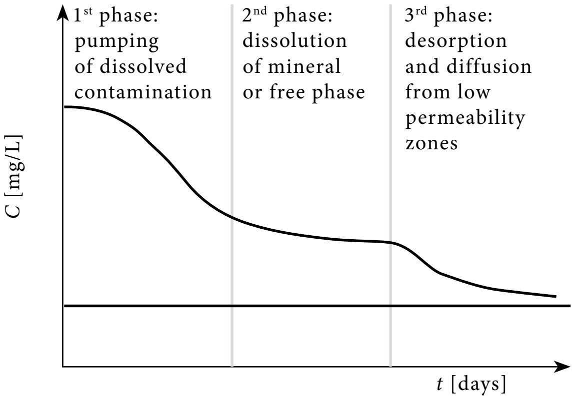

Figure 12.1 Tailing effect during remediation.

12.2 Geochemical Aspects

12.2.1 Desorption of Contaminants

When contamination is in dissolved form only, remediation is relatively straightforward. Time necessary for remediation would be simply

$$t = (V\,n)/Q \qquad 12.1$$

where V is volume of contaminated aquifer, n is porosity, and Q is pumping rate. However, in many cases most of contaminant is in solid phase. When contaminant is adsorbed and adsorption/desorption follows the linear isotherm K_d, resulting time for remediation is obtained by multiplication of the time calculated by equation 8.1 by retardation factor R (Chapter 7.5). Thus,

$$t_{\mathrm{adsorbed}} = (R\ V\ n)/Q \qquad 12.2$$

The equation makes sense because R indicates how many times slower moves a contaminant compared to the ground water flow velocity. Both equations above neglect the effect of dispersion, which results in some tailing compared to the case of piston flow. The exchange factor EF (Deutsch, 1997), defined as a ratio between water concentration before and after flushing of one pore volume, is

$$EF = C_1/C_2 = 1 - (1/R) \qquad 12.3$$

where C_1 and C_2 are dissolved concentrations before and after flushing, respectively. It is evident that when R (and, thus, K_d) increases, the value of exchange factor decreases as a consequence of slower desorption rate. Number of flushings necessary to reduce concentration from initial concentration C_{initial} to limiting concentration C_{limit} is

$$NF_{\mathrm{desorp}} = \log\left(C_{\mathrm{initial}}/C_{\mathrm{limit}}\right) / \log EF \qquad 12.4$$

Situation becomes more complex in the case of non-linear isotherm (Appelo and Postma, 1993). Retardation factor R is defined as

$$R = 1 + (\rho_b/n)(\mathrm{d}S/\mathrm{d}C) \qquad 12.5$$

and for linear isotherm

$$R = 1 + (\rho_b/n)\ K_d \qquad 12.6$$

where dS/dC is equal to K_d e.g., to slope in graph $S = f(C)$, ρ_b is bulk density of solid phase, and n is porosity. For non-linear isotherm such as the Freundlich isotherm, $S = K_F.C^n$, and R becomes

$$R = 1 + (\rho_b/n)(\mathrm{d}S/\mathrm{d}C) = 1 + (\rho_b/n)\ n\ K_F\ C^{n-1} \qquad 12.7$$

Thus, the value of R is no longer constant, but depends on dissolved concentration C. When C is high, retardation is low, (it is even more pronounced for the Langmuir isotherm with upper limit for adsorption), but the value of R increases at low dissolved concentrations. This non-linear desorption can produce a tailing of the curve C vs. t. It is worth mentioning that the process of diffusion from low permeability zones (e.g. physical process), represented as immobile water zones towards high permeability zones (mobile water zones) can produce the same effect.

12.2.2 Dissolution of precipitated minerals

Situation is even more complicated in the case of precipitation of inorganic contaminants as minerals. For example, lead can precipitate as cerussite, $PbCO_3$, Cr(VI) can precipitate as hashemite, $BaCrO_4$, or, after reduction, as amorphous chromium hydroxide, $Cr(OH)_3$(am). The precipitated mineral serves as a source of dissolved contamination during pumping (2nd zone, Fig. 12.2), and maintains dissolved equilibrium concentration with the mineral. The theoretical number of flushings necessary for dissolution of mineral of contaminant is

$$NF_{\mathrm{dissol}} = [(\rho_b/n)C_{\mathrm{solid}}]/C_{\mathrm{eq}} \qquad 12.8$$

where C_{solid} is concentration of contaminant present as a mineral in solid phase and C_{eq} is equilibrium concentration of dissolved contaminant in ground water. This concentration includes free ions and complexes (for example, for lead it is $Pb_{\mathrm{total}} = Pb^{2+} + PbCl^{+} + PbSO_4^{0}$ etc.) and is calculated by a program such as PHREEQC (Parkhurst, 1995).

Total number of flushings is calculated as

$$NF_{\mathrm{total}} = 1 + NF_{\mathrm{dissol}} + NF_{\mathrm{desorp}} \qquad 12.9$$

where 1 represents first volume of contaminant dissolved in ground water. The change of concentration during pumping is shown in Fig. 12.2. First volume of dissolved contamination is pumped out quickly, but dissolution of mineral keeps concentration high. After complete dissolution of mineral, desorption and diffusion from low permeability zones supplies contamination and asymptotic behavior is observed..

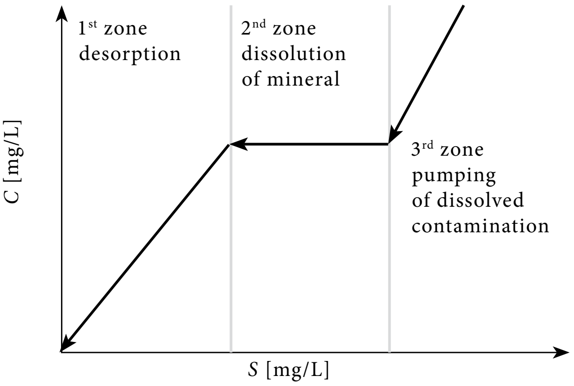

Figure 12.2 Processes during remediation. S and C indicate solid phase and aqueous phase concentrations, respectively. Desorption is considered to be linear and reversible.

12.2.3 Dissolution of Free Phase

Dissolution of free phase of organic contaminants is an analogy of dissolution of minerals of inorganic contaminant. This process is complicated by a common presence of organic contaminants in mixtures. For example, commercial gasoline comprises more than 100 compounds. Solubility of compounds in mixture depends on the Raoult´s Law (Chapter 11) and is lower compared to the solubility of a single compound. Let us consider, for example, mixture of TCE with solubility of 1100 mg/L and 1,2-DCP (dichloropropan) with solubility of 2700 mg/L. Solubilities of both compounds in mixture are in Table 12.1.

Thus, during pumping the dissolution of 1,2-DCP will be faster and mixture of free phase will be enriched in less soluble TCE. This means that transfer of mass and rate of free phase dissolution will be decreasing with time. Remaining mass after each flushing step is equal to

$$M_2 = M_1 - [(S_i^{ef}/MW)\ V_{water}] \qquad 12.10$$

where M_2 and M_1 are remaining and previous masses of free phase, respectively, S_i^{ef} is effective solubility of a compound in mixture, MW is molecular weight of the compound and V_{water} is volume of water in contact with free phases. When the mixture has about 28.95 % of 1,2-DCP and 71.05 % of TCE, the solubilities of both compounds will be the same, equal to 781.6 mg/L. The changes in free phase composition will also result in changes of the composition of dissolved contamination plume. This behavior is sometimes erroneously interpreted as a consequence of biodegradation. Dissolution is further complicated by the lack of equilibrium between fast-flowing water and relatively slow transfer of dissolving free phase.

Slow dissolution of free phase is an analogy of dissolution of inorganic contaminant mineral and seriously complicates remediation. Thus, localization of free product in source zone and its removal or isolation plays a pivotal role in remediation projects.

12.3 Basic Types of Remediation

In this section, we present some typical remediation methods. This outline is by no means complete and much more details can be found in specialized publications such as Suthersan, (1996) and Nyers, (1996).

Pump-and-treat (PT): This is classical method, which works quite well when most of contamination is in dissolved form. However, for reasons indicated above the efficiency of the method becomes limited when adsorbed contamination, free phase of organic contamination, and precipitated mineral of contaminant are present. Even when complete remediation of contaminated aquifer by this method is impossible, the method can be used for *containment* of dissolved plume, e.g., the pumping prevents further spreading of contaminant plume towards potential receptors (water supply wells, surface water bodies etc.). The efficiency of PT depends on heterogeneity of an aquifer and pumping wells have to be properly located to prevent escape of contaminated ground water. The location and spacing of pumping wells is often determined by hydrogeological modeling. The pumped water contaminated by organics is treated above ground in filters with granular activated carbon (GAC) or in air-stripping colons (Nyers, 1996).

Chemical enhancement of PT: This method is used to enhance the transfer of adsorbed or precipitated contaminant from solid phase to pumped ground water (Palmer and Fish, 1992). Typical transfer-enhancing processes are: a) competitive adsorption/desorption (example: phosphate displacing arsenic from adsorption sites), b) complexation of metals (example: citric acid complexing Cr(III)), c) cosolvent effects (example: ethanol increasing solubility of free phase of BTEX), d) application of surfactants (they decrease interfacial tension and increase mobility of NAPLs), e) reduction/oxidation (example: organic matter reducing Cr(VI) to Cr(III), which precipitates as $Cr(OH)_3$), f) precipitation/dissolution (example: injection of alkaline solution causes precipitation of lead as $PbCO_3$). A chemical enhancement system has several subsystems: 1) injection system, 2) reaction zone, 3) extraction system, and 4) treatment system for recovered water with contaminant and reactive agent. Principal problem often is the delivery of reaction agent to contaminated zones. Transport of reaction agent follows preferential flow path and may completely miss contamination. Another problem is disposal of sludge from treatment of pumped water.

Impermeable walls: These walls are made from materials such as bentonite slurry and they have low permeability (<10^{-10} m s^{-1}). They are generally located in source zone of contamination (around free phase zone,

Table 12.1 Solubilities of TCE and 1,2-DCP in mixture.

Molar fraction 1,2-DCP	0	0.1	0.2	0.3	0.4	0.5	0.6	0.7	0.8	0.9	1.0
1,2-DCP	0	270	540	810	1080	1350	1620	1890	2160	2430	2700
TCE	1100	990	880	770	660	550	440	330	220	110	0

around landfills etc.). Their purpose is to stop advective flux across source zone and, thus, to prevent formation of dissolved plume. However, even low permeability materials are permeable for diffusion, which can deliver considerable quantities of contaminants into aquifers.

Impermeabilization of ground surface: This is a relatively simple method which aims to reduce infiltration and, thus, formation of contaminated plume in saturated zone. The impermeable layer can be clay liner, geotextile or combination of both. Typical value of hydraulic conductivity of the layer is $<10^{-10}$ m s^{-1} and a protective layer (for example, gravel) on the top of low permeability layer is required to prevent destruction of the layer by drying and by roots of plants. Common applications are related to landfills and mine tailings sites, where low permeability layer maintains high water saturation and also reduces diffusion flux of oxygen (Chapter 9). A variant of the method is placement of impermeable layer at the base of future source of contamination. An example is construction of low permeability layers and drainage system at the base of projected landfill.

Soil vacuum extraction, (SVE): This is an efficient approach for remediation of unsaturated zone with residual free phase of organic contaminants. Suction is applied in air wells located in unsaturated zone. Flow of air is introduced and a contaminant partitions into air and is carried away towards suction wells. This approach has an advantage compared to the pumping of ground water because the flow rate for air is much higher than for water. This method is applicable only for volatile contaminants with high values of vapor pressure P_i and in permeable soils with high value of intrinsic permeability k. In some cases, the method is combined with air-sparging. The air-sparging is based on injection of air into saturated zone. Air bubbles then rise towards water table and there is partitioning between dissolved contamination and air bubbles depending on the value of Henry Law constant H_{cc} for a given contaminant. When bubbles reach water table, contaminants enter unsaturated zone and they are removed by soil vacuum extraction.

Soil flushing: This method is in the stage of development. It is based on the application of solution of surface-active compounds (surfactants) for flushing of residual free phase in unsaturated zone. Solubility of organic contamination increases and they drain towards the saturated zone, where they are captured by classical pumping methods. Compared to soil vacuum extraction (SVE), the method is only applicable at relatively low depth, but is applicable also for cleaning of capillary fringe, where SVE fails.

Permeable reactive barriers (PRB): These are in-situ reactive zones, where reaction agents are added to create favorable environment for remediation of contaminants. Typical applications include both organic and inorganic contaminants. In the case of acid plume with high metals and sulfate concentrations, the barrier is filled by organic matter and sulfate reduction and precipitation of sulfides take place:

$$2CH_2O + SO_4^{2-} = H_2S + 2HCO_3^- \qquad 12.11$$

$$Me^{2+} + H_2S = MeS + 2H^+ \qquad 12.12$$

where Me^{2+} represents metal. A common reactive material for chlorinated solvents is zero valence iron Fe^0, causing reductive dechlorination:

$$2Fe^0 + 3H_2O + X\text{-}Cl = 2Fe^{2+} + 3OH^- + H_2(g) + \\ + X\text{-}H + Cl^- \qquad 12.13$$

where X represents functional group of chlorinated solvents. The reactive barrier has to be more permeable than the surrounding aquifer because a plume would by-pass the barrier in the opposite case. This fact represents a limitation for the method because in some cases the residence time in the barrier may not be sufficient to complete remediation.

Natural attenuation (NA): This is a process of natural reduction of contaminant concentration, without human involvement. It can be both non-destructive (concentration decreases, but mass of contaminant remains the same, an example is dispersion) or destructive (mass is also reduced, an example is biodegradation). Natural attenuation of petroleum products takes place in relatively oxidizing environment and, in contrast, natural attenuation of chlorinated solvents takes place in relatively reducing environment (see Chapter 11). Basic criterions for evaluation of natural attenuation according to U.S. EPA are:

(1) Trends of dissolved concentrations in the plume have to be determined by several samplings. Nonparametric statistic tests (for example, Mann-Whitney test) are used to check if concentrations are decreasing. Trend of decreasing concentrations is the principal proof of natural attenuation.
(2) Background concentrations of geochemical indicators (electron acceptors O_2, NO_3^- and sulfate) are determined in ground water out of plume. Then we compare background concentrations with concentrations in the plume to decide if intrinsic bioremediation takes place. Products of biodegradation like Fe(II) and methane are sampled only within the plume. Concentration of geochemical indica-

tors can be converted to biodegradation capacity for BTEX. In the case of chlorinated solvents and inorganic contaminants, geochemical indicators are generally used only for qualitative indication of suitability of an environment for natural attenuation.

(3) In the case of organic contamination, laboratory tests in microcosmos with contaminated water and sediments may be run and bacterial population parameters and rates of biodegradation are determined.

Detailed methodology for evaluation of natural attenuation of organic contaminants is in Wiedemeier et al. (1999). Natural attenuation of inorganic contamination and redox conditions in contaminant plumes are discussed by Christensen et al. (2000). The natural attenuation approach is not nothing-to-do approach. Careful monitoring is required to confirm that NA really occurs and calculation of risk for potential receptors is performed to verify potential risks (so called RBCA, Risk Based Corrective Action).

References

Appelo C.A.J., Postma D., 1999: *Geochemistry, groundwater and pollution*, Revised edition, A.A. Balkema, Rotterdam/Brookfield.

Christensen T.H., Bjerg P.L., Banwart S.A., Jakobsen R., Heron G., Albrechtsen H.-J., 2000: Characterization of redox conditions in groundwater contaminant plumes, *J. Contam. Hydrol.* 45, pp. 165–241.

Deutsch W.J., 1997: *Groundwater Geochemistry, Fundamentals and Applications to Contamination*, Lewis Publishers, Boca Raton, New York.

Nyers E.K., 1996: *In Situ Treatment Technology,* CRC Press, Florida.

Mackay D.M., Cherry J.A., 1989: Ground Water Contamination: Pump and Treat Remediation, *Envir. Sci. Technology,* 23(6), pp. 630–636.

Palmer C.D., Fish W., 1992: *Chemical Enhancement to Pump-and-Treat Remediation*, EPA Issue Papers, EPA/540/S-92/001.

Parkhurst D.L., 1995: Users Guide to PHREEQC-A Computer program for Speciation, Reaction-Path, Advective-Transport, and Inverse-Geochemical Calculations, *U.S. Geological Survey Water Resources Investigation Report* 95–4227.

Suthersan S.S., 1996: *Remediation Engineering: Design Concepts,* CRC Press.

Wiedemeier T.H., Rifai H.S., Newell C.J., Wilson J.T., 1999: *Natural attenuation of fuels and chlorinated solvents in the subsurface*, John Wiley and Sons, New York.

Chapter 13: Risk Analysis

13.1 Basic Concepts

Risk analysis often is a last step of contamination studies. There are several stages of risk analysis (LaGrega et al., 1994, Masters, 1998):

(1) *Hazard identification:* this is a process of determining if a particular chemical, which is linked to particular health effects like cancer, birth defects etc. Human data are rather limited, thus data on animals or other test organisms are generally used.

(2) *Dose-response assessment:* in this process the relationship between the dose of a chemical and incidence of health effects is determined. Most tests are performed using high doses on animals and extrapolation to low doses is commonly performed.

(3) *Exposure assessment:* this process involves assessment of exposure concentration, duration and size of population exposed to a particular chemical. Several factors like age and health of exposed population, pregnancy, smoking history, etc., have to be taken into account to evaluate possible synergic effects. In this stage, geochemical and transport models are used to calculate future possible exposure out of the site of contaminant release. For example, when a chemical is released from landfill site and migrates downgradient towards municipal wells in a nearby village, a transport model can be used to predict concentration of the chemical in drinking water from municipal wells in future.

(4) *Risk characterization:* in this stage previous stages are integrated and risk magnitude is calculated. This is compared with a regulatory limit and a decision about possible remediation of a contaminant source may be taken.

There are several possible ways of exposure, including *ingestion* by drinking of contaminated water, *inhalation* by breathing of contaminated air, and by *dermal contact* with contaminated soil. In human body, a chemical can be stored (for example, in fat like DDT), eliminated from body by excretion (in urine etc.) or can be transformed to other compounds (sometimes even more toxic, an example is transformation of trichlorethylene, TCE, to vinylchloride, VC).

Several human organs are especially vulnerable. The liver filters blood and, thus, can be directly damaged by a chemical transported in blood stream. Chemicals damaging liver are called *hepatotoxic.* Examples are arsenic, trichlorethylene (TCE), and anabolic steroids. Kidneys also filter blood and can be damaged by *nephrotoxic* compounds like cadmium, lead and chlorinated solvents. Chemicals acting on blood are called *hematotoxic* and include carbon monoxide and nitrogen compounds. They interfere with blood ability to transmit oxygen. Benzen affects formation of platelets in blood and, thus, also is hematotoxic compound. *Pulmonotoxicity* is related to compounds like asbestos, and quartz dust, which can cause cancer of lungs.

13.2 Concept of Toxicity

Two principal groups are considered: chemicals with *acute toxicity* and chemicals with *carcinogenic effects.* Some chemicals like arsenic belong to both groups.

Acute toxicity refers to effects that may happen within a short period of time after a single exposure to a chemical. Not every exposed individual will react in the same way and a *dose-response curve* shows a percentage of tested population that is affected as a function of dose received. Dose is normalized per kg of body weight and is expressed, for example, in mg/kg. It is assumed that is a *threshold dose*, below which there is no toxic effect. Thus, the dose-response curve for acute toxicity (non-carcinogenic) chemicals does not pass through origin (Fig. 13.1), but starts at some non-zero concentration of a chemical.

In contrast, for substances with carcinogenic effect it is assumed that any exposure to a carcinogen may create some probability of cancer. In that case the dose-response curve passes through origin (Fig. 13.1).

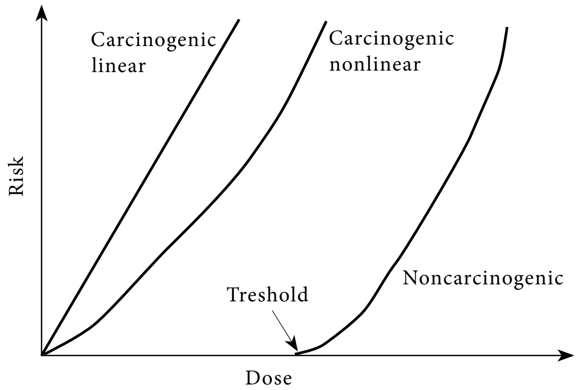

Figure 13.1 Dose-response curves for carcinogens and for non-carcinogens.

In some cases, there are epidemiological data based on the study of human population exposed to a toxic chemical. These studies cannot be generally performed under completely controlled conditions and their results are often interpreted using statistical methods.

However, the dose-response curves are generally based on *animal bioassays* and a *scaling factor* must be used for extrapolation from animals to humans. In general, testing is performed on animals like selected species of rats and tested doses are much higher than expected doses for human population exposures. Several extrapolation methods are used. Commonly used model is the *one-hit model* (Masters, 1998) which gives the relationship between dose (d) and lifetime probability $P(d)$ of cancer as

$$P(d) = 1 - e^{-(q_0 - q_1 d)} \qquad 13.1$$

where q_0 and q_1 are fitting parameters for dose-response curve. When we substitute $d = 0$, we will obtain background risk of cancer. For small values of x, we can develop e^x using the Taylor expansion as $e^x \cong 1 + x$ and assuming that background risk is small, we can write:

$$P(0) = 1 - e^{-q_0} \cong 1 - \left[1 + (-q_0)\right] = q_0 \qquad 13.2$$

Thus, background risk for cancer incidence is equal to q_0. Life-time probability of cancer can be evaluated, using the Taylor expansion again, as

$$P(d) = 1 - (1 - (q_0 + q_1 d)) = q_0 + q_1 d = P(0) + q_1 d \qquad 13.3$$

For low doses, the additional risk of cancer $A(d)$ is

$$A(d) = P(d) - P(0) = q_1 d \qquad 13.4$$

Thus, the model predicts that the additional risk of cancer for low doses is linearly related to dose. There are other models such as *multistage model.* See, for example, Masters (1998).

13.3 Carcinogenic Contaminants

There are several categories of carcinogens according to U.S. EPA.:

Group A: human carcinogens, based on sufficient epidemiological evidence to support a causal relation between exposure to a chemical and cancer.

Group B: probable human carcinogen, divided into *group B1* and *group B2*. For a chemical in group B1, there is limited epidemiological evidence. For group B2, there are insufficient human data, but sufficient evidence of carcinogenecity in animals.

Group C: possible human carcinogens, based on limited animal data, but without human data.

Group D: not classified, both human and animal evidence is insufficient or there are no data at all.

Group E: evidence of non-carcinogenecity, there is evidence about lack of carcinogenic effects in both humans and animals.

The dose-response curve for carcinogenic contaminants is used to calculate the incremental risk of cancer (e.g., above the background incidence). At relatively low doses, the slope of dose-response curve is called *slope factor SF* (also potency factor PF) and dimensionless *incremental risk IR* is calculated as

$$IR = SF\ CDI \qquad 13.5$$

where *CDI* is *chronical daily intake* [mg/kg day] and *SF* is slope factor (slope of dose-response curve) with units [(mg/kg.day)$^{-1}$]. The value of *CDI* is calculated for different exposures (ingestion, inhalation, dermal contact) during 70 years of life time. For example, for ingestion via drinking of contaminated water the *CDI* is

CDI [mg/kg day] = Average daily dose [mg/day]/Body weight [kg] 13.6

The values of slope factor *SF* can be obtained from database of U.S. EPA called IRIS (integrated risk information system), available on the web under U.S. EPA Home Page. Values of incremental risk > 10^{-6} are generally considered as unacceptable, but there is a transition between 10^{-4} and 10^{-6}, when other circumstances are considered.

Problem: Calculate incremental risk for chloroform (class B2 contaminant) with slope factor $SF = 6.1\times10^{-3}$ [mg/kg.day]$^{-1}$ when 70-kg person drinks 2L of water with 0.2 mg/L of chloroform.

Solution:
$CDI = (2.0\times0.2)/70 = 0.00572$ mg/kg.day, then
$IR = 0.00572\times6.1\times10^{-3} = 34.8\times10^{-6}$
e.g., the probability to get cancer is about 35 in 1 million.

13.4 Non-carcinogenic Contaminants

As indicated earlier in the text, there is a threshold concentration for non-carcinogenic contaminants, below which no adverse effects are observed. Furthermore, lack of some elements which are toxic at high administered doses also has a negative impact on human health. Examples are selenium and zinc. Thus, there is some optimum concentration below which and above which there is an adverse effect on human health. In contrast, contaminants like lead, cadmium, and arsenic are not necessary for human organism even at extremely low doses.

The lowest administered dose resulting in a response is called *the lowest observed effect level (LOEL)*. The highest dose without response is called *the no observed effect level (NOEL)*. When adverse effect levels are included, then there are *the no observed adverse effect level (NOAEL)* and *the lowest observed adverse effect level (LOAEL)*.

The concept of *reference dose, RfD* (also called acceptable daily intake) is based on the NOAEL divided by safety factor (uncertainty factor). The safety factor includes uncertainties for extrapolation from animals to humans, for presence of more vulnerable individuals in human population etc. Thus, the reference dose is several orders of magnitude lower than the observed value of NOAEL. Reference dose RfD with units [mg/kg.day] indicates a level of human exposure without an appreciable risk.

Hazard index HI (also called hazard quotient) is calculated as

$$HI = \text{Average daily dose during exposure [mg/kg day]} / RfD\text{[mg/kg day]} \qquad 13.7$$

Results of *HI* are dimensionless. When $HI > 1.0$, the risk becomes unacceptable. Average daily dose *ADD* is calculated only for a period of exposure and not over life time as it is for carcinogenic contaminants. For several contaminants, the hazard index is the sum of individual hazard indexes. Values of reference doses for different chemicals can be found in database IRIS, just like slope factors for carcinogenic contaminants.

Problem: Calculate hazard index for drinking of 2 L of water with 2.0 mg/L of toluene for a person with body weight of 70 kg. The *RfD* for toluene is 0.200 mg/kg.day.

Solution:
First calculate average daily dose *ADD*
$ADD = (2.0 \text{ mg/L} \times 2 \text{ L/day})/70 \text{ kg} =$
$= 0.058 \text{ mg/kg}\times\text{day}$
Hazard index
$HI = 0.058 \text{ mg/kg}\times\text{day}/0.200 \text{ mg/kg}\times\text{day} = 0.14$
$0.14 < 1.0$, suggesting that drinking of the water is safe.

13.5 Risk Analysis Methodology

Several steps are performed during risk analysis (LaGrega et al., 1994). Let us consider a case of a municipal landfill. First of all, contaminants of interest have to be selected and exposure has to be estimated. Data for the source zone, in this case landfill area, are collected. Concentrations of chemicals in water, soil, and air are determined. In this preliminary screening, *toxicity scores TS* for both carcinogens and non-carcinogens are determined using slope factors and reference doses. The toxicity scores for individual contaminants are summed up and contaminants comprising 99 % of toxicity score are selected.

Then exposure is determined at exposure (receptor) points. This exposure point may be directly at source zone or may be located at some distance from source zone. Say the contaminant selected on the basis of toxicity score is lead and exposure point is a water supply well about 400 m downgradient from the landfill. In that case, we have to calculate prediction of future concentration of lead in drinking water from the water supply well. This can be performed using an analytical or numerical model of transport, which are an extension of flow model. Relevant processes for lead transport (advection, dispersion, adsorption, precipitation of lead minerals like cerussite, $PbCO_3$) should be included in the model. If only advection is included in model, then the prediction of lead concentration represents the worst case scenario (maximum level of exposure).

After calculation of exposure, the risk is calculated separately for both carcinogens and non-carcinogens. If the risk is acceptable, natural attenuation processes only may be sufficient to stop spreading of the plume. In contrast, if risk calculated for exposure point is unacceptable, then some remediation technology (pumping and treatment of ground water, reactive barriers etc., see Chapter 12.3) should be used. The approach based on risk analysis is called *Risk Based Corrective Action (RBCA)* and is implemented by the U.S. EPA.

References

LaGrega M.D., Buckhingham P.L., Evans J.C., 1994: *Hazardous Waste Management*, McGraw-Hill Inc., New York, 1146 p.

Masters G.M., 1998: I*ntroduction to Environmental Engineering and Science*, 2nd Edition, Prentice Hall, Upper Saddle River, New Jersey 07458, 651.